Stress Relaxation in Poly(methyl methacrylate) (PMMA)

During Large-Strain Compression Testing Near the Glass Transition Temperature

A Thesis

Presented in Partial Fulfillment of the Requirements for Graduation with Distinction in

Mechanical Engineering at The Ohio State University

By

Dana Vogtmann

Advisor: Dr. Rebecca Dupaix

The Ohio State University

May 2009

Table of Contents

List of Figures

LIST OF TABLES

Abstract

Poly(methyl methacrylate) (PMMA) is a common polymer with useful applications in micro-scale compression-molding. Better understanding of this polymer's behavior when held in compression during molding could greatly improve accuracy when imprinting micro-scale features on the material's surface. Previous work has been done to record the behavior of PMMA under complex loading situations, and from this research a material model has been developed. However, the current model inaccurately predicts how stress in the material will naturally decrease in a sample held in compression at elevated temperatures. This behavior is referred to as "stress relaxation." The purpose of my work is to help improve the current material model by collecting data on PMMA's stress relaxation behavior. To do this, I tested about 50 small samples of PMMA within an environmental chamber heated to near the material's glass transition temperature, T_g, or the temperature at which a rigid polymer transitions to a more rubbery, deformable state. These tests consisted of compressing the samples between two plates at a constant rate and then holding at a constant compression level. During the holding period, I recorded the stress in the material by measuring the force exerted by the sample on the compression plate. Between tests, I varied temperature, compression rate, and the compression level applied during the holding period. I observed differences in the stress relaxation behavior based on changes to each of these variables. I explored these behavior differences further through several data manipulation techniques and through comparisons of the results against a general viscoelastic material stress relaxation model. I have also compared my results with simulations based on the current material model to determine the model's accuracy, which proved to be low for this behavior. Ultimately, I would like to help improve the model's simulation capabilities using the data I have collected. When it is able to accurately predict material behavior under complex loading, this material model will be a valuable aid in creating inexpensive and precisely molded PMMA parts with micro-scale features.

1.0.0 Project Background

Poly(methyl methacrylate) (PMMA) is a common polymer often used on a macro scale as a sheet glass substitute due to its low cost, good processing temperature range, and ability to be molded into most any shape. However, these same abilities also make PMMA ideal for use in ultra-precise, micro- or nano-scale compressive hot embossing applications such as CD molding and microchip base construction. A higher level of understanding of PMMA is currently needed in order to better employ it in this field. There has been extensive recent testing of this material with emphasis on compressive tests, endeavoring to create an accurate model of PMMA's behavior near its glass transition temperature—the temperature at which a polymer transitions from a rigid solid to a more rubbery, deformable state (Palm et al., 2006). Mechanical models of polymers involve connecting, in series and parallel, combinations of linear and non-linear springs and dampers. Research into the actual behavior of the material determines the equations and constants that define these theoretical springs and dampers, and ideally this model should react to loadings in the same way that the actual polymer would. In the case of PMMA, our current model involves two branches connected in parallel, each with a spring in series with a damper. See Figure 1 for a schematic of the PMMA model. This modeling, when sufficiently complete, will help further the understanding of the material which could lead to more efficient and inexpensive precise processing techniques.

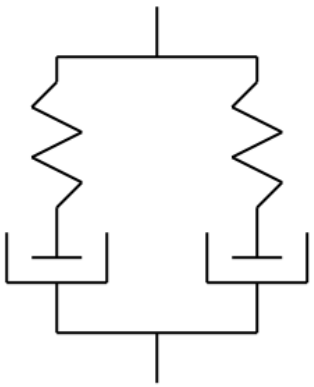

Figure 1: Basic schematic of model

In this project I have attempted to help further this material behavioral research by heating samples of PMMA to near or above the glass transition temperature (about 107°C for PMMA), compressing the samples, holding them in compression, and observing the stress relaxation (how the material deforms) over time. To our knowledge, there had previously been no recorded large-strain relaxation data for PMMA. Since most polymer compression molding techniques involve holding the part inside the mold for a brief period to let it cool to a more rigid state, understanding this portion of the material's behavior is crucial to our ability to model and predict the actual molded shape after emergence from its mold. This prediction is extremely important in high-precision applications.

1.1.0 Objectives

Over the course of my research, I attempted to complete several objectives.

- Collect mechanical data for PMMA in embossing processing regime
  - Vary temperature between 100°C – 130°C (Near the 107°C glass transition temperature)
  - Vary strain rate (the rate at which the material is deformed) between 1 ε/min - 3 ε/min
  - Observe stress relaxation at final strains of .5, 1.0, and 1.5 for long holding periods.
- Graph/Interpret results, including
  - Stress vs. Time
  - Stress vs. Strain
  - Stress Relaxation vs. Total Strain
  - Stress Relaxation vs. Temperature
- Compare results with existing material model specifically focusing on stress relaxation behavior

These original objectives have been met, along with other ways of interpreting the data I obtained, and a comparison of the data with a more generalized material model typically used in viscoelastic relaxation modeling, the Maxwell model.

1.2.0 Equipment Used

The samples of PMMA used for testing were cylinders cut from a large sheet for consistency. This sheet stock was supplied by Plaskolite, Inc. Before deformation, the dimensions were roughly 8.8 mm in height by 10 mm in diameter. Figure 2 shows an example of these specimens.

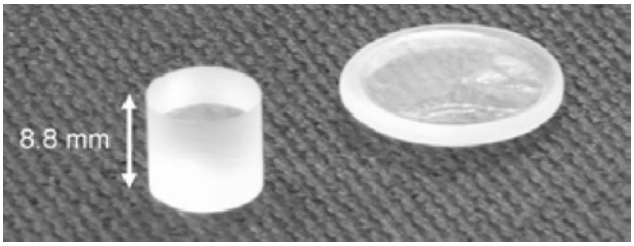

Figure 2: Undeformed and deformed PMMA samples

In order to compress the samples of PMMA for study, I used an Instron 5869 screw driven (electromechanical) materials testing system with an Instron 3119-409 environmental chamber capable of heating to 250°C. The system consisted of a static lower plate and a movable upper plate, both contained within the environmental chamber with temperature control. This setup was connected to an Instron 5800 controller run by Instron Bluehill software. This software allowed me to input a strain profile which would then be translated into movement of the Instron machine's upper compression plate. The software also collected the displacement of the upper compression plate, and data from a 50kN load cell set up to detect force from the sample onto the compression plates. These force and displacement data sets were used to calculate stress (detailed in section 3.1.1), and to verify that the strain profile was correctly input to the system.

2.0.0 Testing procedure

The general method for testing samples was as follows:

1. Program the software with the strain profile at which the sample is to be compressed. This consists of a loading period and a holding period.
2. Prepare the sample for testing and place it between the compression plates within the environmental chamber.
3. Input the desired temperature for the environmental chamber.
4. Wait at least 30 minutes for the sample to heat to the desired temperature.
5. Bring the upper compression plate just barely into contact with the sample.
6. Run the compression program and save the output force data.

Step 1 is discussed in more detail in section 2.1.0. Step 2 is discussed in more detail in section 2.2.0.

2.1.0 Strain Profile Programming

For each combination of strain rate and total strain, a different strain profile had to be added to the Bluehill testing control area. A sample strain profile is shown in Figure 3.

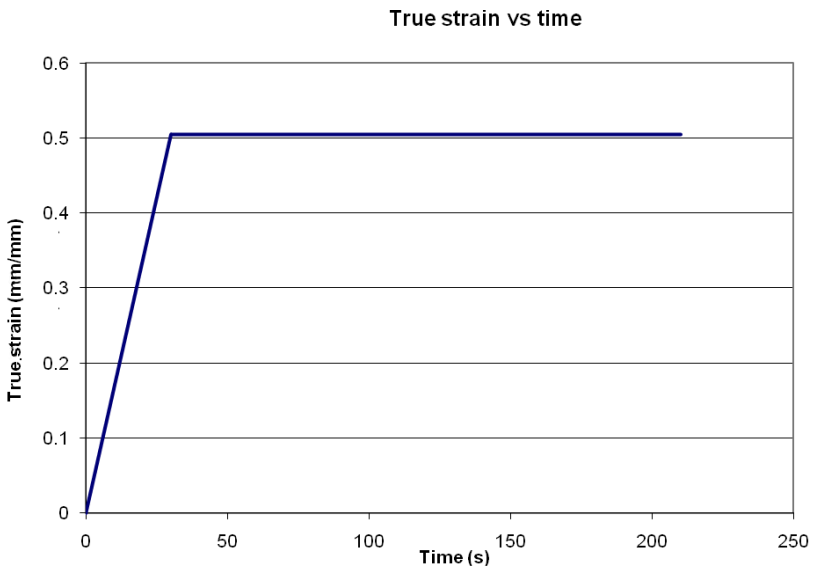

Figure 3: Sample strain profile

These profiles were created by inputting the desired displacement of the force plate over several discrete time intervals. The software allowed for 28 intervals, so I calculated the total time it would take for the strain to reach the desired level at the desired strain rate (call t_{tot}) and set the length of time for the first 27 intervals to $t_{tot}/27$. The last interval was reserved for the holding period. Since I wanted the samples to be compressed at a constant true strain, I approximated this behavior by calculating the necessary displacement for the given strain over the first interval, subtracting the change in height from the original height, and using the new height to calculate the necessary displacement for the given strain over the second interval, and so on. So,

$$\Delta h = h_i * \varepsilon$$

$$h_{i+1} = h_i - \Delta h$$

where Δh is the required change in height over an interval, h_i is the height of the sample at the beginning of the interval, and h_{i+1} is the height at the end of the interval. The start and end strain was input for each interval, with values ranging from 0 to the desired total strain. For the final interval, the strain level was held constant over a long period of time.

2.2.0 Sample Preparation

To prepare the samples for testing, I left each prefabricated sample in a desiccator for at least 24 hours prior to the test to control the amount of moisture present. Once the samples were prepared and the testing profile entered in the Bluehill software, I placed a thin sheet of Teflon, lubricated with WD-40, on both the top and bottom compression plates and placed the PMMA sample between the two sheets of Teflon. See Figure 4 for a schematic of this setup.

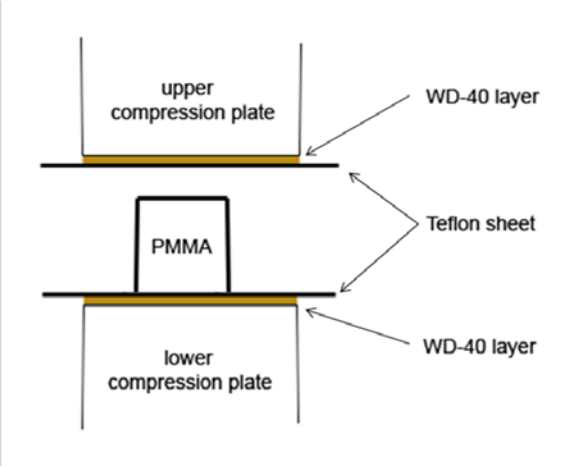

Figure 4: Experimental setup

The lubricated Teflon sheets were used to allow the sample to expand laterally with greatly reduced friction without introducing the polymer directly to the lubrication.

2.3.0 Experimental Variables

Throughout the entire testing phase, I used different values for temperature, strain rate and total strain, though not all combinations were tested. A test matrix follows in Table 1.

Table 1: Test matrix (blue cells indicate test was performed)

Total Strain	Temperature					Strain Rate
	95°C	105°C	110°C	125°C	135°C	
0.5ε						1.0 ε/min
1.0 ε						1.0 ε/min
1.5 ε						1.0 ε/min
1.0 ε						3.0 ε/min
1.5 ε						3.0 ε/min

My original test matrix consisted of temperatures from 105-125°C, at 1.0/min strain rate, with varied total strains. Some tests at 3.0/min were done to investigate strain rate dependence, and tests at temperatures of 95°C and 135°C were added later to investigate an unexpected trend in the temperature dependence of relaxation rate, which will be discussed in section 3.3.1.

2.4.0 Repeatability

For each set of parameters used, I tested two samples. From this, I was able to ensure that my results were very repeatable. For tests using the same parameters, the curves I obtained were nearly identical for all but a few parameter sets. If any of the sets of data did not match up well, I ran another test to confirm which curve seemed to be more accurate. Figure 5 shows a comparison between two stress-time curves tested with the same parameters.

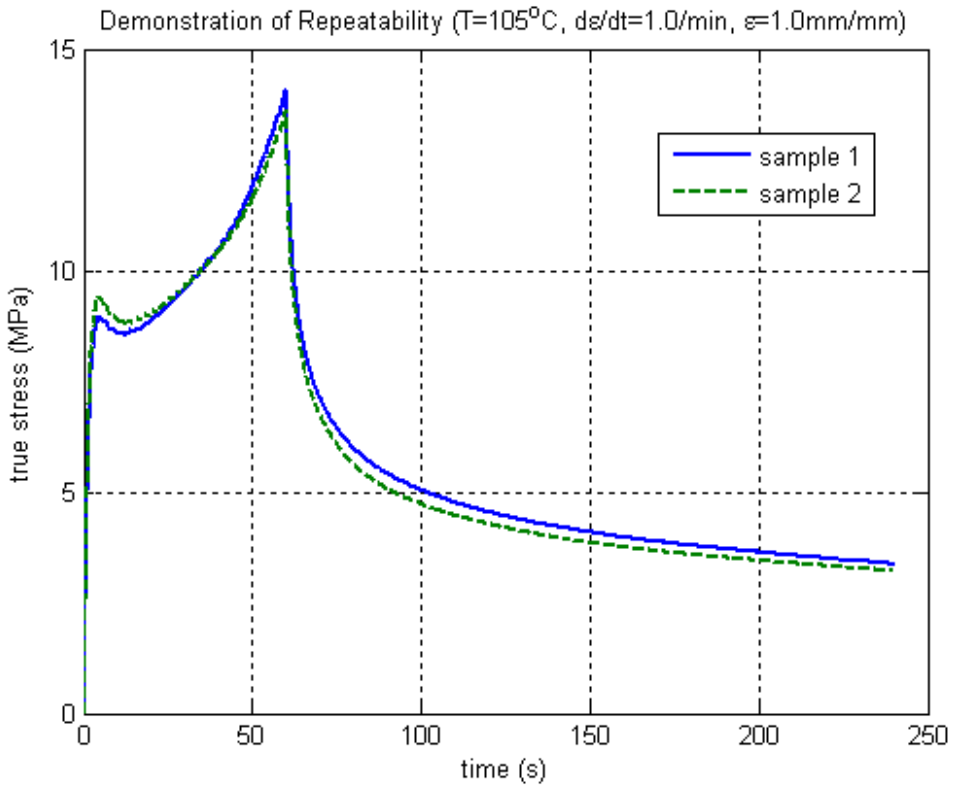

Figure 5: Two samples tested under the same parameters

Comparisons between tests run at the same parameters for all other sets were similarly close to one another, with deviations tending to stay within about 5%.

3.0.0 Findings

Over the course of my project, I collected large amounts of data and manipulated the data in different ways in order to more directly compare the reactions of the PMMA samples under different loading conditions and temperatures. This section describes some of the basic plots obtained from the collected force data, and some of the plots created from more complicated manipulation of this data

3.1.0 Basic Plots

This section presents some basic plots created essentially directly from the data collected by the load cell measuring the force from the samples on the compression plate, with very little manipulation.

3.1.1 Stress vs Time

The main results I obtained from the tests described in section 2 were stress vs time plots. True stress was obtained from the force-displacement data collected by the Instron Bluehill software by assuming constant volume in the samples. A cylinder volume, V, is given as

$$V = h\pi r^2$$

where h is the height of the cylinder and r is the radius of the cross section. At constant volume, and for the total displacement value at any time, $\Delta h(t)$, the assumed radius at any time, r(t), can be calculated as

$$r(t) = r_0 + \Delta r(t) = \sqrt{\frac{V}{\pi(h_0 - \Delta h(t))}}$$

where h_0 is the initial height, r_0 is the initial radius, and $\Delta r(t)$ is the total change in radius at any time.

By using this equation, we can determine the assumed radius of the sample for any displacement. Using the fact that stress in a sample is equal to the force over the cross sectional area, and that we can find the area for any time using the above equations, we can find the stress at any time, $\sigma(t)$, by using

$$\sigma(t) = \frac{F(t)}{2\pi * r(t)}$$

where F(t) is the force data from any point in time.

Plotted over time, this data gives us the stress-time curve for a sample. I have included Figure 6 here as a representative of these plots. Appendix A contains a stress vs. time plot for each of set of parameters tested.

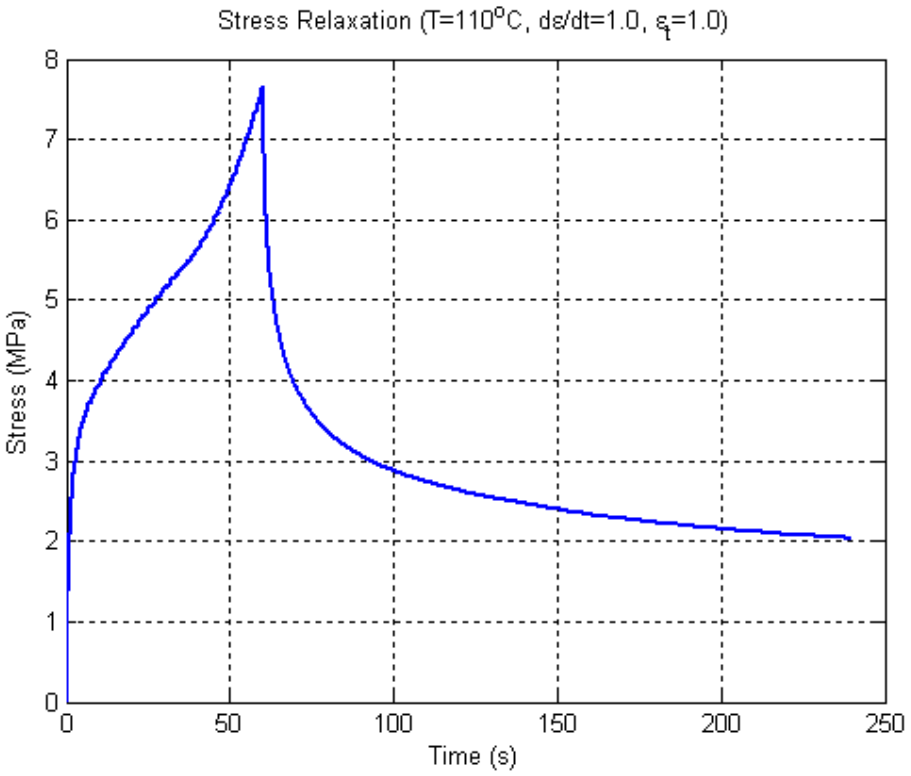

Figure 6: Representative stress vs. time plot

Each plot features, for the first phase, a general nonlinear increase of the stress over time, which corresponds to the loading phase of the test procedure. Samples tested at lower temperatures display a fairly clear yield point and strain hardening behavior, while those tested at higher temperatures appear more fluid-like, with no clear yield point or strain hardening. At the end of the loading phase, the stress reaches a peak point when the desired strain level is reached. For reference, this peak occurs at 60 seconds for the sample in Figure 6. After this point, the stress steadily drops for the remainder of the test while the strain is held constant. Figure 7 shows how the strain input relates to the stress output over time.

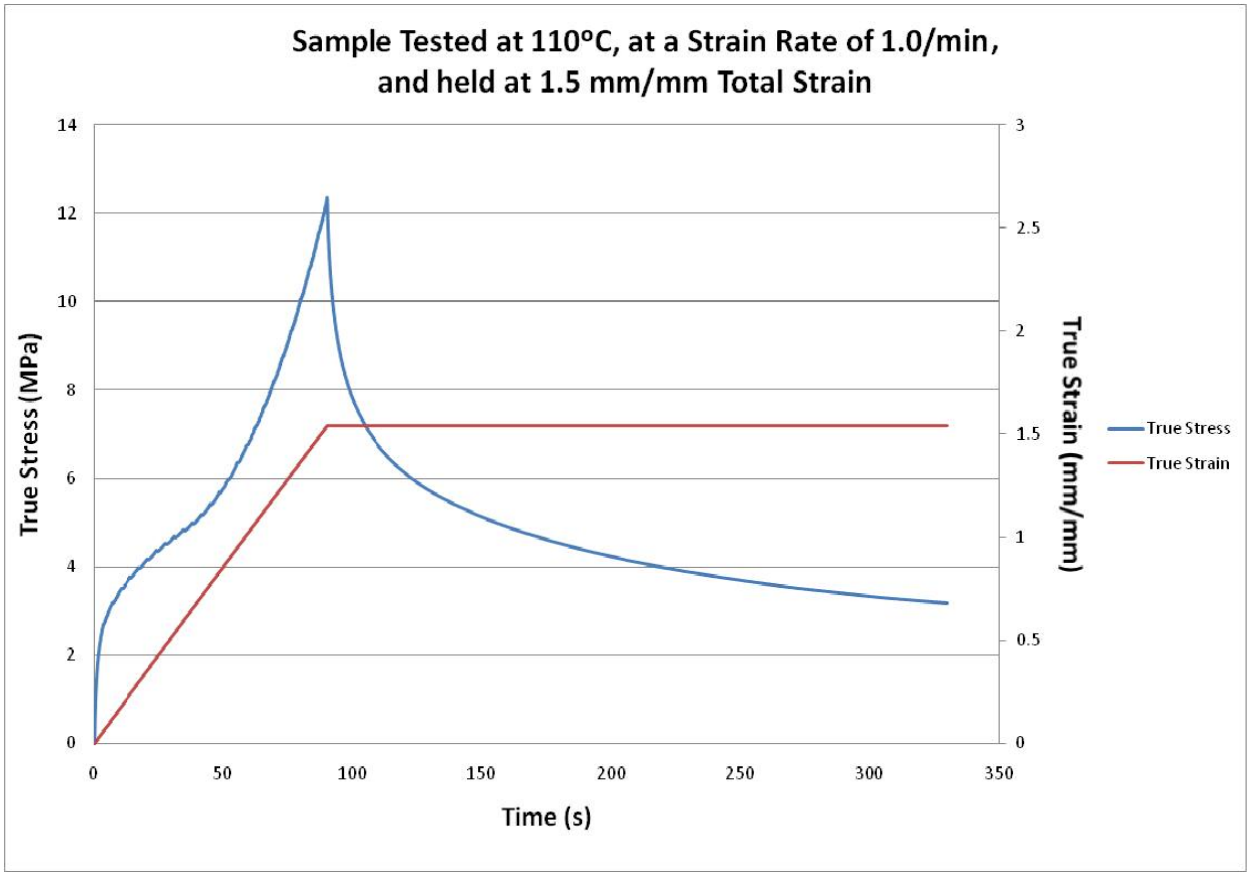

Figure 7: Stress output's relation to strain input

From this plot, it can be seen how the increase in stress relates to the loading period on the strain input profile, and how the relaxation of stresses begins during the holding period after the strain input has reached the total desired strain.

By varying the input temperature, strain rate, and total strain, the behavior of the stress-time plots can change significantly. Figure 8 shows the variation in behavior of samples tested at different temperatures.

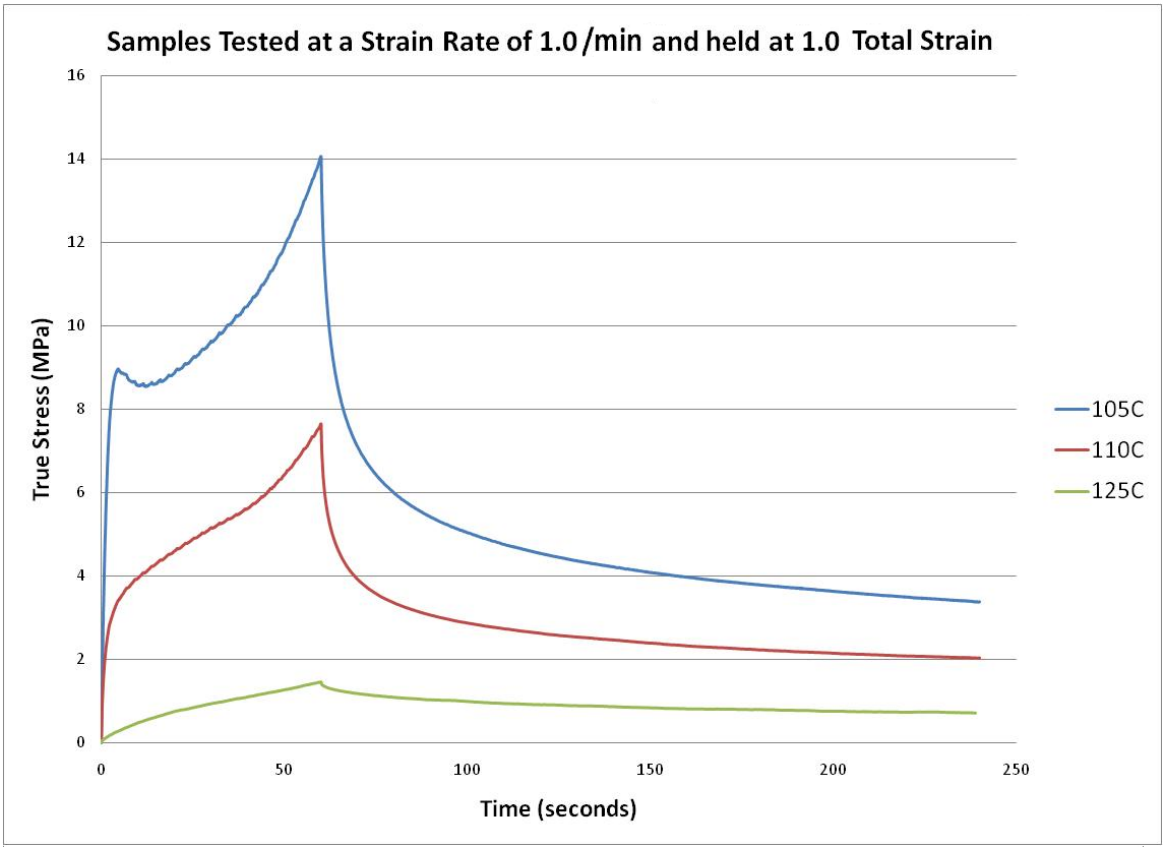

Figure 8: Behavior at different temperatures

All three of the curves in Figure 8 were tested at the same strain rate and total strain. As the temperature is increased, the peak stress in the system is lowered. This is due to the increased compliance of PMMA at higher temperatures, exhibiting typical polymer behavior. This behavior is consistent for all tested combinations of strain rate and total strain.

Figure 9 shows the variation in behavior of samples tested at different total strain levels.

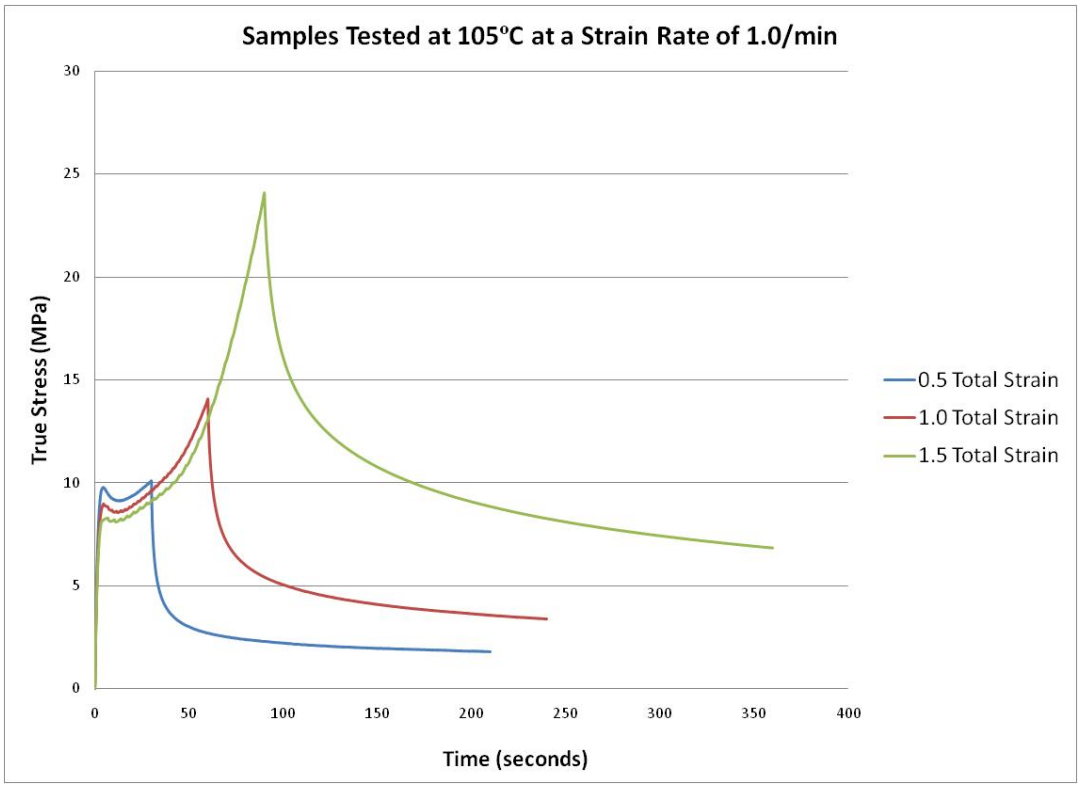

Figure 9: Behavior at different total strain levels

All three of the curves in Figure 9 were tested at the same temperature and strain rate. Because the total strain is increased in these plots by simply leaving the loading phase on longer, the curves follow roughly the same path of increasing stress until the given total strain is reached and the holding phase begins. So, as the total strain is increased, the peak stress occurs later and higher. This behavior is also consistent for all tested combinations of temperature and strain rate.

Figure 10 shows the variation in behavior of samples tested at different strain rates.

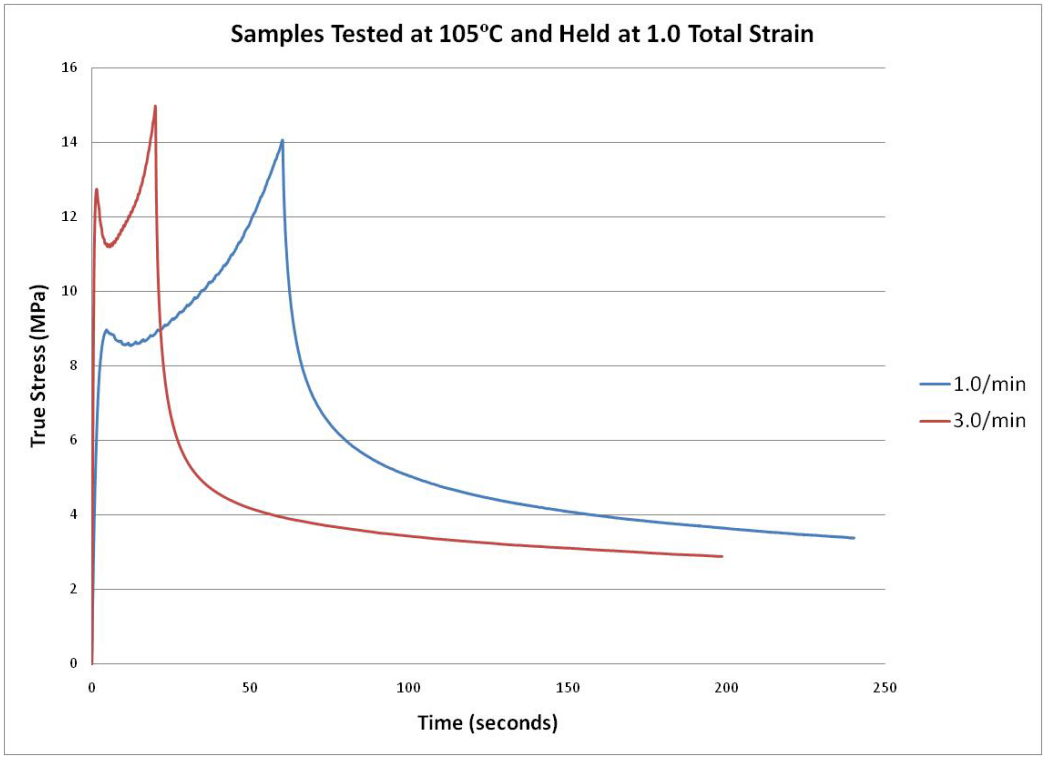

Figure 10: Behavior at different strain rates

Both of the curves in Figure 9 were tested at the same temperature and total strain level. The test done at 3.0/min reaches the total strain much more quickly than the test done at 1.0/min. Because of this, the peak stress in the 3.0/min curve occurs earlier than that of the 1.0/min curve. Additionally, the peak stress in the 3.0/min curve is somewhat higher than that of the 1.0/min curve. This behavior is due to some of the stress in the system relaxing during the loading period. Because the loading period is longer for the 1.0/min, more stress would have already relaxed by the peak stress point.

3.1.2 Stress vs. Strain

Because all of my samples were tested at a constant loading rate, the shape of the stress-strain curves look identical to the stress-time curves for the loading period, with a straight vertical line at the total strain level, representing the relaxation of stresses at that constant strain. Figure 11 shows a representative stress-strain curve. This curve corresponds to the stress-time curve from Figure 6, and the loading period portion of the curve can be seen to be identical, with only the x-axis values being different by a factor of the strain rate, since

$$t = \varepsilon/(d\varepsilon/dt)$$

So, the peak stress, which occurs here at 1.0mm/mm true strain, occurs at a time of

$$t=(1.0\varepsilon\ /1.0\ \varepsilon/\text{min})\ *60\ \text{s/min} = 60\text{s}$$

on the stress-time curve.

Figure 11: Stress vs strain representative plot

This similarity to the stress-time curve during the loading phase, with a vertical line at the hold strain, holds true over all tested samples, so the rest of the stress-strain curves have not been included.

3.2.0 Adjusted Stress vs. Time

Since each stress vs. time plot begins at a different time and at a different peak stress value, the relaxation behaviors from plot to plot are difficult to directly visually compare, even qualitatively. To get a sense of the rate at which the stresses relax out of a sample tested under a given set of parameters, I created adjusted stress relaxation plots. Figure 12 shows a representative adjusted plot.

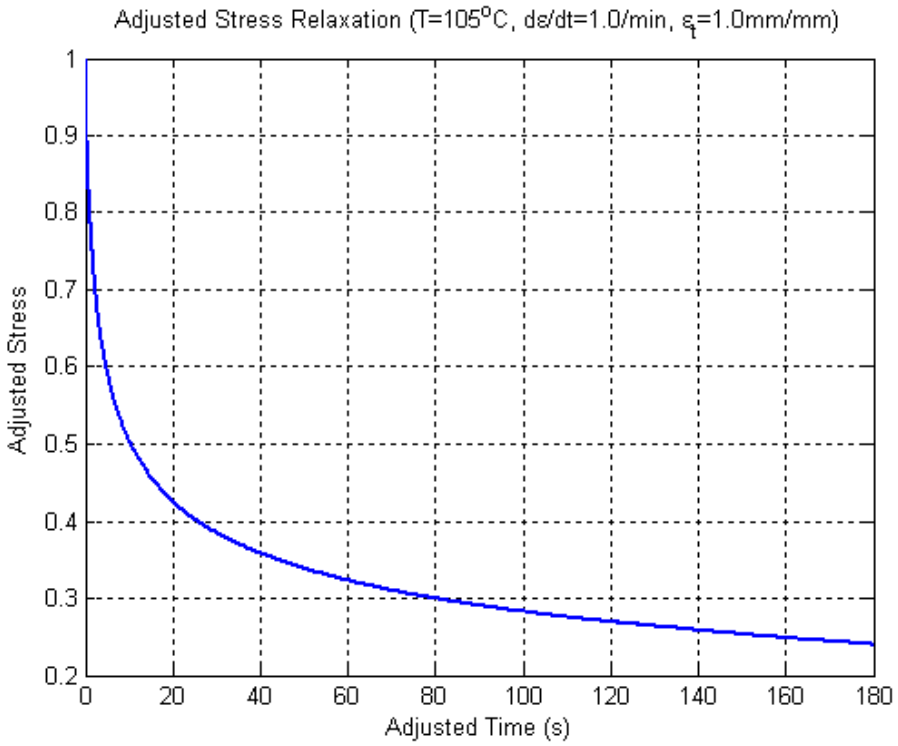

Figure 12: A sample adjusted stress plot

To create these plots, I took the stress data from each test and cut off every stress-time point preceding the peak stress point. I then divided each of the remaining stress values by the peak stress value and subtracted the first time value from each of the remaining time values. This causes every adjusted stress-time plot to begin at the point (0,1) on the adjusted time/adjusted stress plane. These plots can be seen as representing the decimal percentage of the total induced stress remaining in the system at any time after the start of the relaxation period.

Because each plot begins at the same point, they can easily be compared both qualitatively and quantitatively with one another. Figures 13-17 show the data taken over each combination of strain rate and total strain at each temperature.

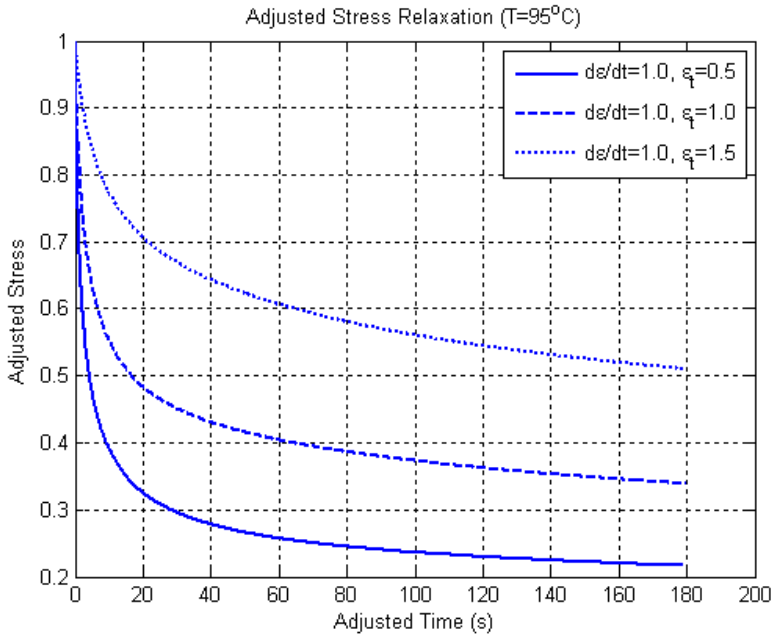

Figure 13: Comparison of adjusted stress at 95°C

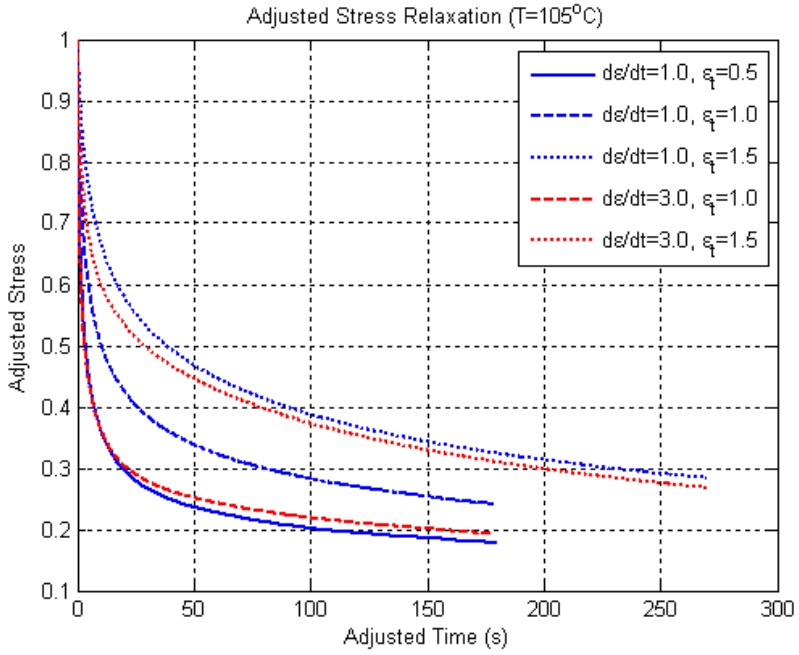

Figure 14: Comparison of adjusted stress at 105°C

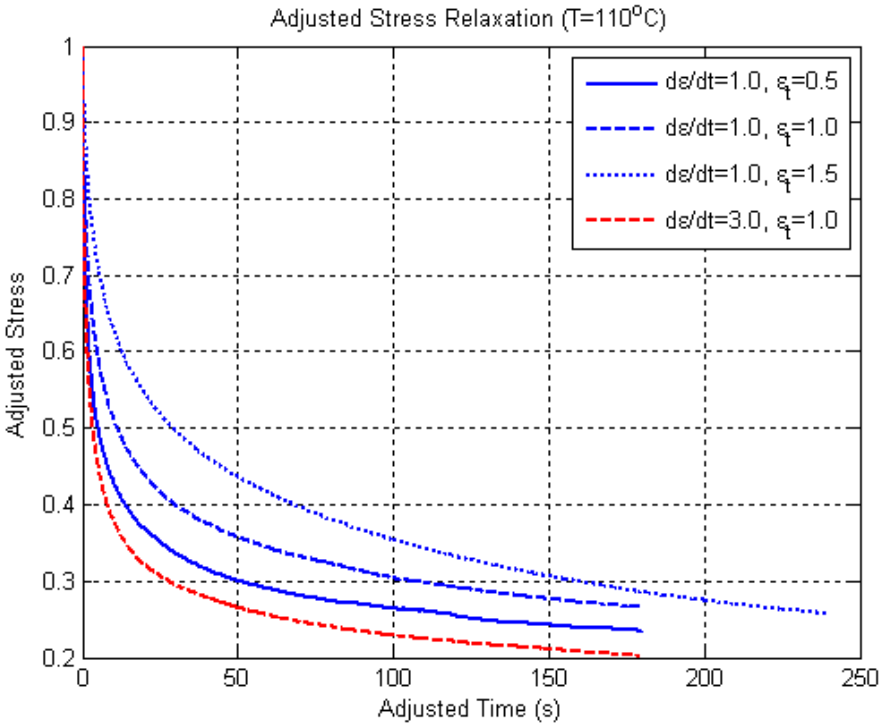

Figure 15: Comparison of adjusted stress at 110 °C

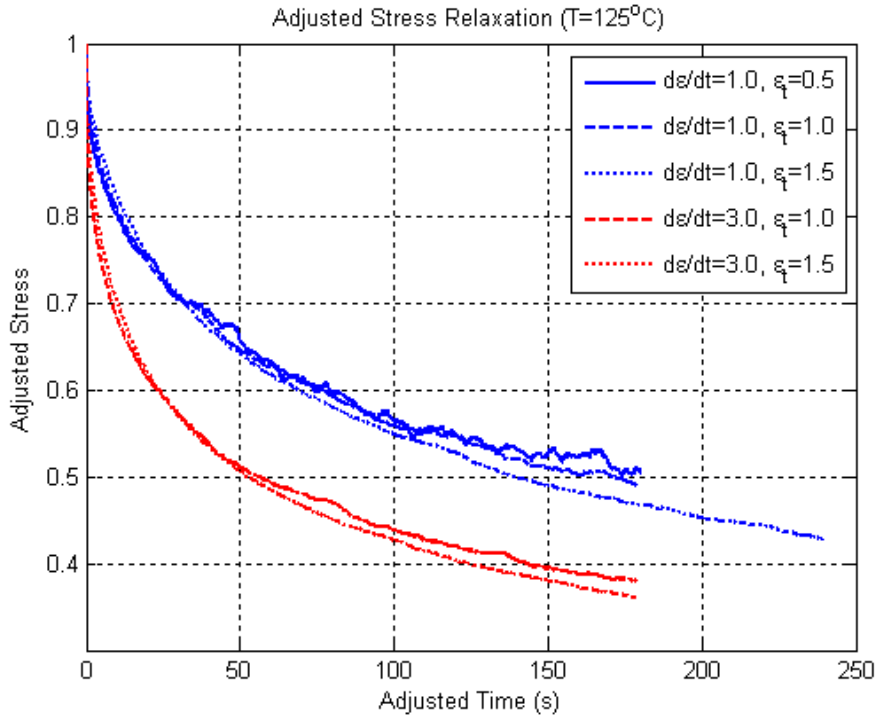

Figure 16: Comparison of adjusted stress at 125°C

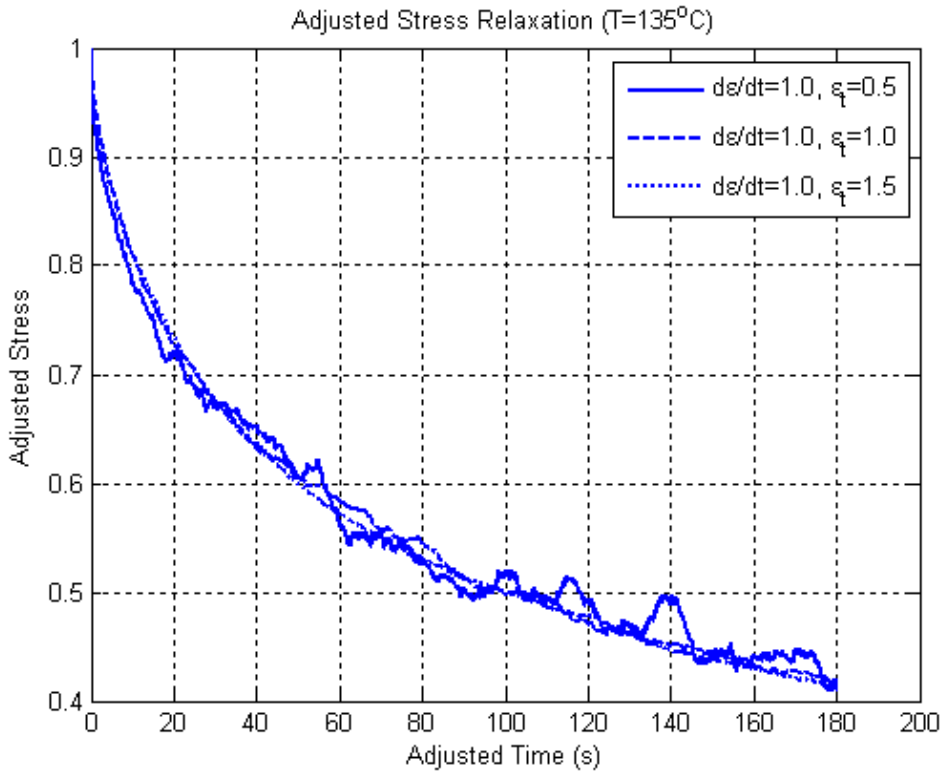

Figure 17: Comparison of adjusted stress at 135°C

These plots can help identify which factors are influencing the relaxation rate at different temperatures. It can be seen most clearly in Figure 14 that at low temperatures, the total strain level has more of an effect on the relaxation rate than the loading strain rate. In Figure 16, it is quite clear that this trend has reversed at higher temperatures, and the strain rate has much more of an effect than the total strain level. This behavior is due to the polymer's tendency to act as a rigid solid at lower temperatures, therefore reacting similarly to strain regardless of how quickly it was applied, and its tendency to act as a viscous liquid at higher temperatures, therefore relaxing more during the loading period and causing the level of strain not to matter as much as how quickly it was applied.

Other interesting behaviors based on these plots are described in the next section and subsequent subsections.

3.3.0 Relaxation Rate (50 second indicator values)

One way to show the speed at which a given sample is relaxing is to take the percentage of stress left in the system at a set amount of time after the beginning of the relaxation period, and compare this value to values taken from samples tested under different parameters. I chose 50 seconds for a few reasons: I let each test run at least this long, this time is neither during the initial slope nor after the leveling off point for most of the samples, and because none of the samples appear to "switch places" after this time.

I isolated these data points for each test by taking the value of adjusted stress at an adjusted time of 50 seconds, off the plots described in section 3.2.0. I then compared these points for each set of testing parameters over temperature, strain rate, and total strain.

3.3.1 Temperature Dependence

While looking at the data presented in section 3.2.0, I noticed that at temperatures of 105°C and 110°C, samples tested at higher strains were relaxing more quickly, while at 125°C, samples tested at higher strains were relaxing more slowly. Figure 18 shows this behavior over 105°C, 110°C, and 125°C, using the method described above.

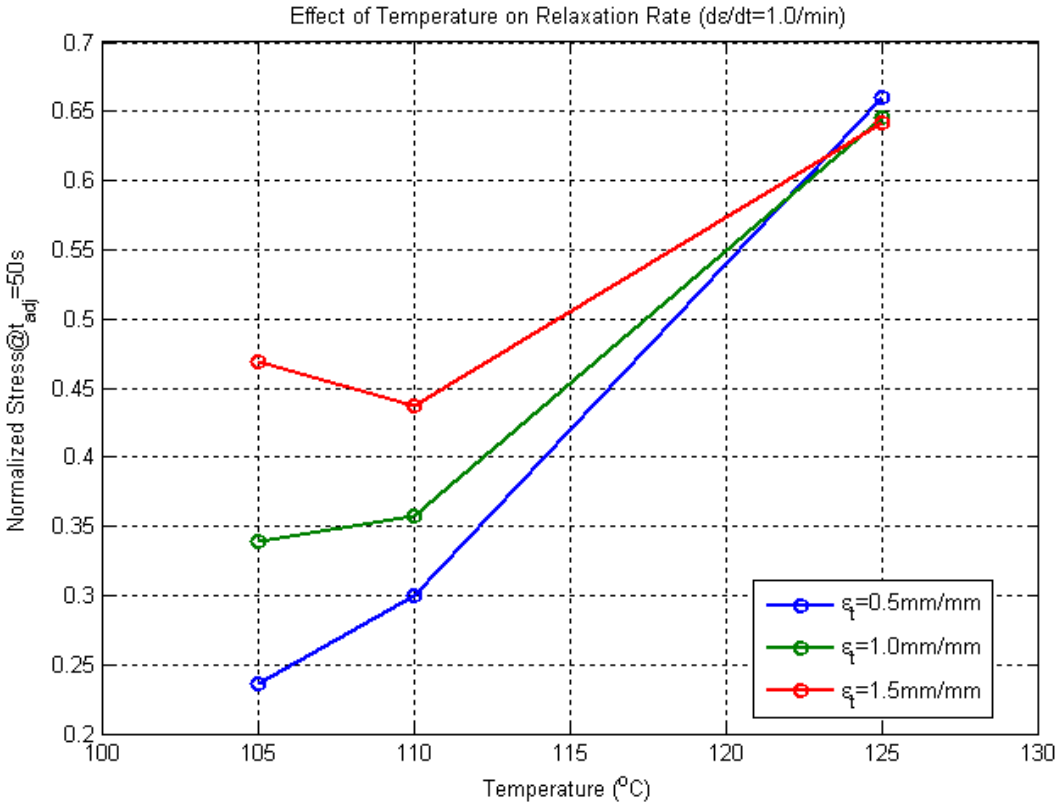

Figure 18: Relaxation left in the system for each system: dependence over three temperatures

Note the crossovers of the curves just before 125°C. This behavior is possibly caused by the higher influence of viscous fluid properties of polymers at temperatures much higher than their glass transition temperatures. Since there is more influence from the damping properties of the material, more of the stress is relaxing out of the material before the holding phase begins. Because larger strains (at the same strain rate) are loaded for a longer period of time, it is possible that so much stress has relaxed out by the end of the loading period that there is less total stress in the system than expected. Since there is less stress in the system, it will not relax out as rapidly.

To further investigate this behavior, I added two more temperatures for testing, 95°C and 135°C. Before this testing, it was difficult to predict the behavior at higher temperatures—whether the curves would switch back, or continue to diverge, or just continue to converge. Figure 19 shows the temperature dependence, with 95°C and 135°C added.

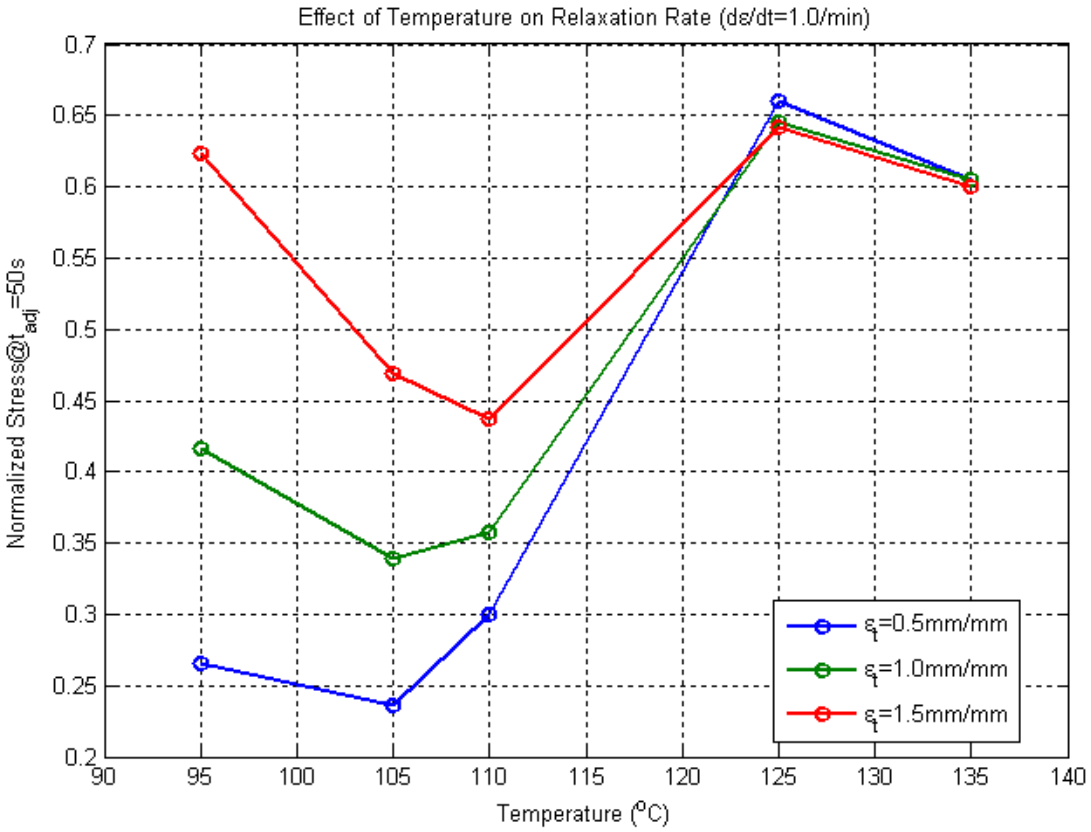

Figure 19: Relaxation left in the system for each system: dependence over five temperatures

The important behavior at higher temperatures appears to be the convergence of the relaxation rate at different total strains. For the same strain rate at higher temperatures, the rate of relaxation seems to be almost the same regardless of the total strain put into the system. It is also interesting that the relaxation rate for the same loading profile does not simply increase or decrease as temperature is raised, but rather increases in speed, then decreases, then increases again. This is a good indicator of the complex nonlinear, temperature-dependent viscoelastic behavior of the polymer.

3.3.2 Strain Rate Dependence

I also plotted this 50 second relaxation rate indicator values over the two loading strain rates tested. Figure 20 shows this dependence.

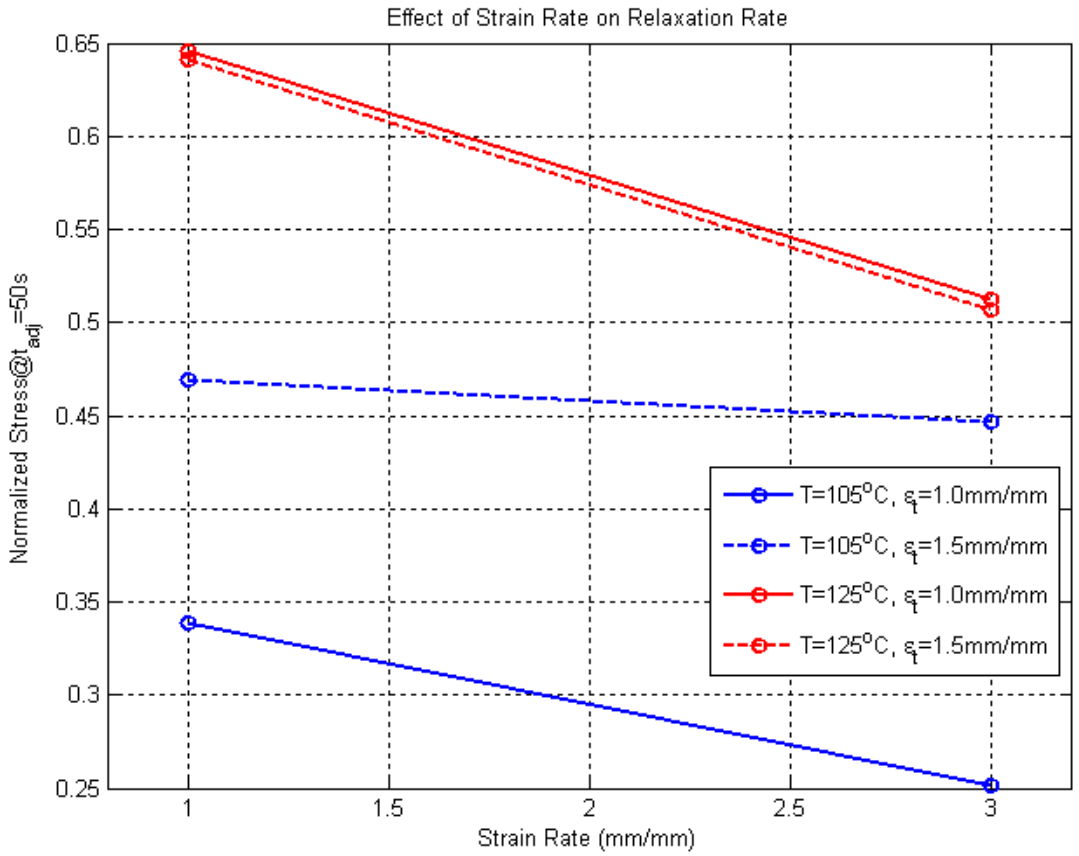

Figure 20: Effect of loading strain rate on relaxation rate

I only tested samples at two different strain rates, and only have complete strain rate comparison data for two temperatures, but behavior based on the limited data appears consistent. For each set of parameters compared here, the relaxation rate seems to increase with increased strain rate, as for the 3.0/min case there is less residual stress in the system at 50 seconds into the holding period. More testing would be necessary to see if this trend continues in this fashion at higher or lower strain rates.

3.3.3 Total Strain Dependence

Finally, I plotted the 50 second relaxation rate indicator values over the total holding strain. Figure 21 shows this dependence.

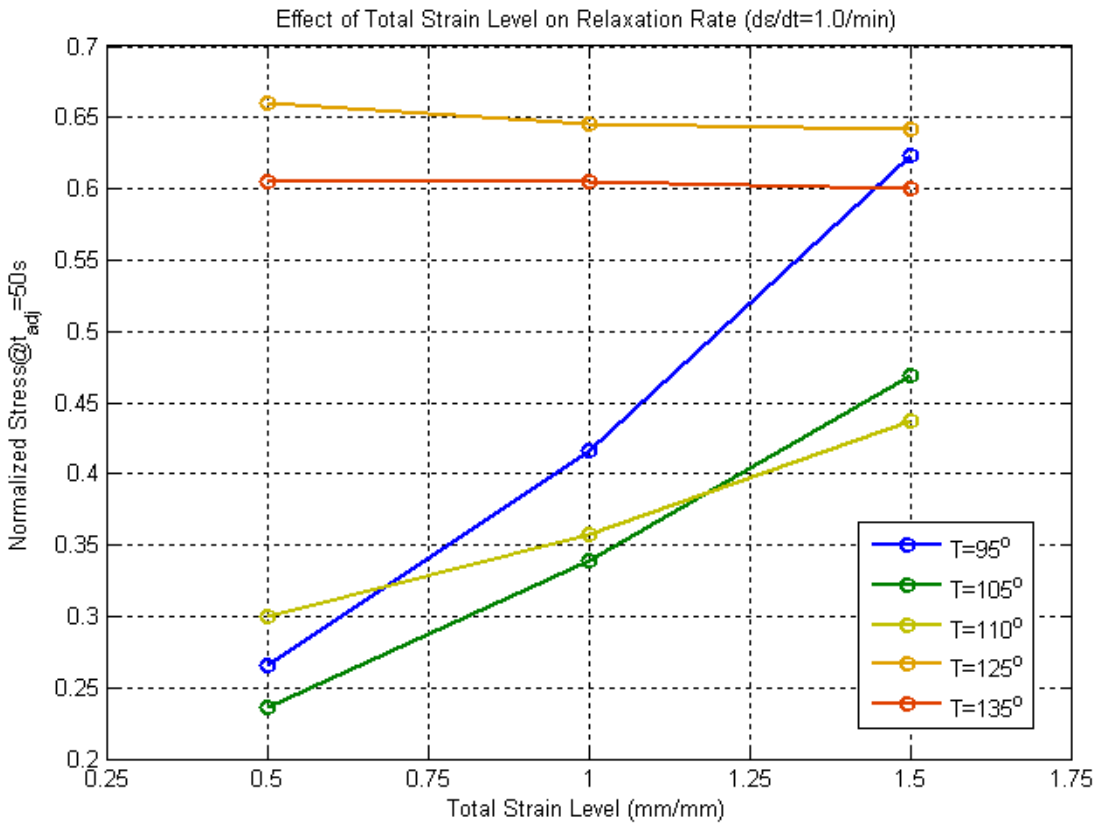

Figure 21: Effect of total strain level on relaxation rate (at a strain rate of 1.0/min)

The samples' relaxation rate dependence on total strain level varies vastly by temperature. This plot is another way of seeing the behavior described in section 3.3.1. Here, it is easier to see how the relaxation rate at cooler temperatures depends greatly on the total strain, while at warmer temperatures the relaxation rate does not depend much on total strain at all, and how the dependence is inverted.

3.4.0 Relaxation Modulus

Relaxation modulus is a different way of plotting the stress data obtained from relaxation tests. It is created by dividing the stress curve by the total applied strain and plotting this data on a log time scale. For an ideal relaxation test, where the strain is instantaneously applied and the material behaves linearly, the relaxation modulus curve will not depend on the total strain. The equation for the modulus, E(t), is

$$E(t)=\sigma(t)/\varepsilon_o$$

where $\sigma(t)$ is the stress at any time and ε_o is the magnitude of the instantaneously applied strain (Ferry, 1980).

Because my tests were done with loading over time, I used a modified relaxation modulus, $E_m(t)$, created by dividing the relaxation data by the hold strain, so

$$E_m(t)= \sigma_h(t)/\varepsilon_{or}$$

where $\sigma_h(t)$ is the stress at any time during the holding period and ε_{or} is the magnitude of the ramp-applied strain during the holding period (the total strain level). This modified relaxation modulus varies with different strain rates. For a linear material, the modified relaxation moduli created under different loading conditions should converge after a time about 10 times the length of the loading period. However, the loading times for my tests were long, with holding periods of much less than 10 times the loading periods, so this behavior is difficult to confirm. But it is expected that this behavior would not occur, because the material has shown mostly nonlinear behavior at these strains. Figures 22-26 contain the modified relaxation modulus for each test conducted, grouped by the temperature at which the test was conducted.

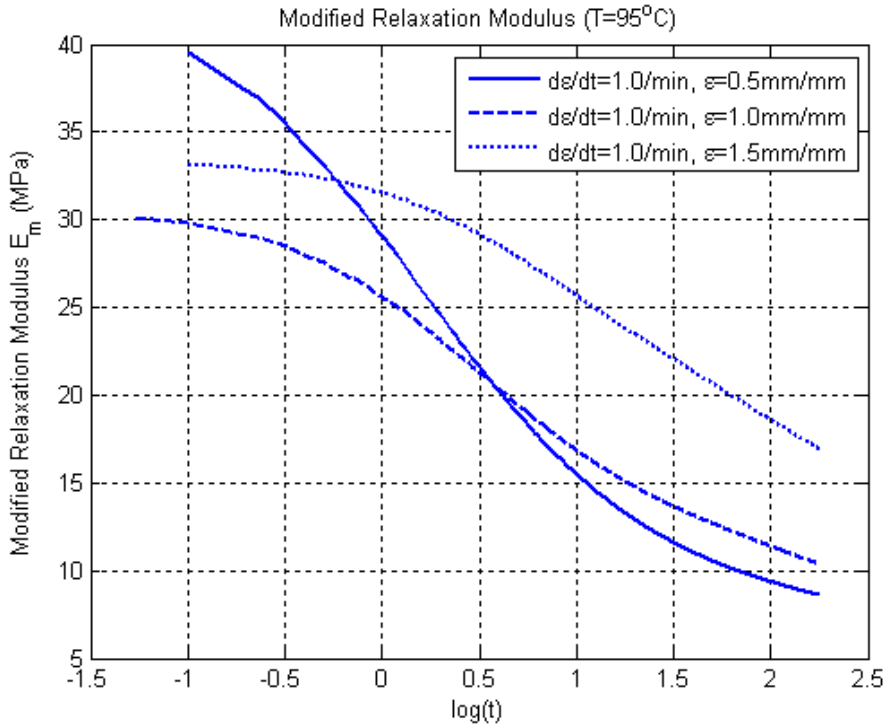

Figure 22: Modified relaxation moduli at 95°C

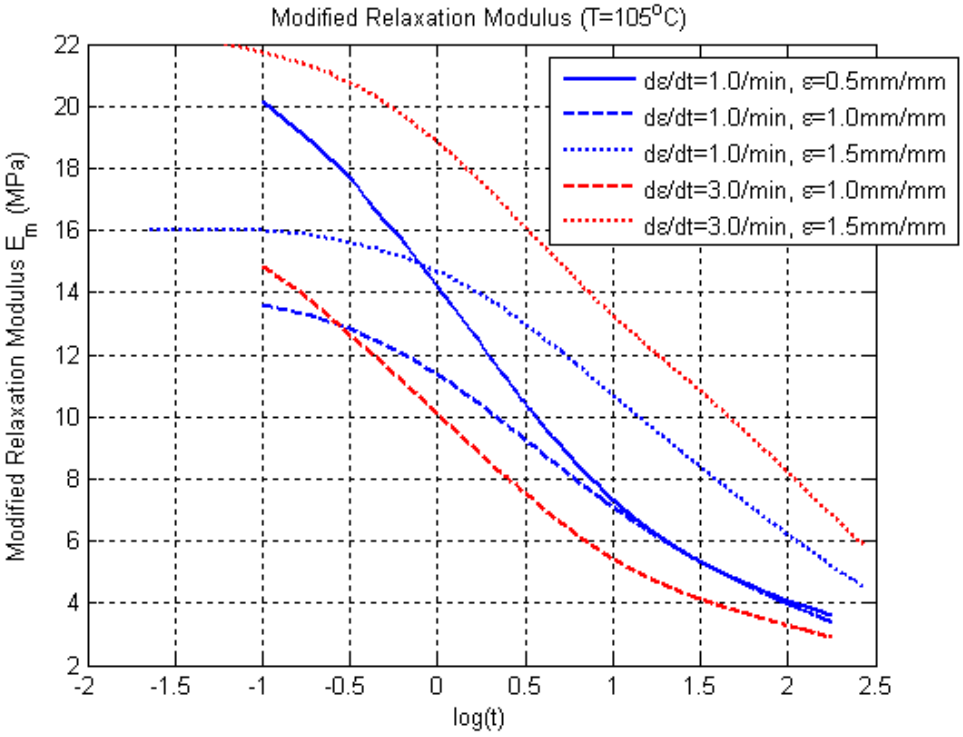

Figure 23: Modified relaxation moduli at 105°C

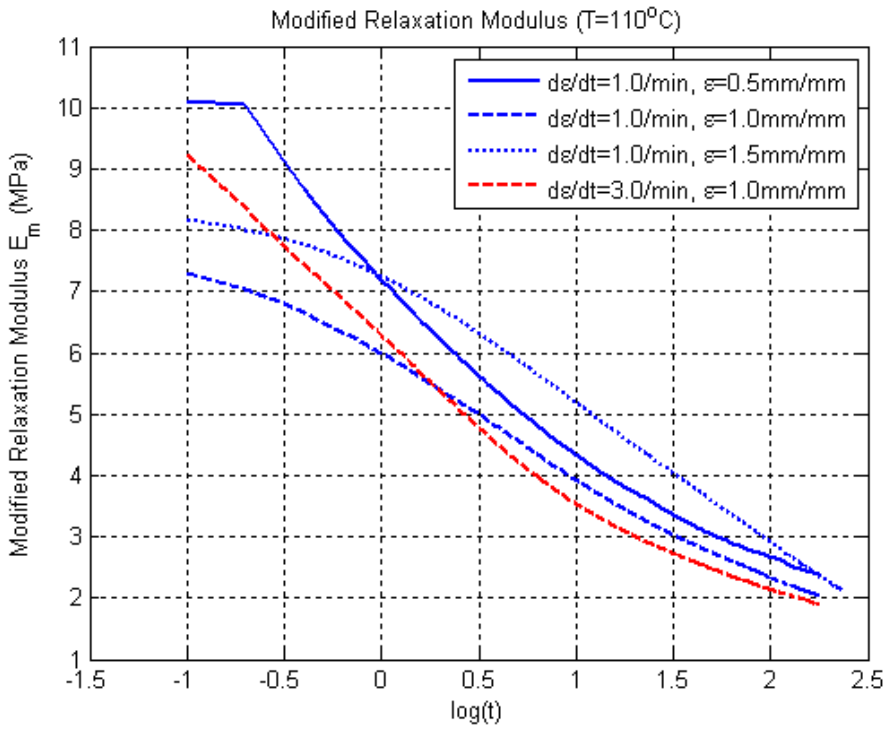

Figure 24: Modified relaxation moduli at 110°C

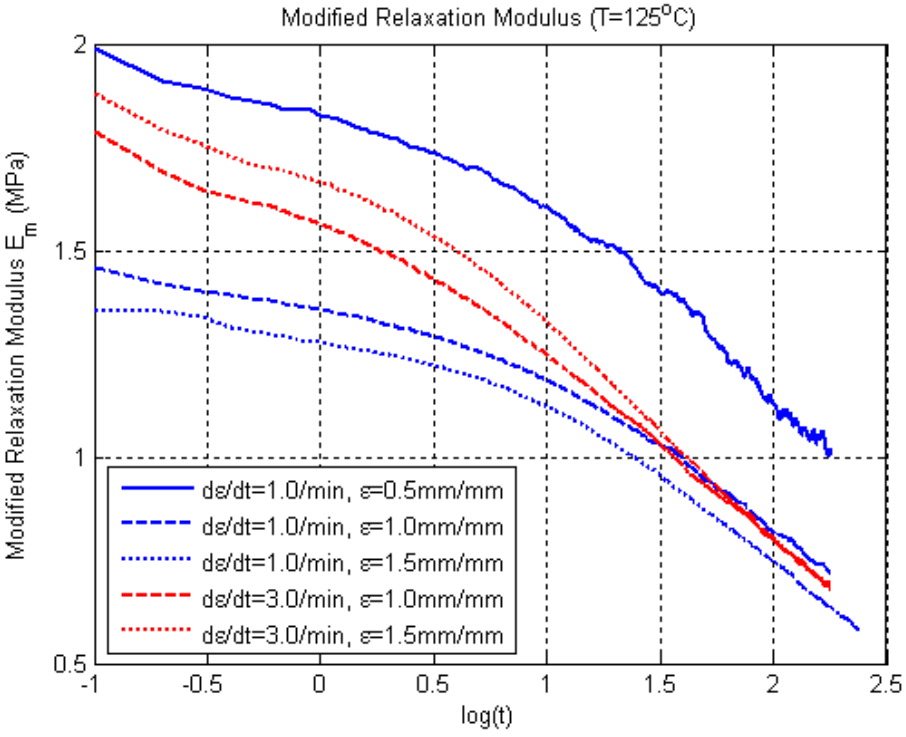

Figure 25: Modified relaxation moduli at 125°C

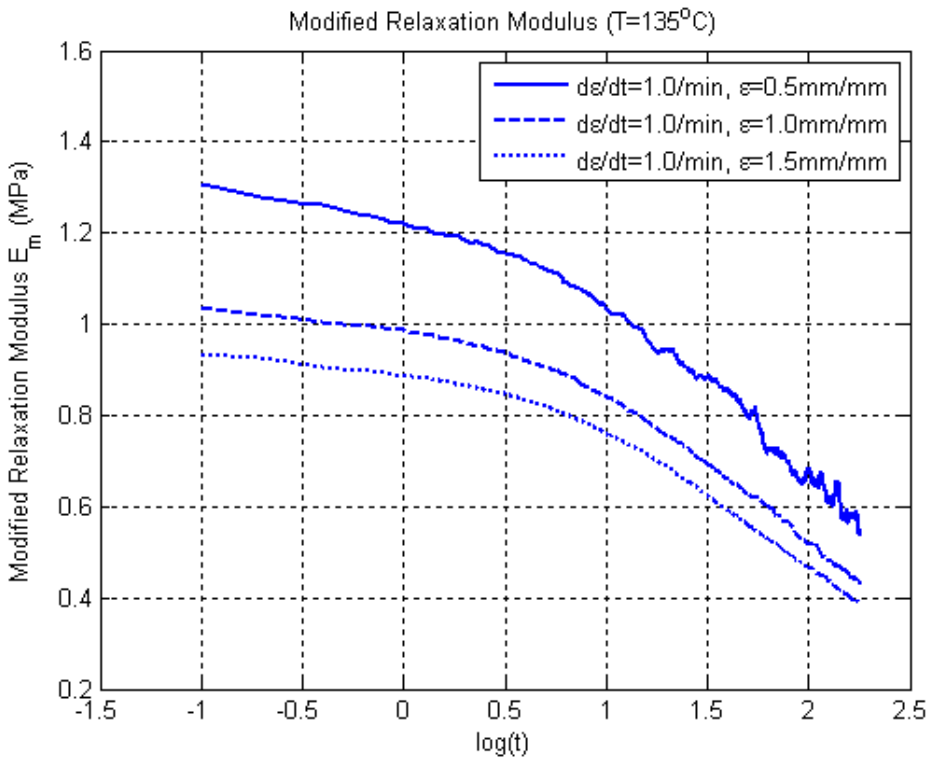

Figure 26: Modified relaxation moduli at 135°C

If the material were linear in behavior, the curves would, in general, look much more uniform in shape than they do. The moduli presented in Figure 26 are actually fairly uniform, indicating that the material behaviors more linearly at higher temperatures than at lower temperatures. This is consistent with our expectations.

Additionally, I compared the moduli for the same strain rate and total strain at each of the temperatures used. Figure 27 shows this comparison.

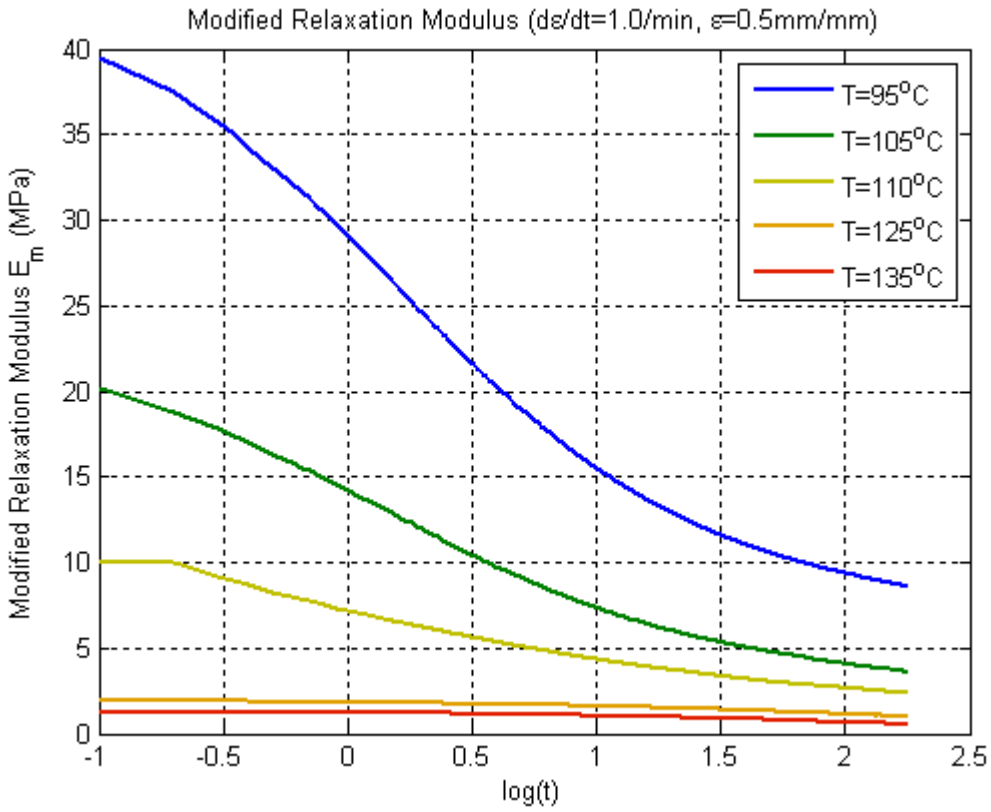

Figure 27: Modified relaxation moduli over five temperatures

This plot shows a fairly consistent time-temperature dependence for the relaxation modulus, which suggests the relaxation behavior over temperature may be linear. For a linearly temperature-dependent material, these curves should superimpose on one another when shifted horizontally, allowing for a single modulus to be described for a reference temperature (usually the glass transition temperature), with the modulus for any other temperature being obtainable by subtracting a log-scale shift factor, a_T, described in theory by the Williams-Landel-Ferry (WLF) equation:

$$a_T = \frac{-C_1(T - T_r)}{C_2 + T - T_r}$$

where T is any temperature, T_r is the reference temperature, and C_1 and C_2 are constants with $C_1 \approx 17.44$, and $C_2 \approx 51.6$ K when T_r is the glass transition temperature (Ebewele, 2000). Figure 28 shows time-temperature superposition for this data.

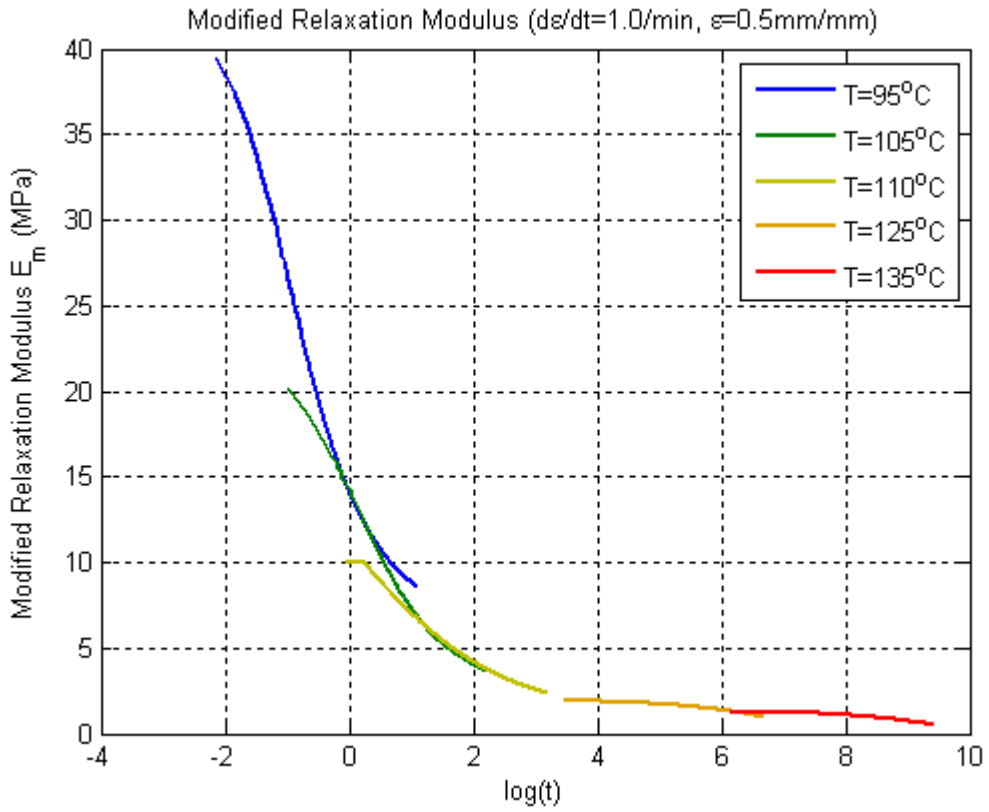

Figure 28: Time-temperature superposition

For this data, the curves are not perfectly superimposed on one another—there are distinct entrance and exit points for most temperatures. These could be caused by the ramped loading in my experiments or possibly by nonlinearities. However, the data does appear to roughly describe an overall modulus shape which could possibly be used a basis to help determine temperature dependence in the overall material model. The shift factors for this plot were determined by superimposing single points and by inspection, rather than using the WLF equation. Table 2 shows the time shift factors I used to create Figure 28, compared with the shift factors determined using the WLF equation, using 105°C as the reference temperature, as this is quite near the glass transition temperature for PMMA.

Table 2: Comparison of time-temperature superposition shift factors

Temperature (°C)	Shift Factors (log(sec))	
	Actual Factors Used	WLF Equation Factors
95	1.14	4.19
110	-0.951	-1.54
125	-4.45	-4.87
135	-7.51	-6.41

With the exception of the shift factor corresponding to 95°C, the WLF equation appears to be a good predictor for the actual shift factors necessary to superimpose the modified relaxation moduli for PMMA onto one another, particularly given that the actual factors used are estimations. Because the constants in the WLF equation are based on typical behavior of a large range of linearly temperature-dependent polymers, this indicates that, above T_g, PMMA exhibits temperature dependence quite typical of linear polymers. The very different shift factor value at 95°C is probably an indication that PMMA exhibits much more nonlinear behavior at temperatures below T_g.

Finally, in addition to the properties discussed in this section, the modified relaxation modulus can be used to help determine parameters for the generalized Maxwell model, which will be further explained in section 4.2.2.

4.0.0 Behavioral Modeling

While the current material model attempts to simulate the behavior of the material under a large range of loading conditions and temperatures, it is also useful to model the behavior of the individual samples.

4.1.0 Log curve fits

To show a very basic model of the individual samples' behaviors, I have fit logarithmic trendlines to the adjusted relaxation data. In Figures 29-31, the colored lines are the adjusted collected data, and the thin black lines overlaid on each are the trendlines, fitted using Microsoft Excel's "Add Trendline" function, which creates a least squares fit logarithmic trendline. The equation generated by this function is shown next to each trendline.

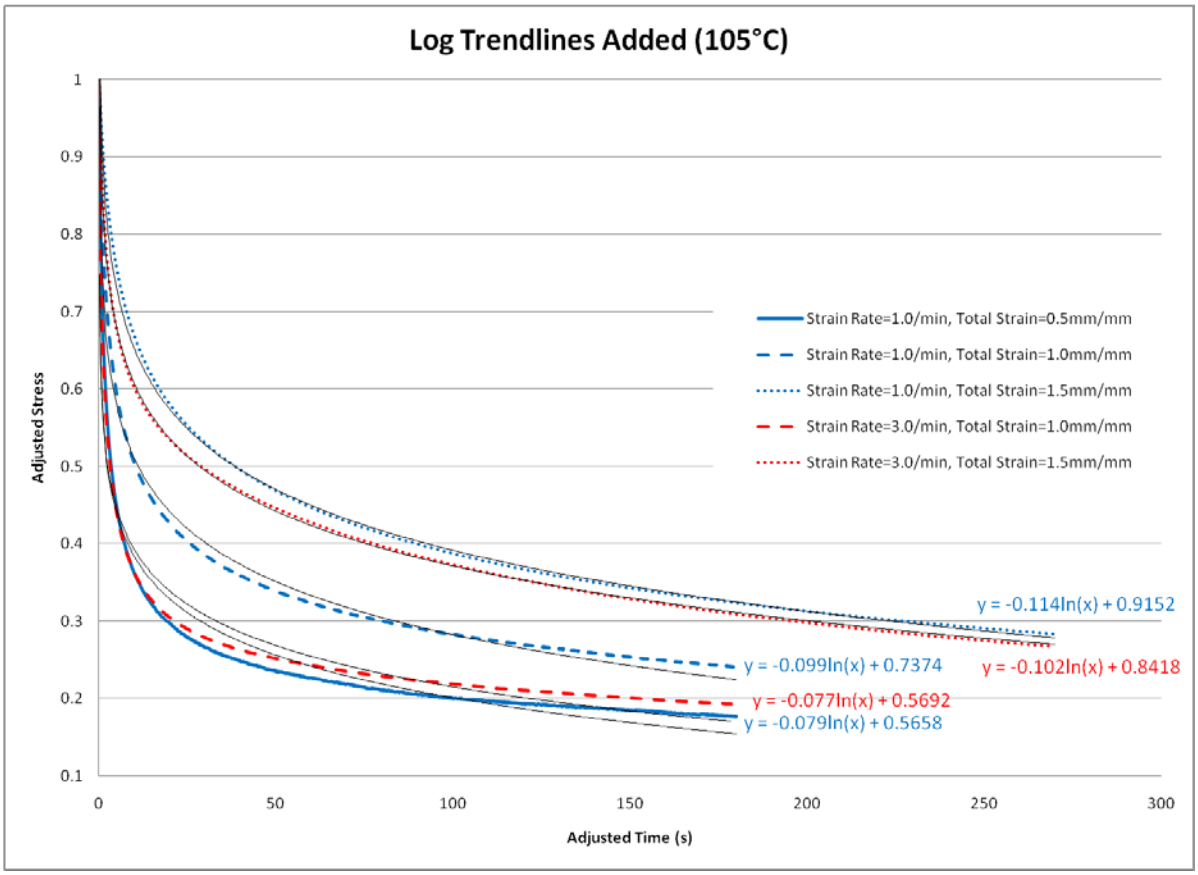

Figure 29: Logarithmic curve fits at 105°C

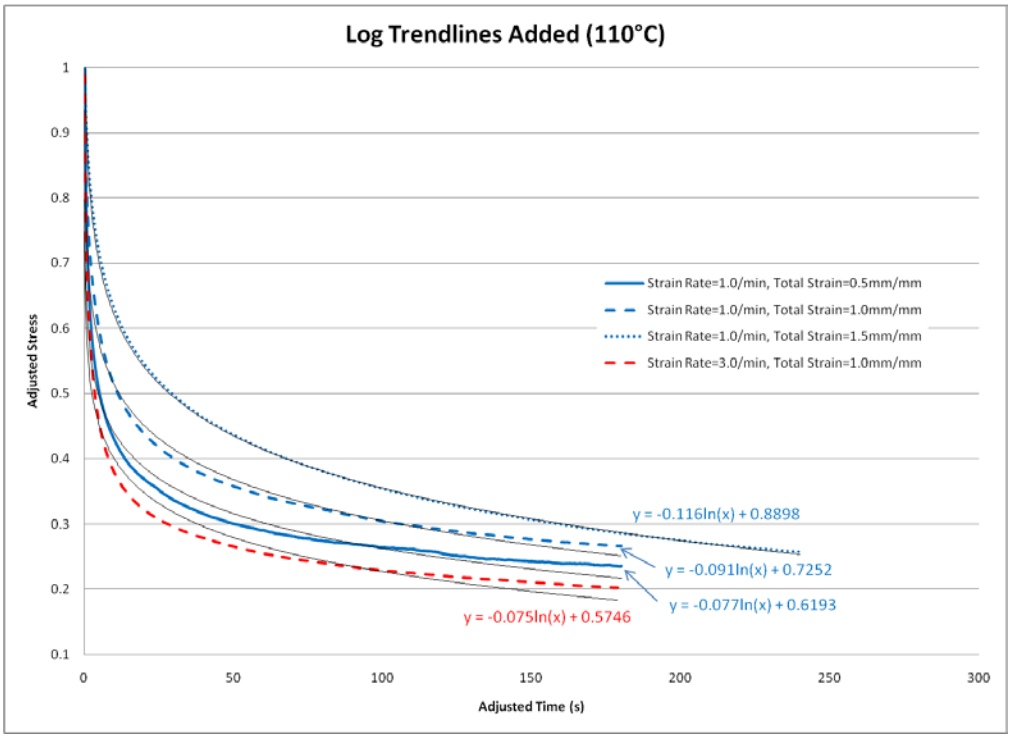

Figure 30: Logarithmic curve fits at 110°C

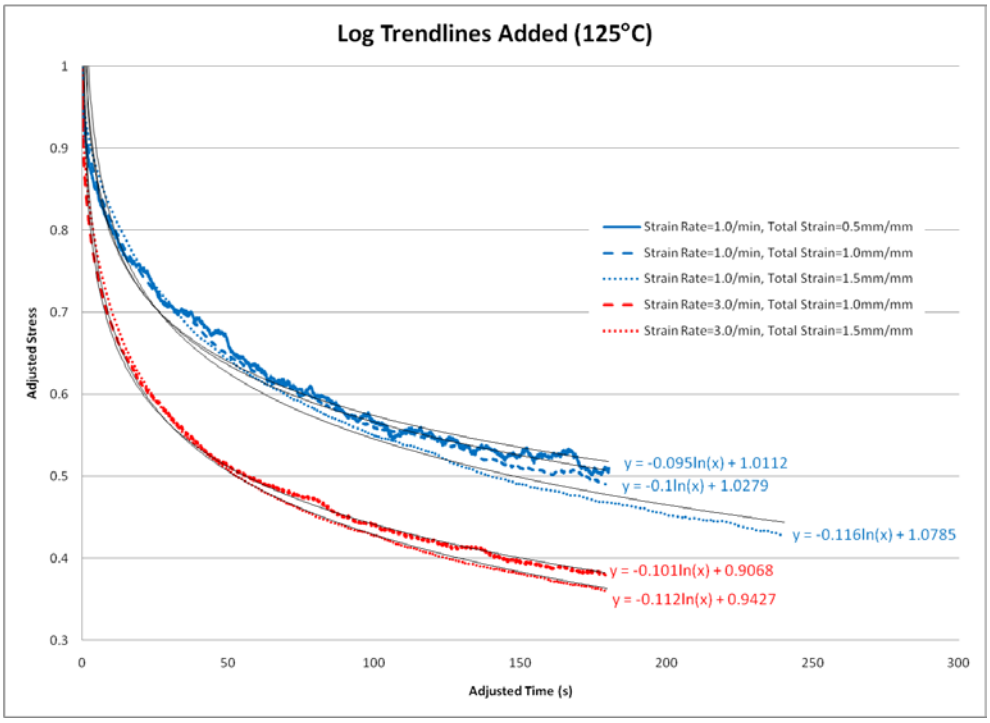

Figure 31: Logarithmic curve fits at 125°C

In general, these curves fit very well. This is unsurprising, as we expected the relaxation behavior of the material to be fairly logarithmic.

4.2.0 Maxwell model

The Maxwell model is a tool used to simulate the viscoelastic properties of polymers, and is generally used for simulations of stress relaxation. In its more basic form, the model consists of a spring and damper in series. In relaxation, the spring acts as the elastic part of the polymer's viscoelastic property, instantaneously deforming under a load and causing the resulting stress. The damper acts as the viscous fluid part of the viscoelasticity, slowly absorbing the stress caused by the deformation of the spring as the model is held under a simulated strain. For an instantaneously applied strain, the stress at any time t for this model is

$$\sigma(t) = E_m * \exp(-t\left(\frac{E_m}{\eta_m}\right))$$

where ε is the strain being applied to the model at time t, E_m is the spring constant, and η_m is the damper coefficient.

The generalized Maxwell model is a set of two or more spring-damper systems in parallel. For solids, the damper coefficient of the first set is generally set to infinity, leaving just the spring for that set alone, with the spring constant set to the limit of the relaxation modulus. For an instantaneously applied strain, the stress at any time t for this model is

$$\sigma(t) = E_\infty + \Sigma\left[E_{mi} * \exp(-\frac{t}{\tau_i})\right]$$

where E_∞ is the limit of the relaxation modulus, E_i is the spring constant for the i^{th} spring-damper system, and τ_i is η_i/E_i where η_i is the damper coefficient for the i^{th} spring-damper system. Figure 32 shows a schematic of a generalized Maxwell model.

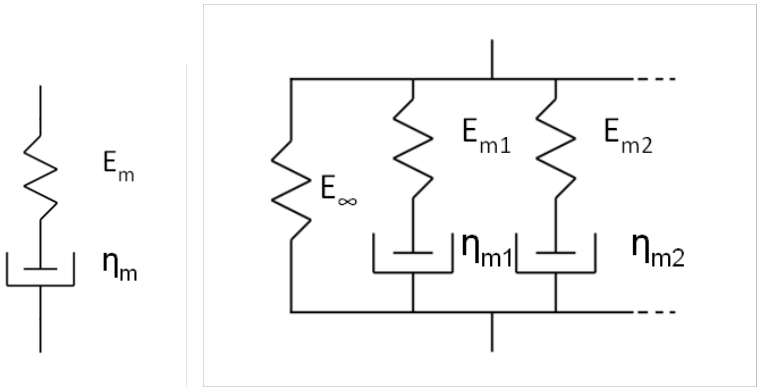

Figure 32: Maxwell model schematics: simple (left) and generalized (right)

4.2.1 Simple Maxwell

A single spring-damper system is the easiest to model, but as I will show, it is difficult to fit to the gathered data. For the simple Maxwell model, the strain rate can be related to stress by the following differential equation:

$$\frac{d\varepsilon}{dt} = \left(\frac{d\sigma}{dt} \frac{1}{E_m} \right) + \frac{\sigma}{\eta_m}$$

Using this equation, I created a simulation using Simulink to simulate a ramp input on a simple spring-damper model. Figure 33 shows this model.

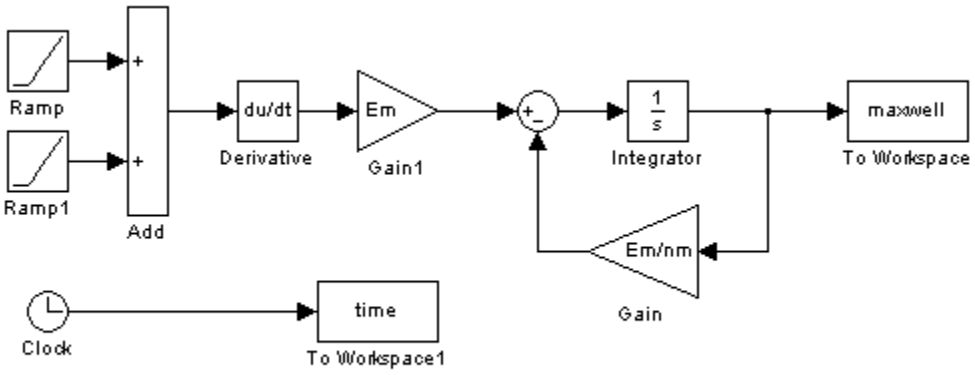

Figure 33: Simple Maxwell Simulink model

The model uses the strain profile as an input, created by two ramps, the first of which starts at t=0 and has a slope equal to the desired strain rate. The second ramp comes on after the desired total strain has been reached and has a negative slope equal to the strain rate, causing the input signal to hold constant. There are two variables, Em and nm, which correspond to E_m and η_m in the Maxwell differential equation. The output of the model is stress. If the model is valid, then with the correct input profile, the coefficients Em and nm should be able to be found to approximate the experimentally determined stress relaxation curve for that strain input.

However, this simple model cannot describe the actual behavior of the relaxation very well. Figures 34 and 35 show two different approaches to approximating the behavior of the material.

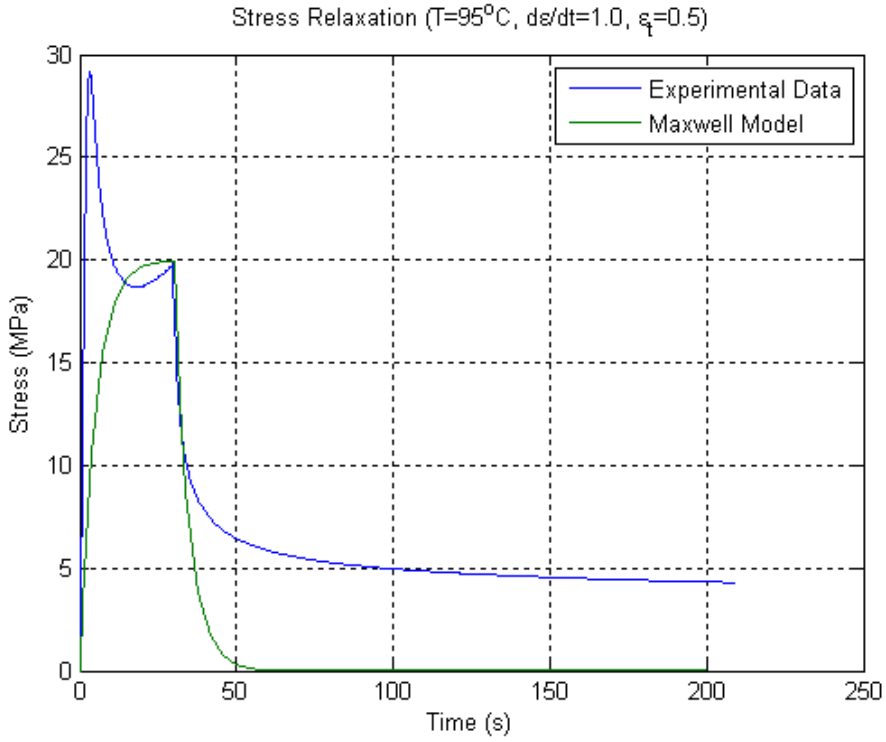

Figure 34: Simple Maxwell simulation: fit to initial slope (E_m=250, η_m=1200)

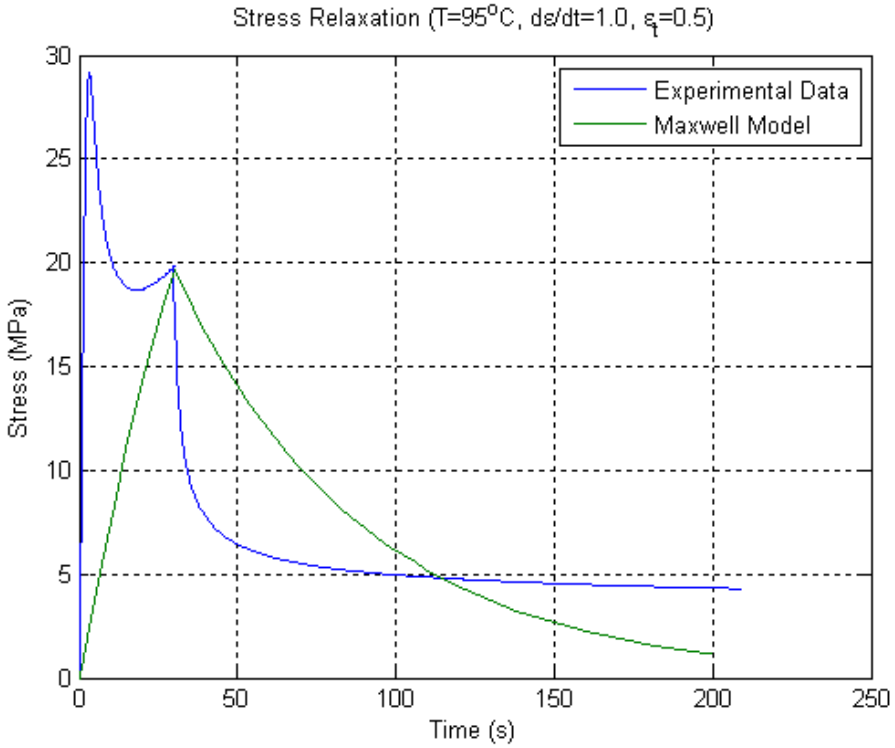

Figure 35: Simple Maxwell simulation: fit to an asymptotic limit (E_m=50, η_m=3000)

Both of these were modeled using the same strain profile, but with different values for Em and nm. The curve in Figure 34 does a decent job of approximating the initial slope of the relaxation portion of the collected data, but a poor job of representing the final value. The curve in Figure 35 attempts to approximate the final asymptotic behavior of the relaxation curve, but it does a poor job of representing the initial slope. Neither curve does very well with the data between the initial slope and the final asymptote.

Fortunately, this model can be improved with the addition of more spring-damper systems.

4.2.2 General Maxwell

With the addition of further sets of springs and dampers, more coefficients must be determined to ensure good fit of the model to the collected data. Assuming that the first η_m term has been set to infinity, with E_∞ corresponding to the steady state stress value of the relaxation curve, the differential equation for this more generalized model looks like:

$$\frac{d\varepsilon}{dt} = \left(\frac{d\sigma}{dt} \frac{1}{E_\infty} \right) + \Sigma \left[\left(\frac{d\sigma}{dt} \frac{1}{E_{mi}} \right) + \frac{\sigma}{\eta_{mi}} \right]$$

To fit each constant E_{mi} to the curve for the sample tested at T=95°C, dε/dt=1.0, and ε=0.5, I used a collocation method described in (Ferry,1980) wherein each spring-damper pair is fit to a representative point along the relaxation modulus. I used the modified relaxation modulus plot described in section 3.4.0, specific to these parameters, to determine the number of decades that the bulk of the relaxation actually spans. For this case, the relaxation spans about three decades, so 4 points were used, plus an initial 5th point. So, I picked the collocation times spaced one decade in time apart, picking the cases from the relaxation modulus data at t_{ci}=[0, 0.1,1,10, 100] . The modified modulus values corresponding to the collocation times are called $E_{Rm}(t_{ci})$. Because log 0 is undefined, $E_{Rm}(t_{c1})$ was simply picked as the initial

value. The values for $\tau_i=\eta_{mi}/E_{mi}$ are then picked to be $2t_{ci}$ or [0.002, 0.2, 2, 20, 200]. Because τ may not be zero, τ_1 was chosen as $0.1*\tau_2$. The spring constant values, E_i, were determined using

$$[A][E]=[E_{Rm}(t_c)-E_{Rm\infty}]$$

Where [A] is an nXn matrix (n being the number of collocation times chosen) where $A_{ji}=e^{-tj/\tau i}$, [E] is a nX1 matrix, to be determined, consisting of the values of E_i, and $[E_{Rm}(t_c)-E_{Rm\infty}]$ is a nX1 matrix consisting of the values of $E_{Rm}(t_{ci})-E_{Rm\infty}$, with $E_{Rm\infty}$ being defined as the steady state value of the modified relaxation modulus.

This method of choosing parameters yields the curve fit seen in Figure 36.

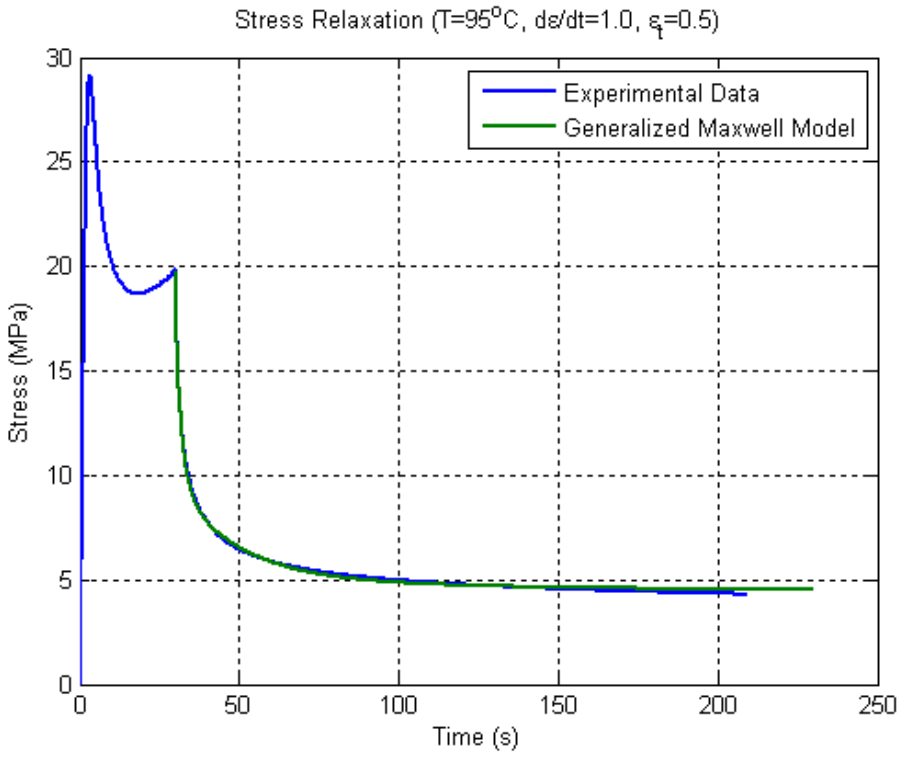

Figure 36: Generalized Maxwell model curve fit

This curve fits the data quite well. However, this model is acting as though the material has been instantaneously strained, but this is not the case. Using an expanded version of the previous Simulink simulation (Previous model: Figure 33; expanded model: Figure 37), I applied a ramp input to the model using the coefficients determined for the curve fit in Figure 36. Figure 38 gives a comparison of this model with the corresponding experimental data.

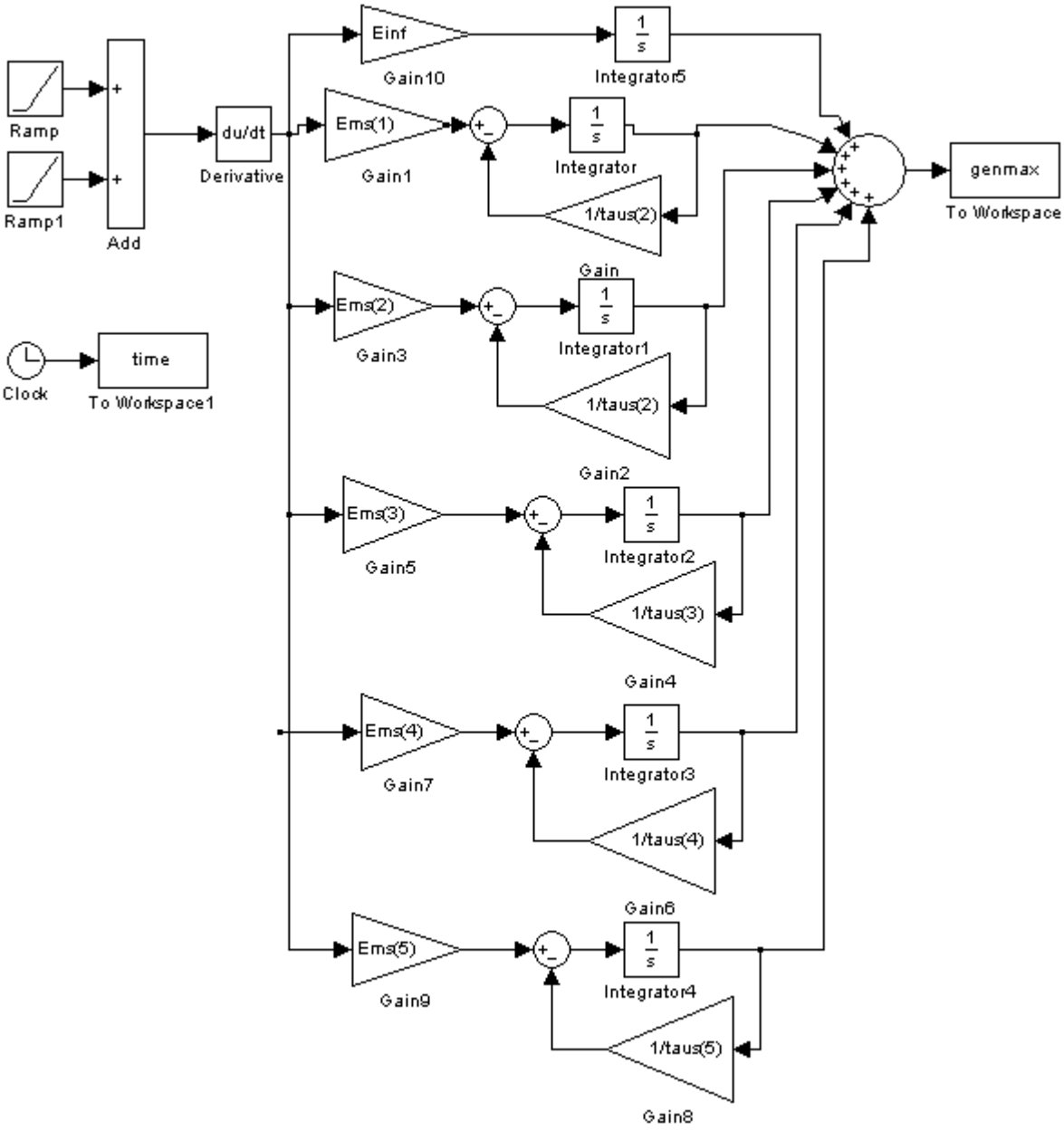

Figure 37: Expanded Simulink model

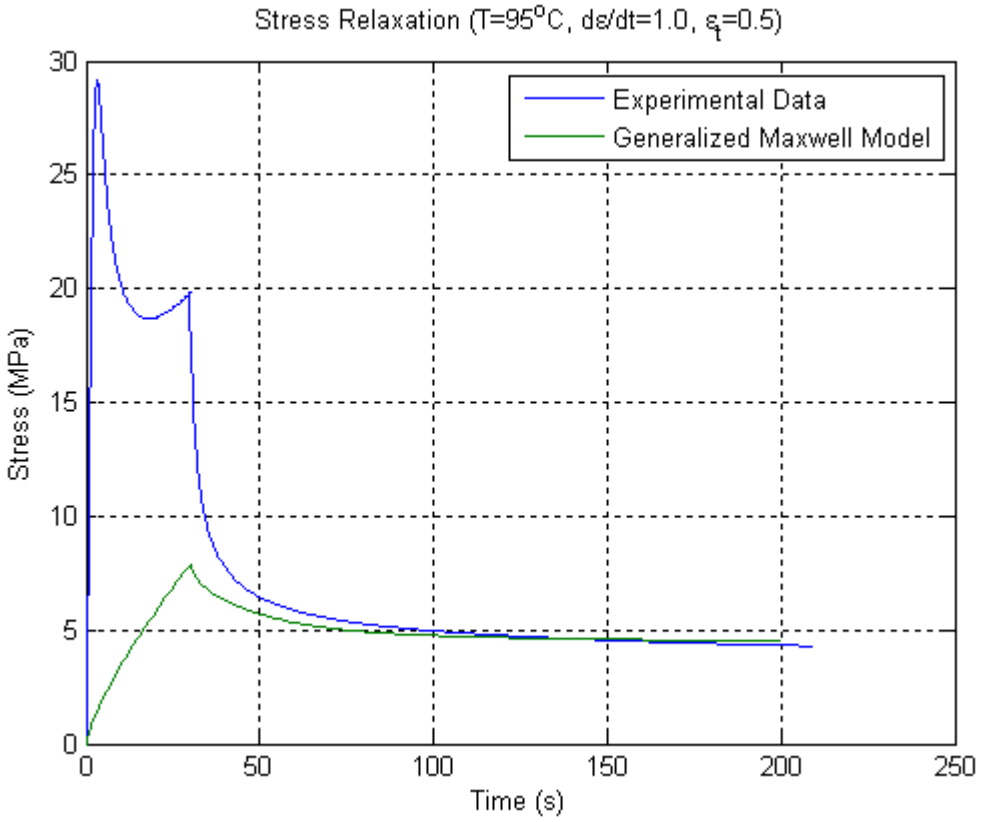

Figure 38: Maxwell model simulation with ramp input

The curve clearly does not fit the first part of the experimental data well—it significantly underpredicts the maximum stress value, so the simulation's relaxation curve begins much too low, though it seems to converge after about 100 seconds. A likely explanation for this behavior is that the time-dependent dampers begin absorbing stress from the instantaneous springs during the loading period, much more than the actual viscous fluid behavior of the polymer would absorb stress during the loading period. The convergence with the later part of the data shows that it is modeling the non time-dependent behavior well. This plot suggests that a model with nonlinear time-dependant damping is more ideal for capturing the behavior of the polymer.

For another comparison, I ran the simulation with the same spring and damper constants, but a different strain input, and compared this simulation with the experimental data at these parameters at the same temperature. In theory, if the material were completely linear, the same linear model could be run with a different input, and the resulting curve would match similarly well with the experimental curve for that input. An example of this simulation is shown in Figure 39. In this case I have compared a simulation designed for the (T=95°C, dε/dt=1.0, ε=0.5) case with the (T=95°C, dε/dt=1.0, ε=1.5) case.

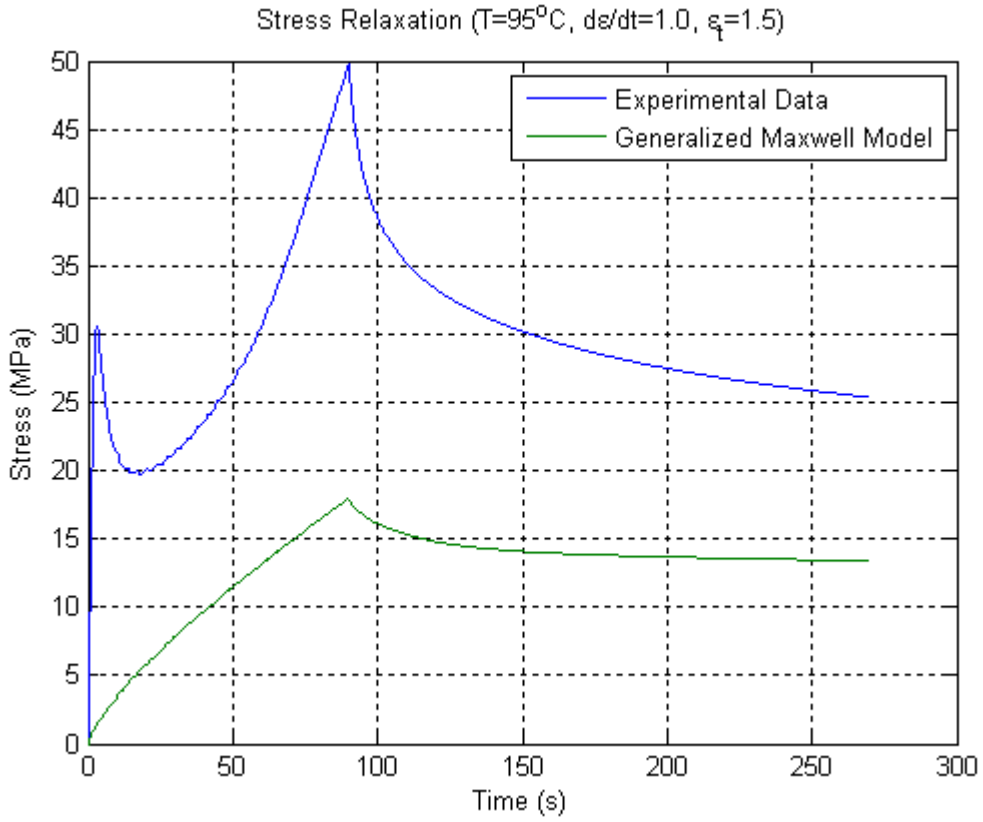

Figure 39: Experimental data compared to a simulation using coefficients fit to a different sample

The model here does not match up nearly as well with the experimental curve as it did with the curve for which it was created. This indicates that the Maxwell model is not a very good predictor of the material behavior overall. The model is meant for instantaneously applied small strains, so the fact that it does not work well is as expected.

5.0.0 Current Material Model

The material model used for this project, the Dupaix-Boyce model, has been used to capture stress-strain loading behavior from temperatures near T_g up to 130°C (Palm et al.,2006 & Ghatak, 2007). Some of these comparisons can be seen in Figures 40 and 41, from (Ghatak 2007). The model does an excellent job of capturing this behavior near the glass transition temperature.

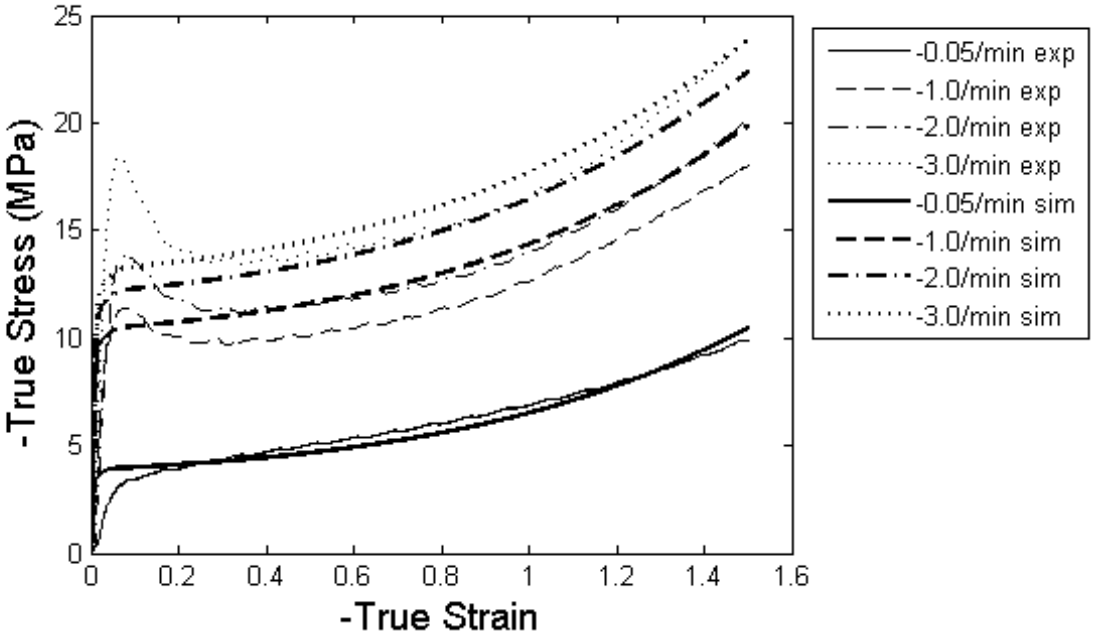

Figure 40: Experimental and simulation results for uniaxial compression tests at 102°C. (Ghatak, 2007)

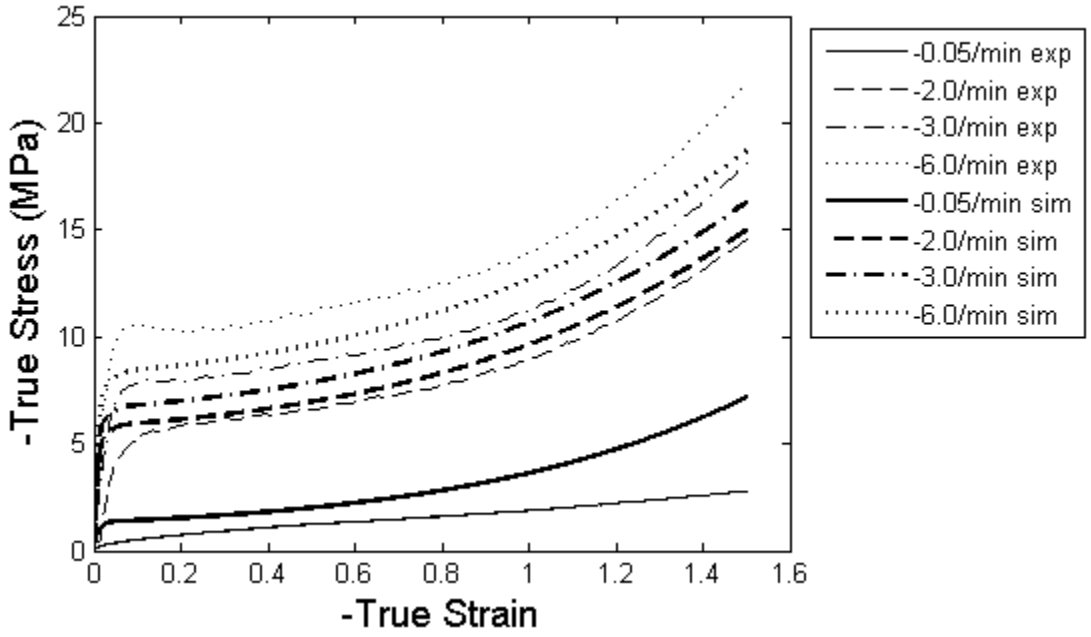

Figure 41: Experimental and simulation results for uniaxial compression tests at 110°C. (Ghatak, 2007)

Unlike the Maxwell model, the Dupaix-Boyce model is specific to PMMA, and includes nonlinear elements which allow it to better capture the loading period of the stress-time curves, and to better predict the material's behavioral dependence on temperature and loading conditions. Figure 42 shows a more detailed schematic of the model.

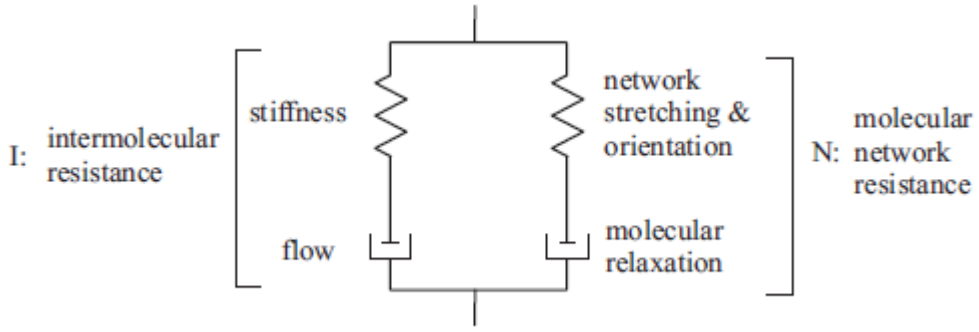

Figure 42: Schematic of the Dupaix-Boyce model

The model has two branches, the intermolecular (I) and network (N), where the total stress is equal to the sum of the stress in each branch: $T=T_I+T_N$, and the total force is equal to the force in each branch: $F=F_I=F_N$. Some brief constitutive equations follow:

$$\mathbf{T}_I = \frac{1}{J_I} C^e \left[\ln \mathbf{V}_I^e \right] \qquad \mathbf{T}_N = \frac{1}{J_N} \frac{\nu k\theta}{3} \frac{\sqrt{N}}{\bar{\lambda}_N} L^{-1}\left(\frac{\bar{\lambda}_N}{\sqrt{N}} \right) \left[\bar{\mathbf{B}}_N^e - \left(\bar{\lambda}_N \right)^2 \mathbf{I} \right]$$

These two equations describe the springs in the I branch and N branch, respectively. Because the T terms in both equations refer to stress, and the V_I and λ_N terms refer to strain, it can be seen how these spring equations relate the stress output to the strain input.

$$\dot{\gamma}_I^p = \dot{\gamma}_{0I} \exp\left[-\frac{\Delta G_I \left(1 - \tau_I / s_I \right)}{k\theta} \right] \qquad \dot{\gamma}_N^p = C \left(\frac{\alpha / \alpha_c - 1}{\alpha_0 / \alpha_c - 1} \right) \left(\frac{\alpha}{\alpha_c} \frac{\tau_N}{\nu k\theta} \right)^{1/n}$$

These two equations refer to the dampers in the I branch and N branch, respectively. Because the γ^p-dot terms in both equations refer to the strain rate, and the τ terms refer to stress, it can be seen how these damper equations relate the strain rate input to the stress output.

A more in-depth but brief explanation is given by Ghatak (2007) and a much more detailed explanation of the model is given by Dupaix and Boyce (2007).

There are 15 constants used in this model, a brief description of each and their current values can be found in Table 3.

Table 3: Material constants for the Dupaix-Boyce material model (Ghatak, 2007)

	Material Property	Symbol	Value
Initial Elastic Behavior	Glassy Modulus	μ_g	325 MPa
	Rubbery Modulus	μ_r	50 MPa
	Temperature Shift	$\Delta\theta$	30 K
	Transition Slope	X_g	-3 KPa/K
	Rate Shift Factor	ξ	3 K
	Glassy Bulk Modulus	B_g	1.0 GPa
	Rubbery Bulk Modulus	B_r	2.25 GPa
Flow Stress	Pre-exponential Factor	$\dot{\gamma}_{0I}$	7.5×10^{13} 1/s
	Activation Energy	ΔG	2.12×10^{-19} J
Resistance Elasticity	Rubbery Orientation Modulus	$\nu k\theta$	8.0 MPa
	Entanglement Density	N	500
Molecular Relaxation	Temperature Coefficient	D	1.7×10^{4} 1/s
	Second Temperature Parameter	Q/R	1.42×10^{7} K
	Power-law Exponent	$1/n$	6.67
	Cutoff Orientation	α_c	0.0012

5.1.0 Comparisons with the Model

The goal of the stress relaxation experiments I have carried out on PMMA was to compare the behavior I observed with Dr. Dupaix's material model and see how well the model is predicting this behavior. This section outlines these comparisons.

Near the glass transition temperature is where the model simulates material behavior best. Figure 43 shows comparison at 105°C, a temperature right at the glass transition temperature range.

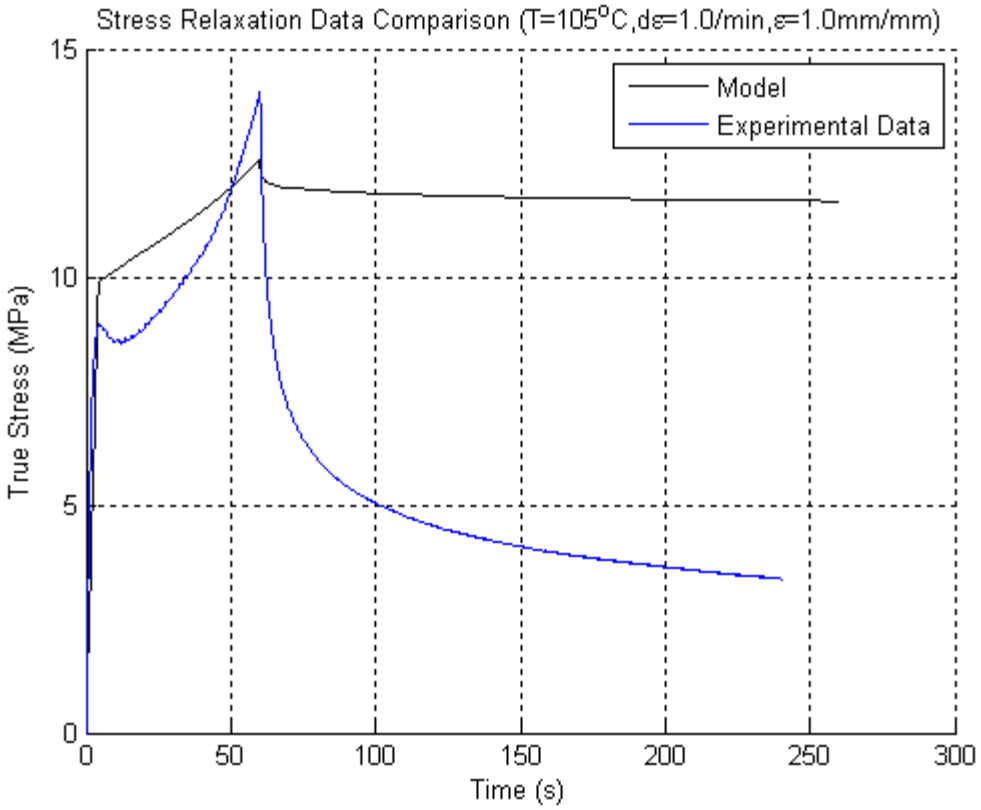

Figure 43: Stress-time data comparison with the material model

The model predicts the behavior of the curve fairly well before the relaxation portion, with the yield point and maximum stress being quite close to the corresponding points on the experimental curve. However, the model does not predict nearly enough relaxation to match the experimental behavior.

At temperatures lower than the glass transition temperature, the model is significantly underpredicting the loading portion of the stress-time curve. Again, the model does not predict enough relaxation. Figure 44 shows an example of a lower-temperature simulation.

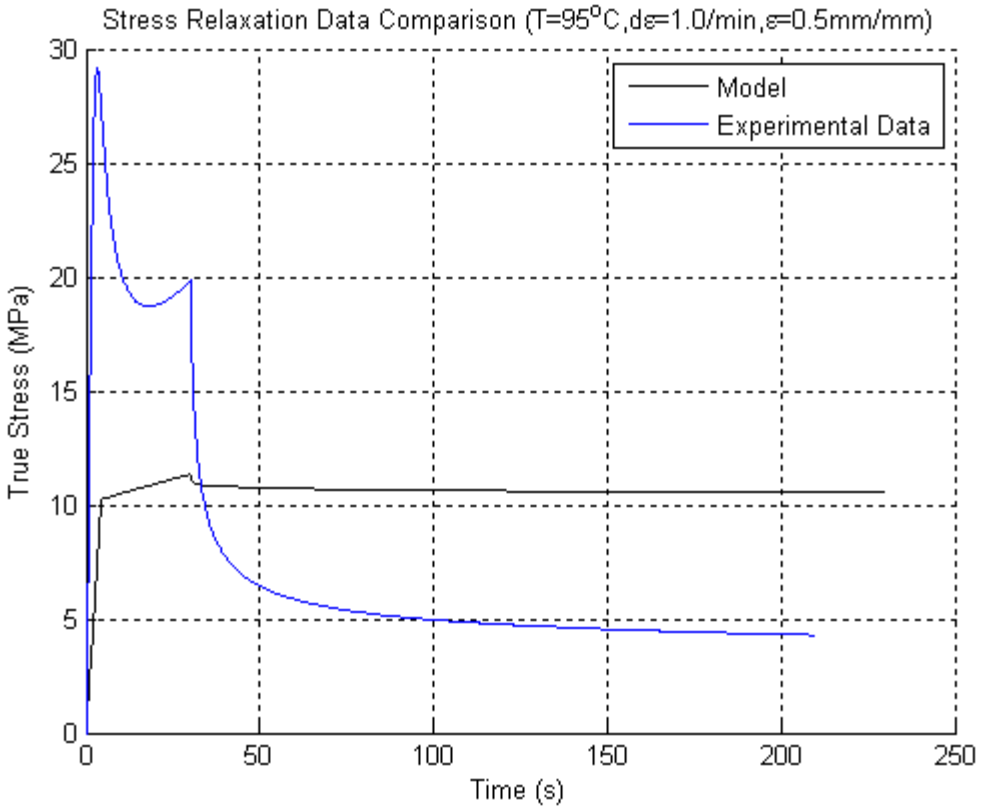

Figure 44: Comparison with the model at 95°C

At temperatures much higher than the glass transition temperature, the model is significantly overpredicting the entire stress-time curve. Figure 45 shows an example of a higher-temperature simulation.

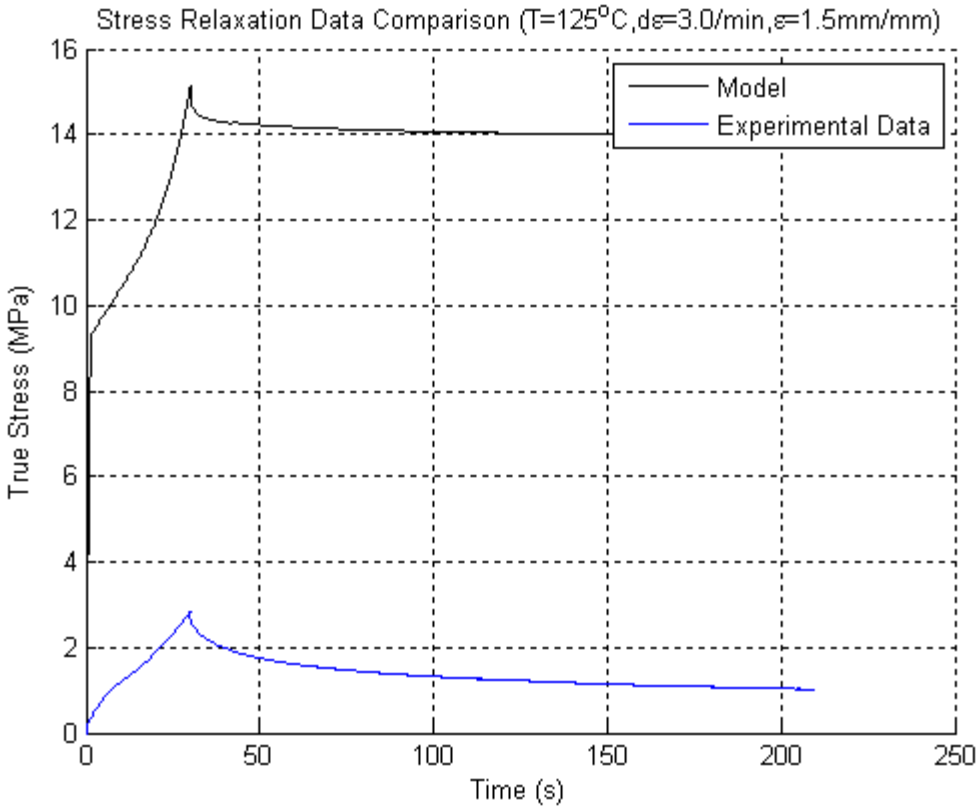

Figure 45: Comparison with the model at 125°C

However, for some simulations at higher temperatures, the amount of relaxation in the system actually appears to be roughly correct. This is likely because the model is predicting too much stress in the overall system, and so the percentage of relaxation of the total system stress is still much too low.

Simulations of all the tests I performed, along with the corresponding experimental data, can be found in Appendix B.

6.0.0 Conclusions from Results

Most of the general characteristics of the material's stress-time behavior were similar to what was expected for polymer large-strain relaxation tests. In particular, the general changes in behavior based on variation of my three test parameters were not unexpected. However, as we previously did not have quantifiable relaxation data for PMMA at large strains, the data from these tests will be useful in editing the material model for better predictions of the specific behavior of PMMA over complex loading conditions.

There were also some fairly unexpected results gathered from these tests. The testing turned out to be highly repeatable, possibly more so than originally expected, so we know that the relaxation behavior is nicely predictable given the right model. Additionally, the temperature dependence was found to be more linear than originally expected for temperatures above T_g. And for higher temperatures, the effect of relaxation during the loading period was higher than originally expected. For applications of PMMA involving hot-embossing at temperatures well above T_g, these high-temperature behaviors could be very important to know about and be able to predict.

The behavioral modeling of the material yielded some interesting results. Logarithmic curve fits of the adjusted relaxation curves described the behavior very well. The simple Maxwell model did not work as well as I had hoped, but this is not unexpected, due to the assumptions inherent to the model. The generalized Maxwell model fit the curve much better, and was even somewhat representative of the actual behavior with ramped loading conditions applied to a simulation of the model. It was as expected, however, that the same set of parameters did not describe the material as well under different loading conditions.

Finally, I found that the current material model does not simulate stress relaxation well. In general, it is not showing enough relaxation. When using a material model to determine mold geometry and procedure in hot embossing, underprediction of stress relaxation could lead to incorrect prediction of

springback in the part. This would lead to mold geometries that seem like they will produce the desired surface profile, but actually produce an incorrect profile because the springback was not well predicted. Better prediction of springback will allow for less trial and error in the mold design procedure, saving time and money. The relaxation aspect of the material behavior also helps determine how much residual stress will remain in the embossed part. Because these residual stresses can cause the material to look "foggy" rather than completely clear, as PMMA normally is, understanding the level of stress left in the part could be important for parts which need to be perfectly clear after embossing.

7.0.0 Future Work

Over the course of my project, much possible work for the future has arisen. A large amount of work could be done in some systematic editing of the material model, so that it continues to represent the behavior of the material during loading at temperatures near T_g, while improving its representation of the material during constant-strain holding. Possibly, in addition to just editing the constants already present in the model, the molecular-network-side damper may be of more use if its contribution to the model is significantly redesigned. In its current state, its influence approaches zero after a certain amount of time into the loading period. A greater influence from this damper at later times could cause the relaxation portions of the simulations to drop lower and more closely reflect the behavior of the experimental results.

Additionally, there are more tests which could be carried out to verify the model's accuracy under different conditions, once it has been altered to better represent the data already collected, or to aid in these alterations. In particular, there may be some interesting behavior relating to the strain rate, but it is currently difficult to see trends in strain rate dependence behavior, since I only tested at two strain rates. It may also be useful to test at a few faster loading conditions with longer hold times, in order to confirm or reject the theoretical convergence of the modified relaxation modulus.

More testing temperatures between 110°C and 125°C may also be useful to more closely determine the point where the stress relaxation rate becomes directly rather than inversely proportional to the total strain input. Testing at more than one strain rate at 135°C could also help determine if the adjusted relaxation curves converge for different strain rates, as they do for different strain levels.

Another way of interpreting relaxation rate, which may also be useful, would be to determine the time at which a sample begins to level off (i.e. a settling time) or the time at which the adjusted curves reach a given percent of stress (i.e. a time constant) rather than taking the percent of the stress at a given time. This may simply give similar dependence results as those obtained from looking at the 50 second relaxation rate values, or it could possibly give different insights into the behavior of the material under different conditions.

There is much interesting work left to be done in completely characterizing the stress relaxation behavior of PMMA at large strains. Hopefully, this project and subsequent work will be able to add to the all the material characterization work already done, and will help the PMMA material model better represent the polymer in this area.

References

Dupaix, R.B., Boyce, M.C., 2007, Constitutive modeling of the finite strain behavior of amorphous polymers in and above the glass transition, *Mechanics of Materials*, **39**: 38-52.

Ebewele,, R.O. “Polymer Science and Technology”, CRC Press, 2000.

Ferry, J.D., “Viscoelastic Properties of Polymers”, John Wiley and Sons, 1980.

Ghatak, A., Dupaix, R.B. “Material Characterization and Continuum Modeling of Poly(methyl methacrylate) (PMMA) for Hot Embossing Applications”, The Ohio State University, 2007.

Palm, G., Dupaix, R. B., and Castro, J., 2006, “Large Strain Mechanical Behavior of Poly(methyl methacrylate) (PMMA) Near the Glass Transition Temperature,” Journal of Engineering Materials and Technology, **128**, pp. 559-563.

Appendix A

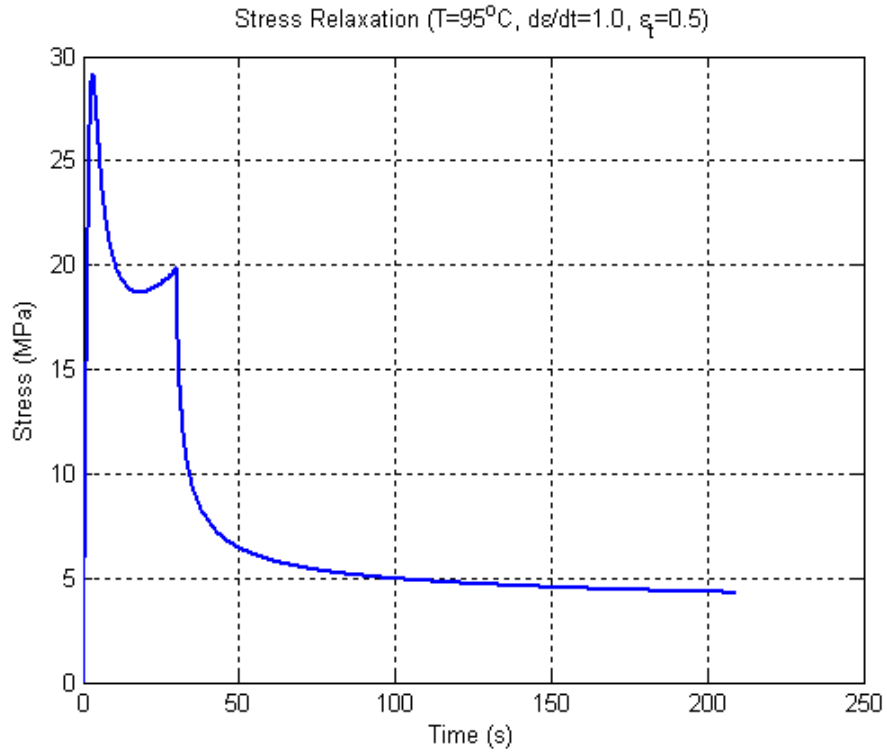
Stress Relaxation (T=95°C, dε/dt=1.0, ε_f=0.5)
Stress (MPa)
Time (s)
0
5
10
15
20
25
30
0
50
100
150
200
250

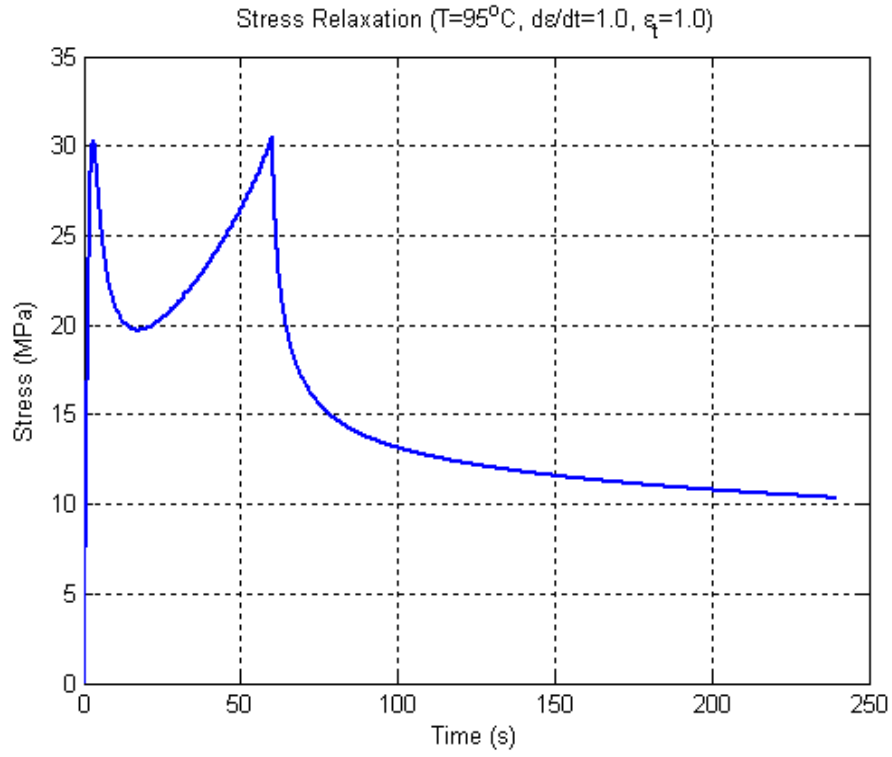
Stress Relaxation (T=95°C, dε/dt=1.0, ε_f=1.0)
Stress (MPa)
Time (s)
0
5
10
15
20
25
30
35
0
50
100
150
200
250

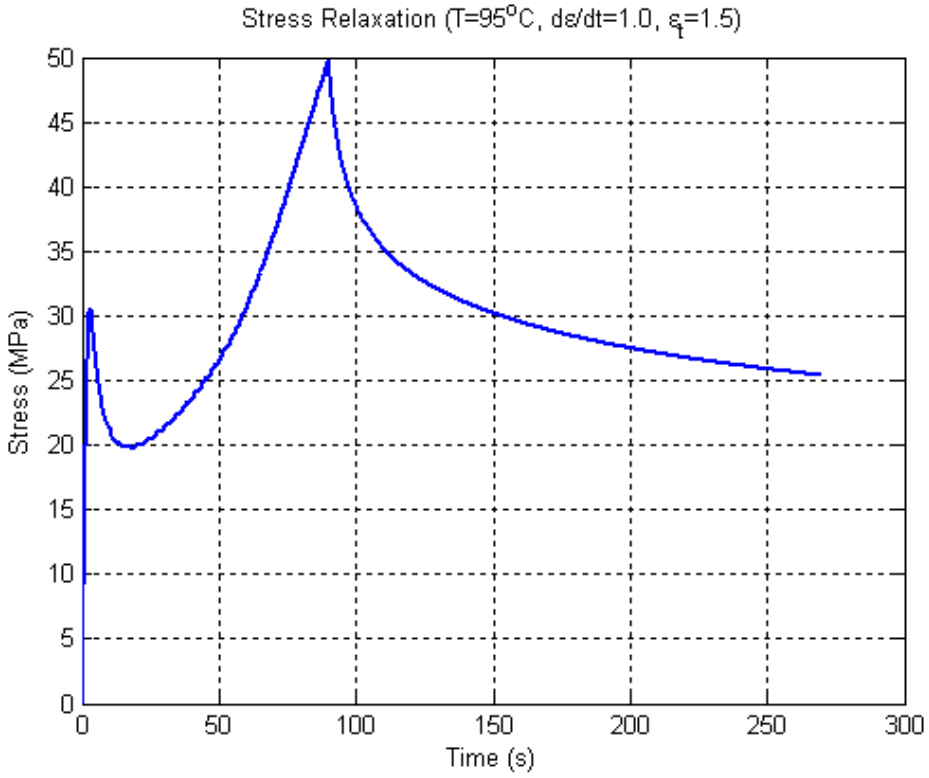
Stress Relaxation (T=95°C, dε/dt=1.0, ε_f=1.5)
Stress (MPa)
Time (s)
0
5
10
15
20
25
30
35
40
45
50
0
50
100
150
200
250
300

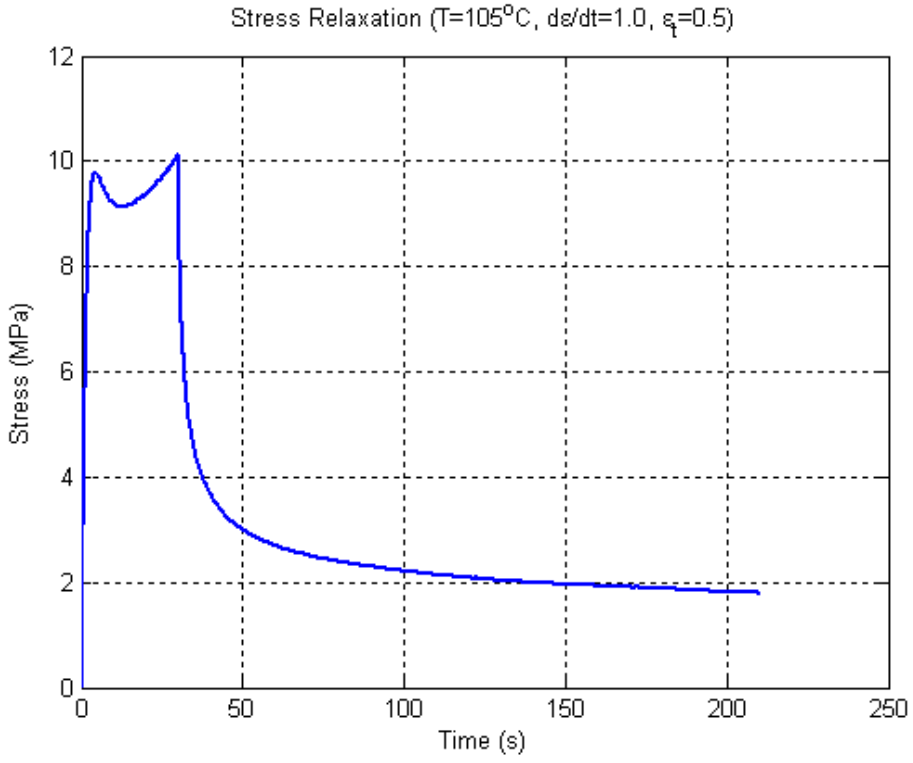
Stress Relaxation (T=105°C, dε/dt=1.0, ε_f=0.5)
Stress (MPa)
Time (s)
0
2
4
6
8
10
12
0
50
100
150
200
250

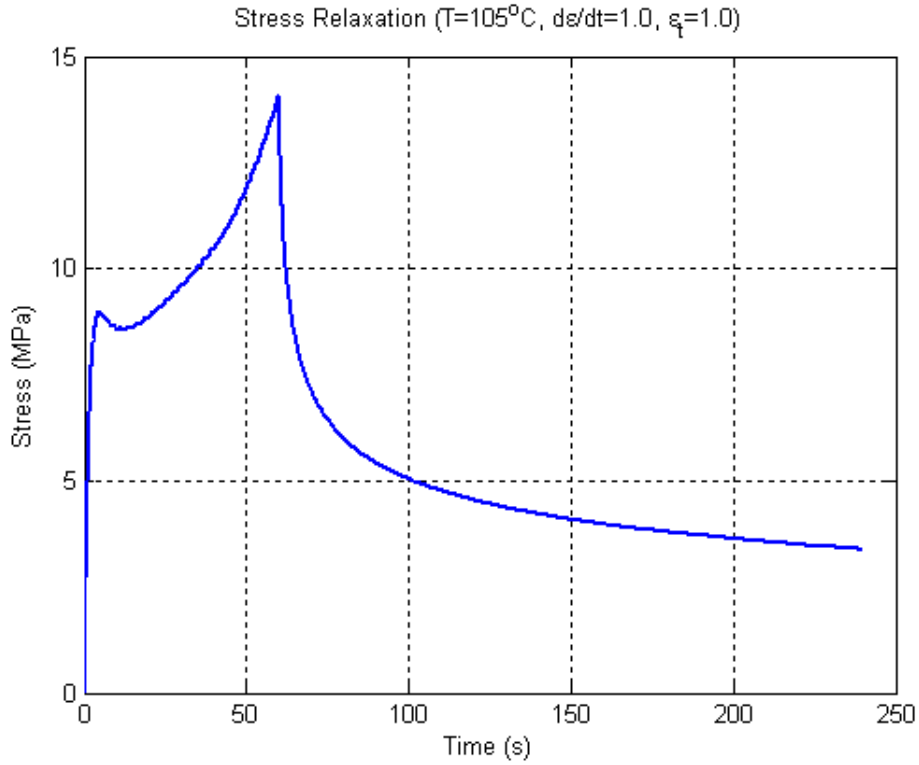
Stress Relaxation (T=105°C, dε/dt=1.0, ε_t=1.0)
Stress (MPa)
Time (s)
0
5
10
15
0
50
100
150
200
250

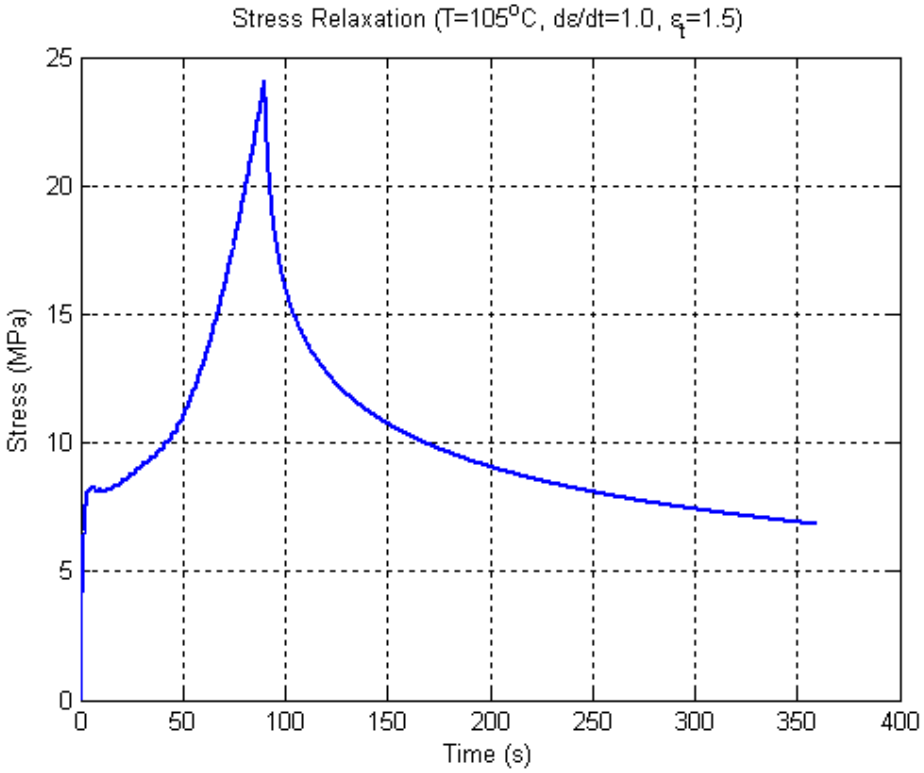
Stress Relaxation (T=105°C, dε/dt=1.0, ε_t=1.5)
Stress (MPa)
Time (s)
0
5
10
15
20
25
0
50
100
150
200
250
300
350
400

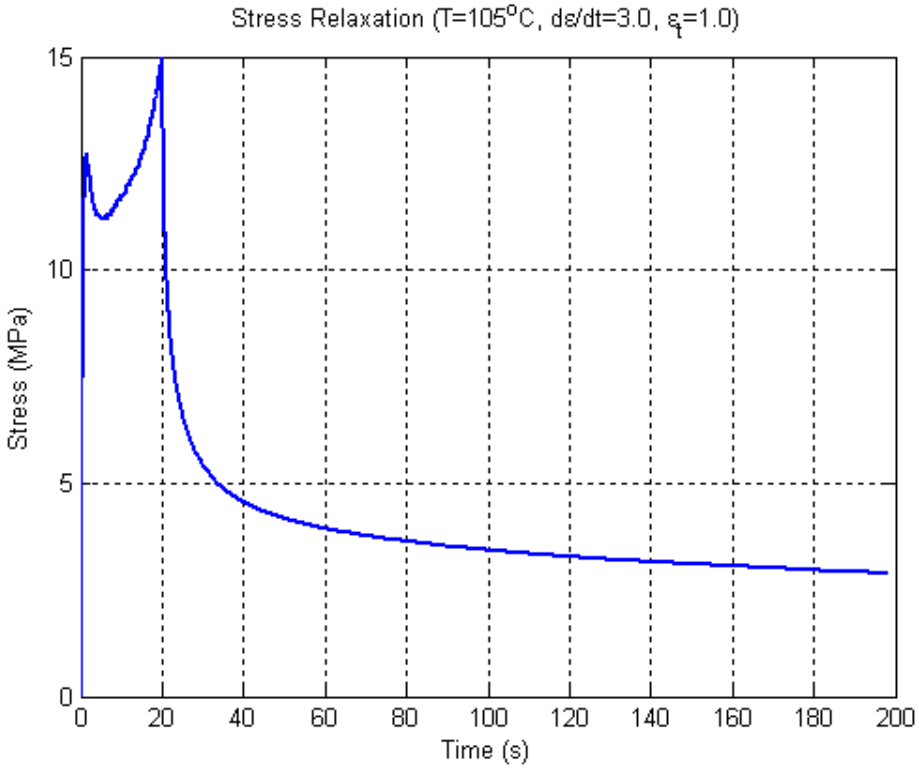
Stress Relaxation (T=105°C, dε/dt=3.0, ε_f=1.0)
Stress (MPa)
Time (s)
0
5
10
15
0
20
40
60
80
100
120
140
160
180
200

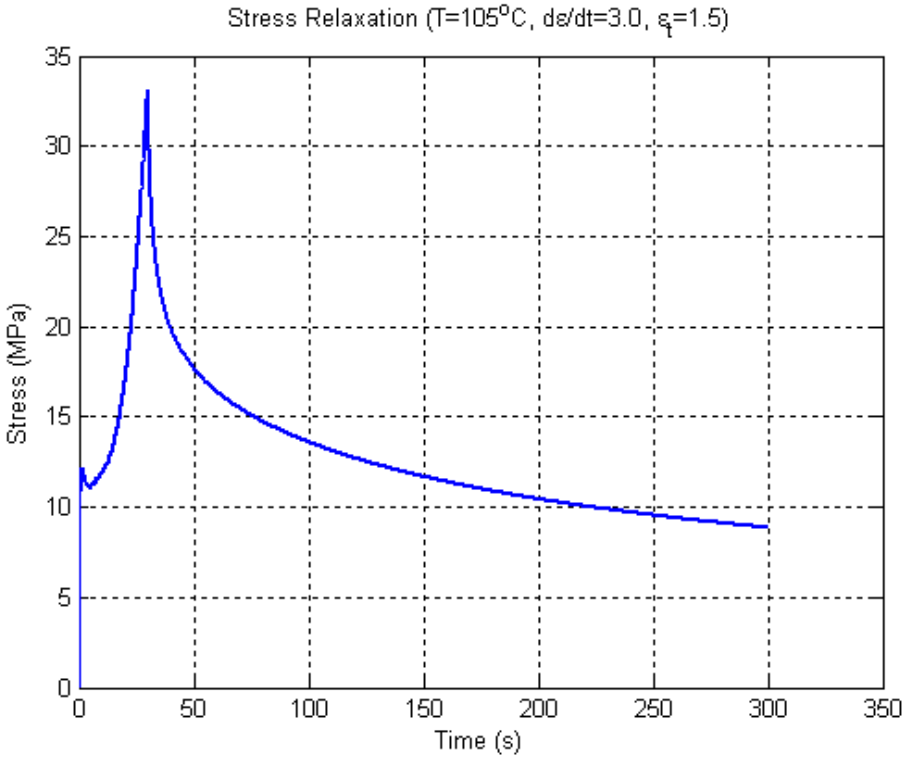
Stress Relaxation (T=105°C, dε/dt=3.0, ε_f=1.5)
Stress (MPa)
Time (s)
0
5
10
15
20
25
30
35
0
50
100
150
200
250
300
350

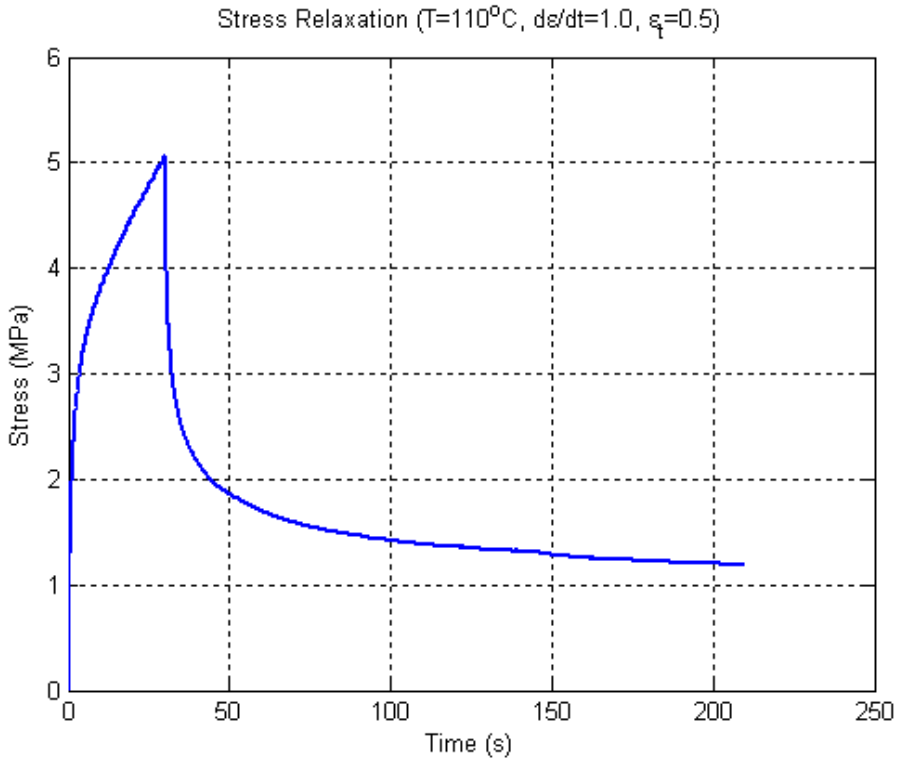
Stress Relaxation (T=110°C, dε/dt=1.0, εt=0.5)
Stress (MPa)
Time (s)
0
1
2
3
4
5
6
0
50
100
150
200
250

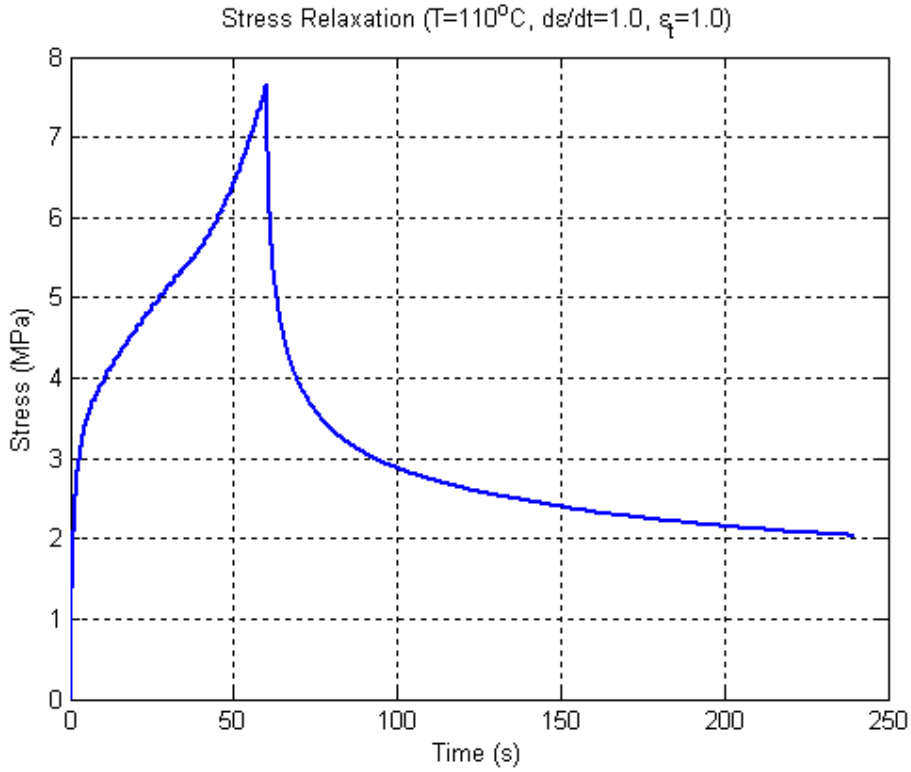
Stress Relaxation (T=110°C, dε/dt=1.0, εt=1.0)
Stress (MPa)
Time (s)
0
1
2
3
4
5
6
7
8
0
50
100
150
200
250

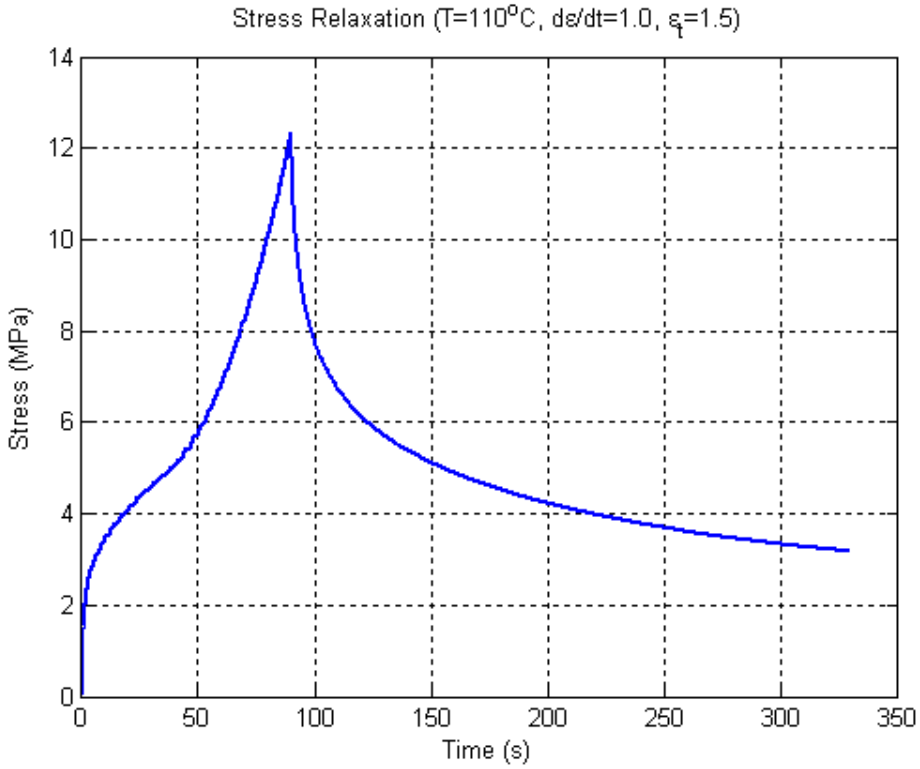
Stress Relaxation (T=110°C, dε/dt=1.0, ε_f=1.5)
Stress (MPa)
Time (s)
0
2
4
6
8
10
12
14
0
50
100
150
200
250
300
350

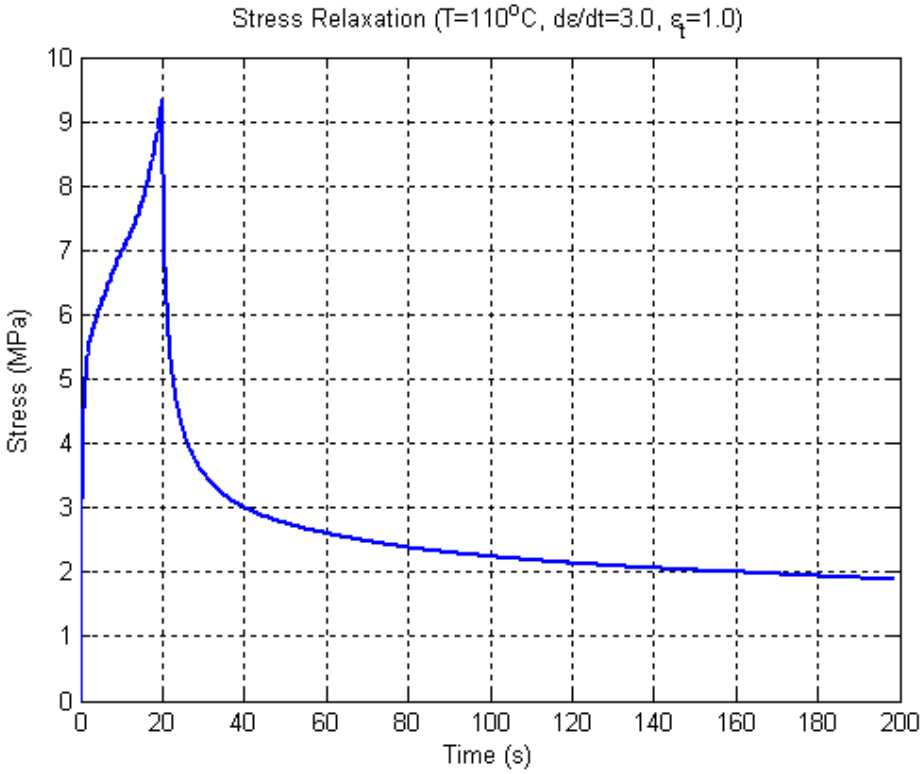
Stress Relaxation (T=110°C, dε/dt=3.0, ε_f=1.0)
Stress (MPa)
Time (s)
0
1
2
3
4
5
6
7
8
9
10
0
20
40
60
80
100
120
140
160
180
200

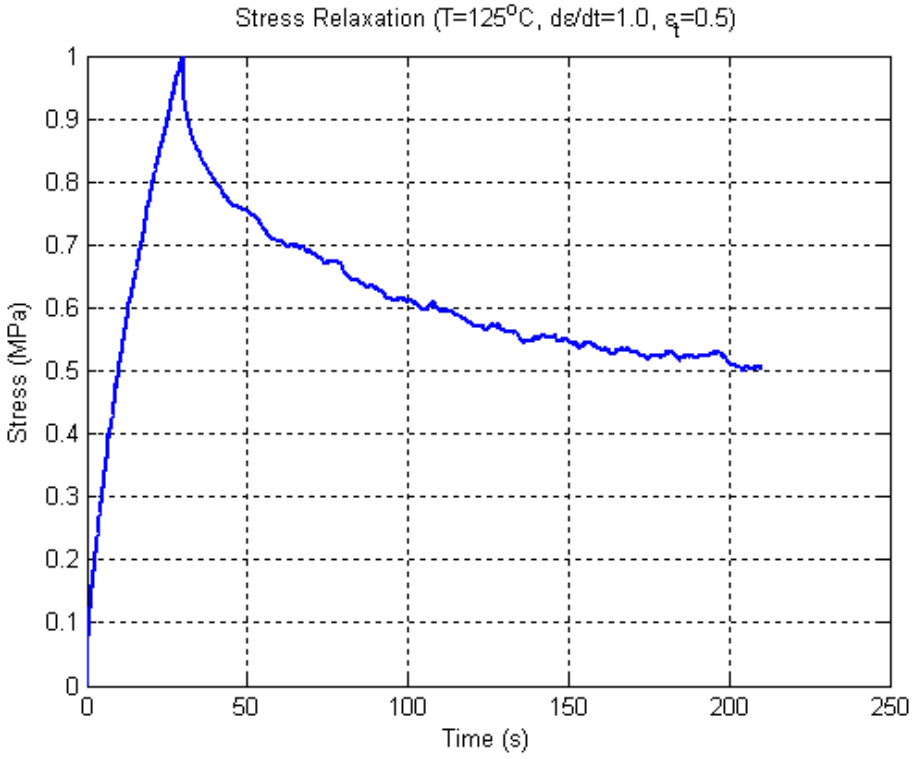
Stress Relaxation (T=125°C, dε/dt=1.0, ε_t=0.5)
Stress (MPa)
Time (s)
0
0.1
0.2
0.3
0.4
0.5
0.6
0.7
0.8
0.9
1
0
50
100
150
200
250

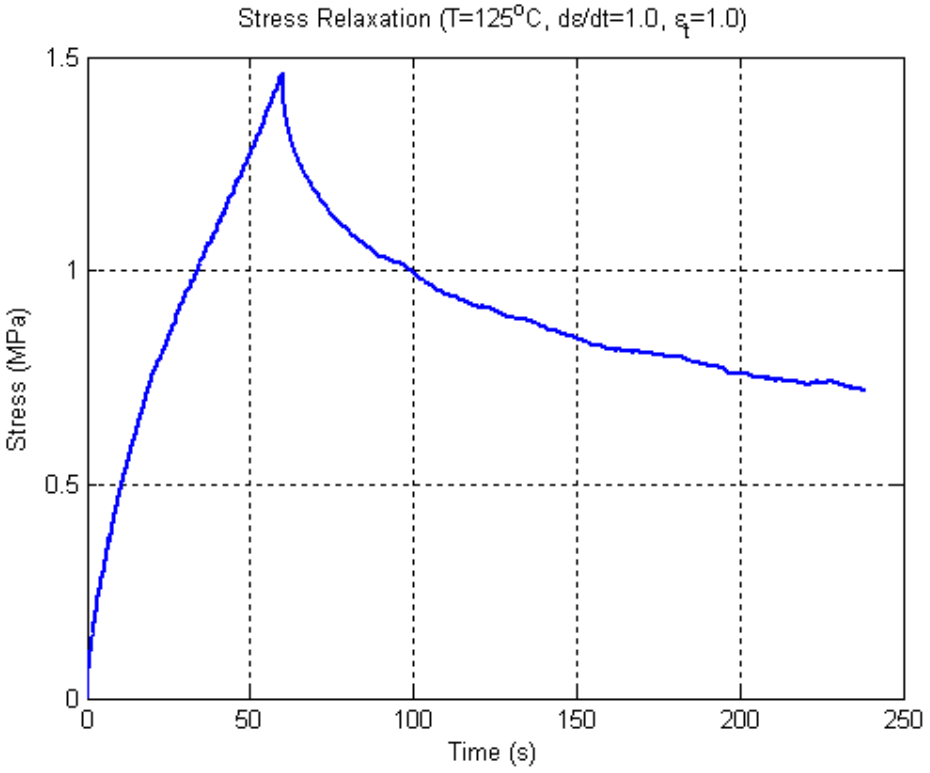
Stress Relaxation (T=125°C, dε/dt=1.0, ε_t=1.0)
Stress (MPa)
Time (s)
0
0.5
1
1.5
0
50
100
150
200
250

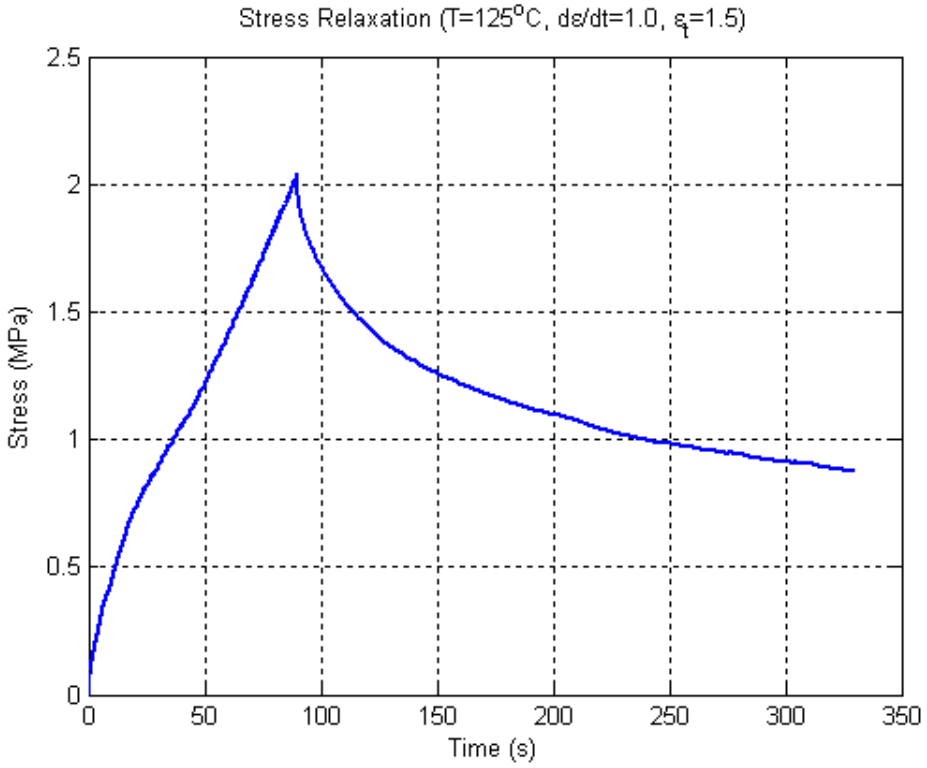
Stress Relaxation (T=125°C, dε/dt=1.0, ε_f=1.5)
Stress (MPa)
Time (s)
0
0.5
1
1.5
2
2.5
0
50
100
150
200
250
300
350

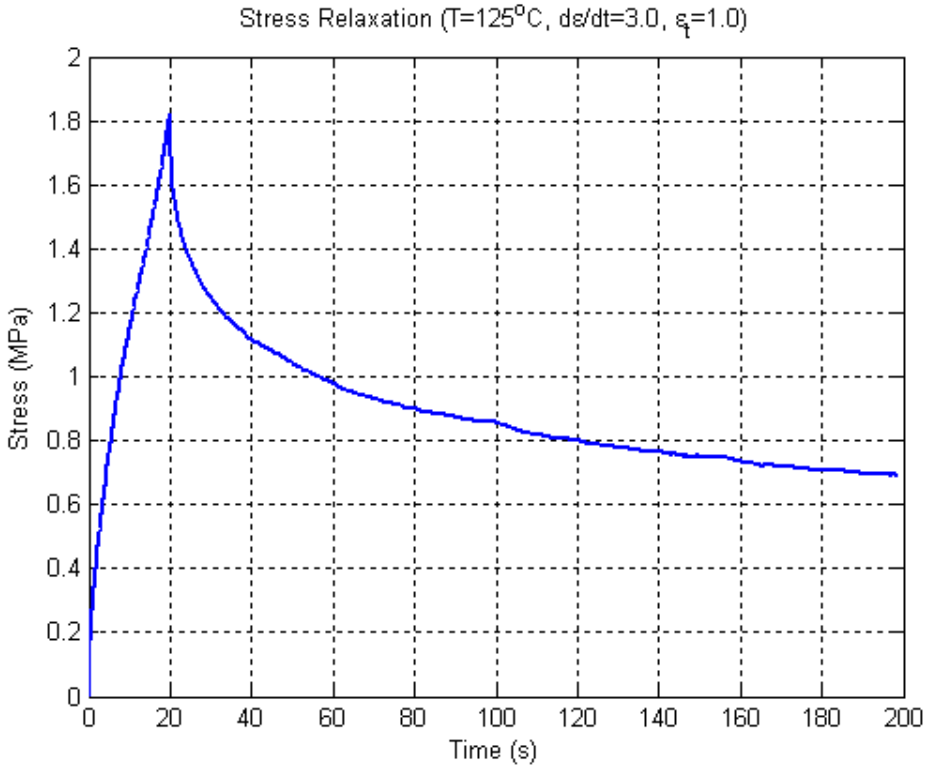
Stress Relaxation (T=125°C, dε/dt=3.0, ε_f=1.0)
Stress (MPa)
Time (s)
0
0.2
0.4
0.6
0.8
1
1.2
1.4
1.6
1.8
2
0
20
40
60
80
100
120
140
160
180
200

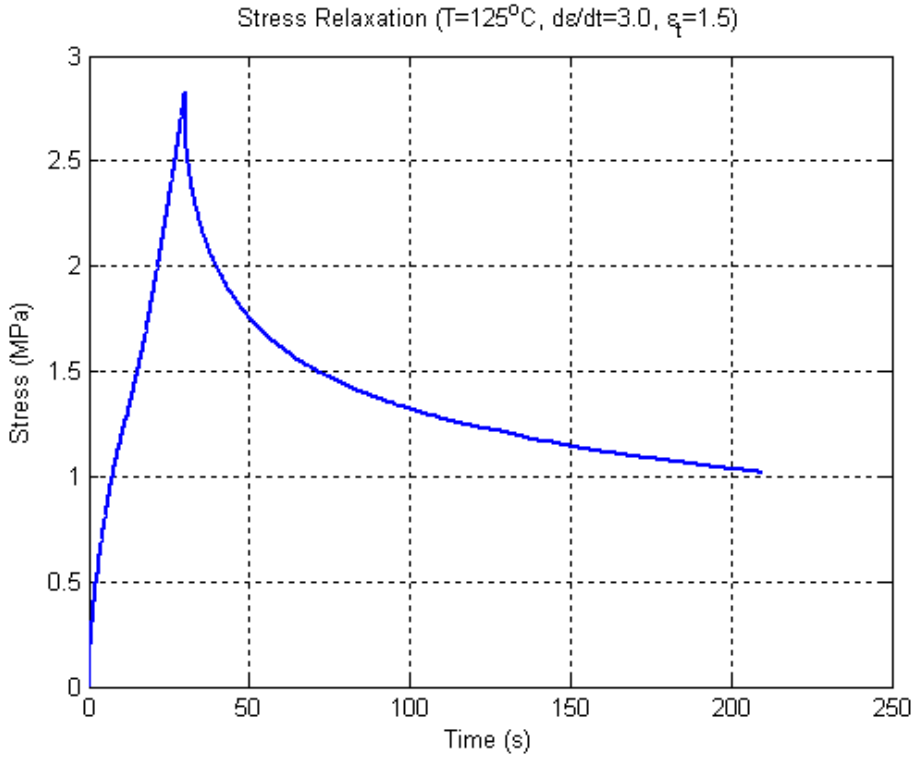
Stress Relaxation (T=125°C, dε/dt=3.0, ε_t=1.5)
Stress (MPa)
Time (s)
0
0.5
1
1.5
2
2.5
3
0
50
100
150
200
250

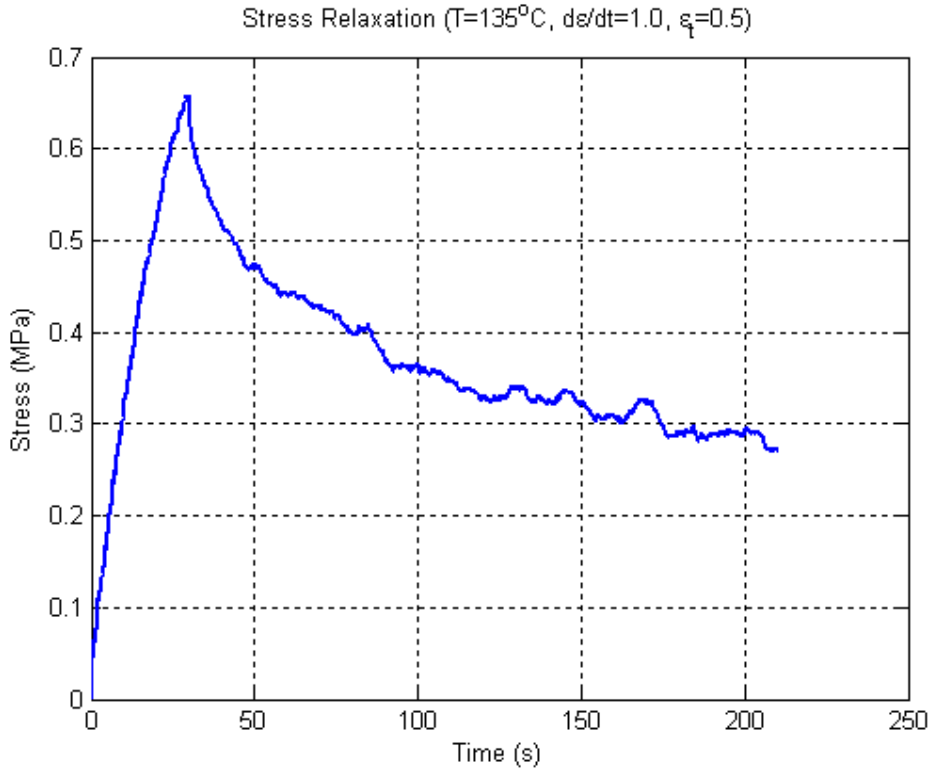
Stress Relaxation (T=135°C, dε/dt=1.0, ε_t=0.5)
Stress (MPa)
Time (s)
0
0.1
0.2
0.3
0.4
0.5
0.6
0.7
0
50
100
150
200
250

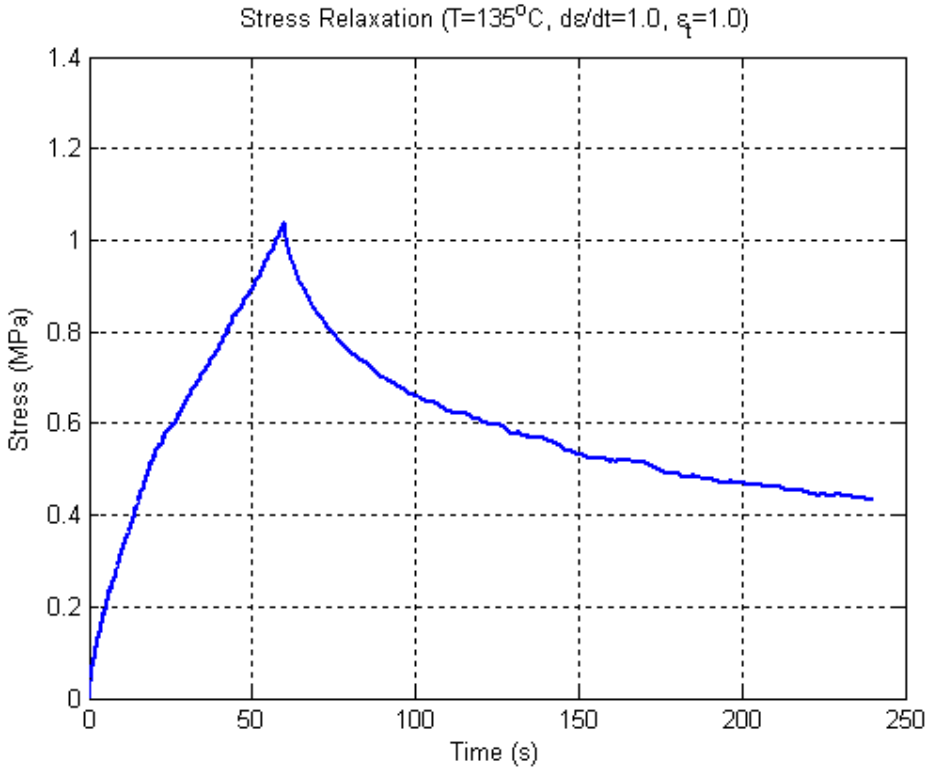
Stress Relaxation (T=135°C, dε/dt=1.0, ε_t=1.0)
Stress (MPa)
Time (s)
0
0.2
0.4
0.6
0.8
1
1.2
1.4
0
50
100
150
200
250

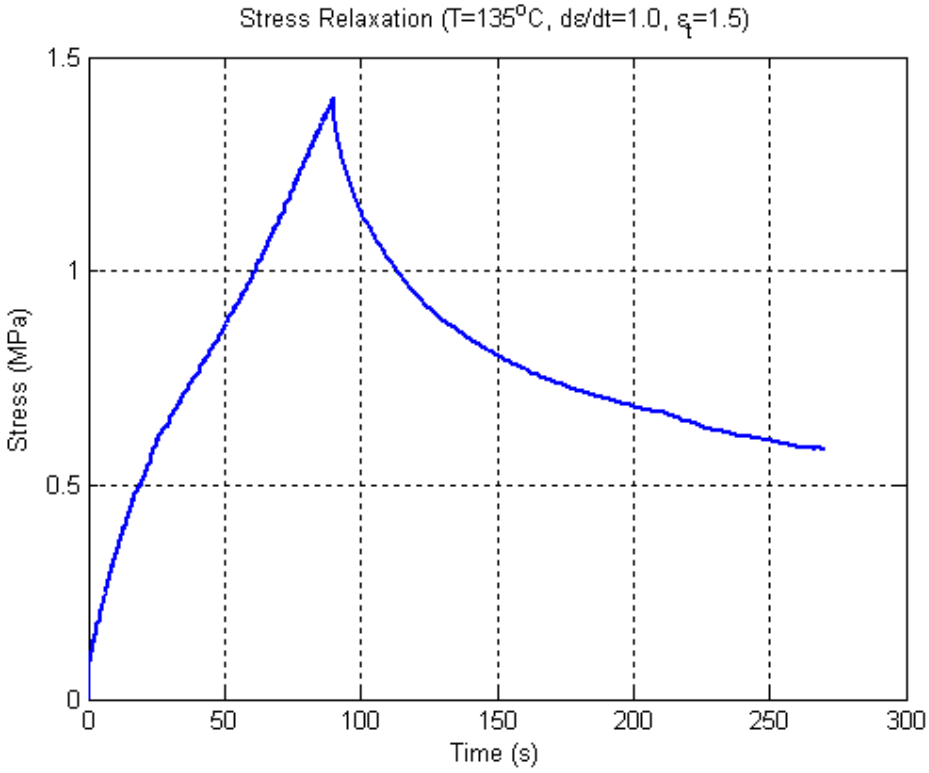
Stress Relaxation (T=135°C, dε/dt=1.0, ε_t=1.5)
Stress (MPa)
Time (s)
0
0.5
1
1.5
0
50
100
150
200
250
300

Appendix B

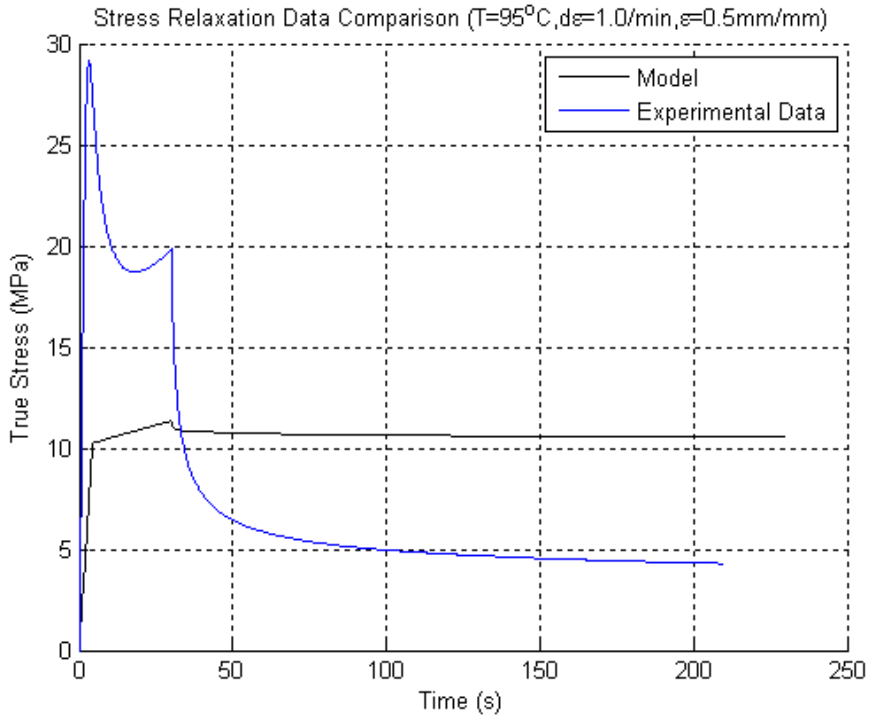
Stress Relaxation Data Comparison (T=95°C,dε=1.0/min,ε=0.5mm/mm)
Model
Experimental Data
True Stress (MPa)
Time (s)
0
5
10
15
20
25
30
0
50
100
150
200
250

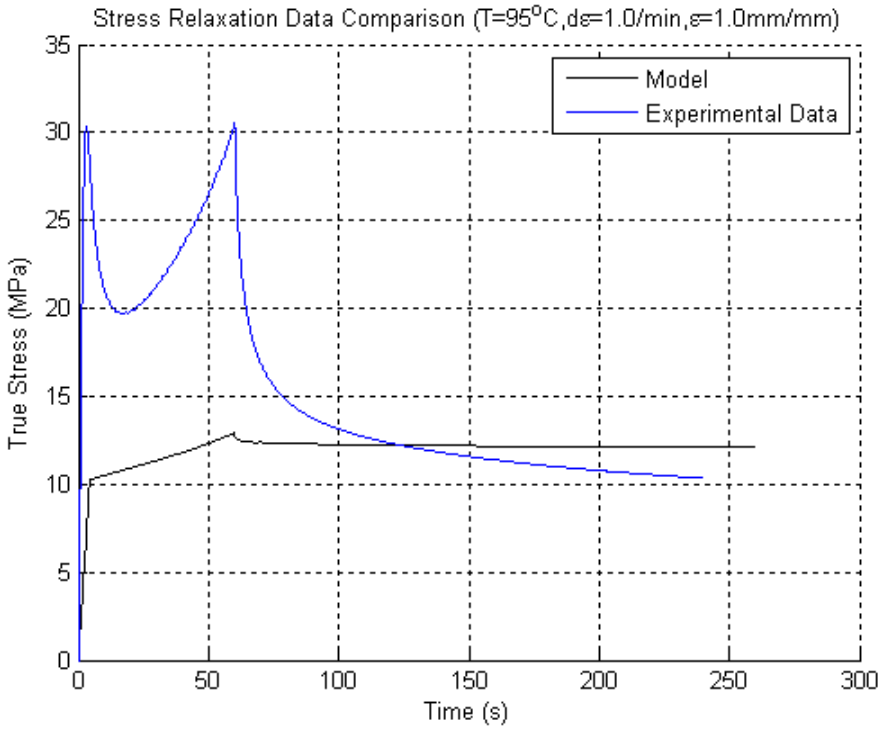
Stress Relaxation Data Comparison (T=95°C,dε=1.0/min,ε=1.0mm/mm)
Model
Experimental Data
True Stress (MPa)
Time (s)
0
5
10
15
20
25
30
35
0
50
100
150
200
250
300

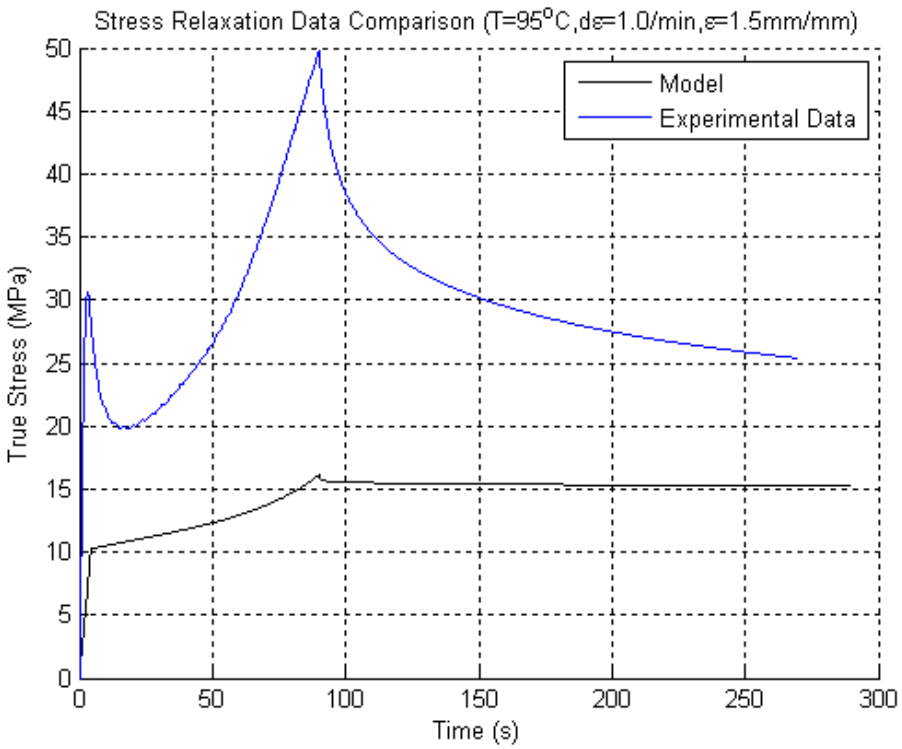
Stress Relaxation Data Comparison (T=95°C,dε=1.0/min,ε=1.5mm/mm)
Model
Experimental Data
True Stress (MPa)
Time (s)
0
5
10
15
20
25
30
35
40
45
50
0
50
100
150
200
250
300

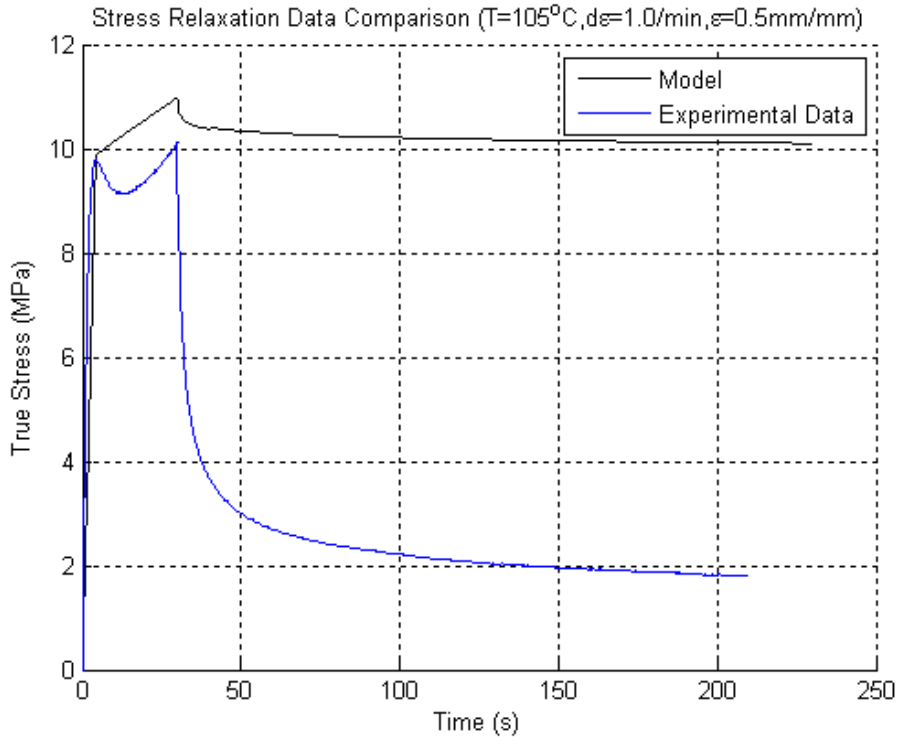
Stress Relaxation Data Comparison (T=105°C,dε=1.0/min,ε=0.5mm/mm)
Model
Experimental Data
True Stress (MPa)
Time (s)
0
2
4
6
8
10
12
0
50
100
150
200
250

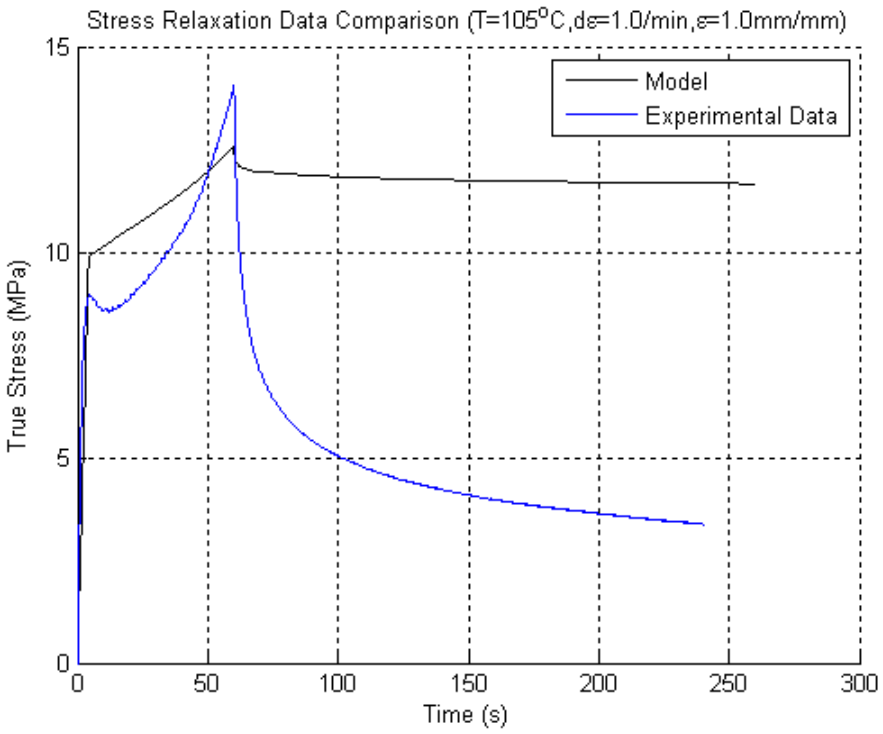
Stress Relaxation Data Comparison (T=105°C,dε=1.0/min,ε=1.0mm/mm)
Model
Experimental Data
True Stress (MPa)
Time (s)
0
5
10
15
0
50
100
150
200
250
300

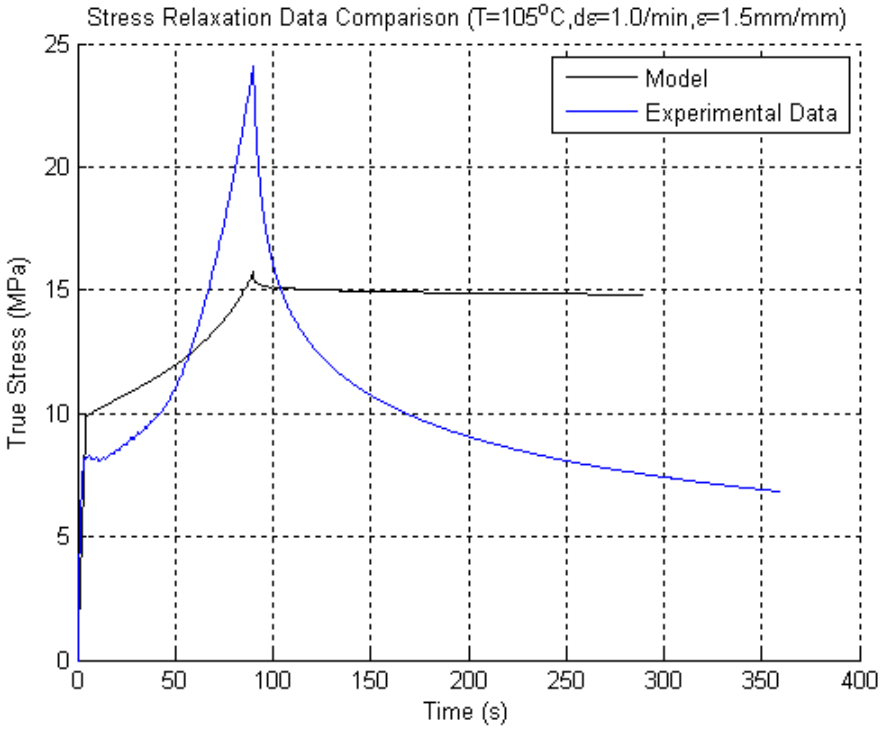
Stress Relaxation Data Comparison (T=105°C,dε=1.0/min,ε=1.5mm/mm)
Model
Experimental Data
True Stress (MPa)
Time (s)
0
5
10
15
20
25
0
50
100
150
200
250
300
350
400

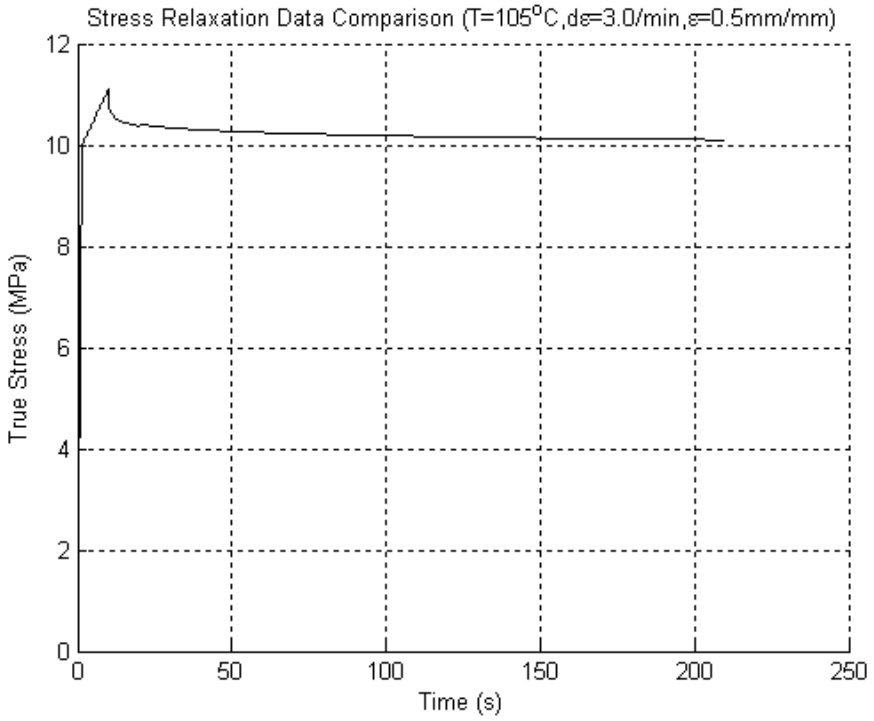
Stress Relaxation Data Comparison (T=105°C,dε=3.0/min,ε=0.5mm/mm)
True Stress (MPa)
Time (s)
0
2
4
6
8
10
12
0
50
100
150
200
250

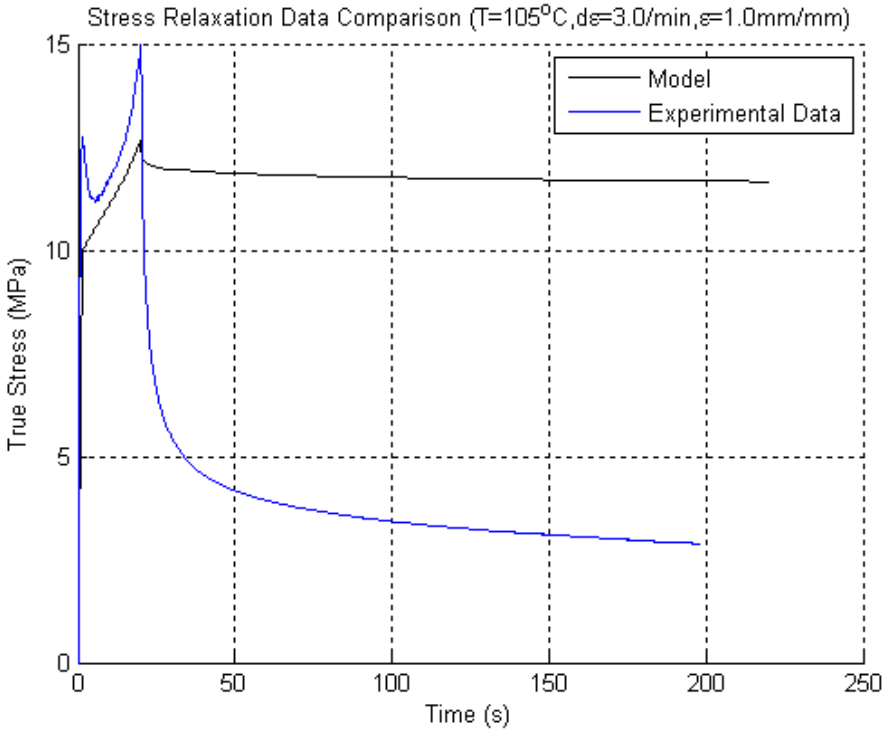
Stress Relaxation Data Comparison (T=105°C,dε=3.0/min,ε=1.0mm/mm)
Model
Experimental Data
True Stress (MPa)
Time (s)
0
5
10
15
0
50
100
150
200
250

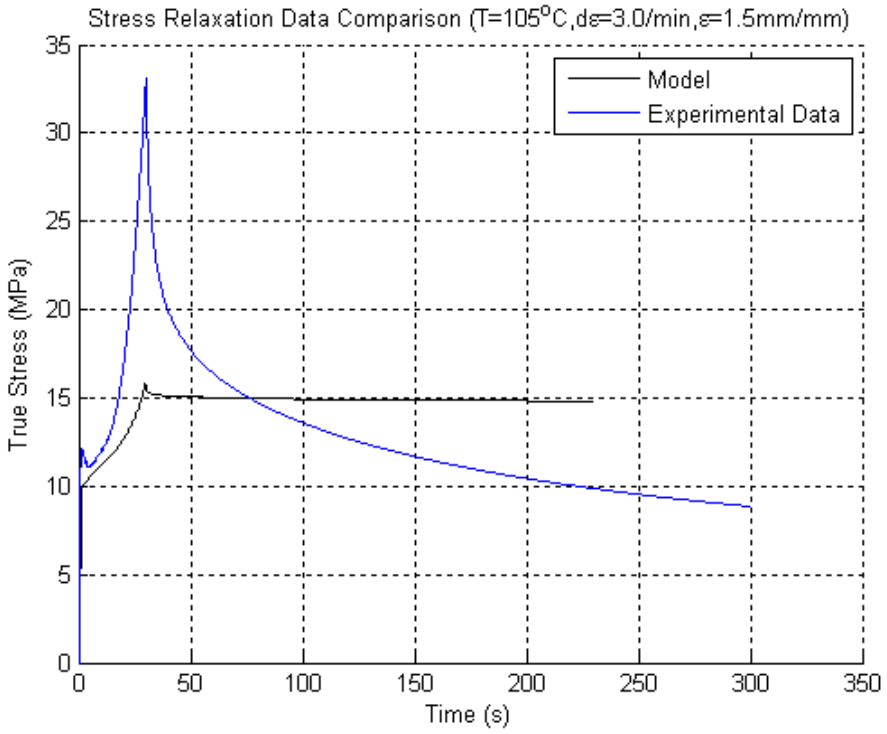
Stress Relaxation Data Comparison (T=105°C,dε=3.0/min,ε=1.5mm/mm)
Model
Experimental Data
True Stress (MPa)
Time (s)
0
5
10
15
20
25
30
35
0
50
100
150
200
250
300
350

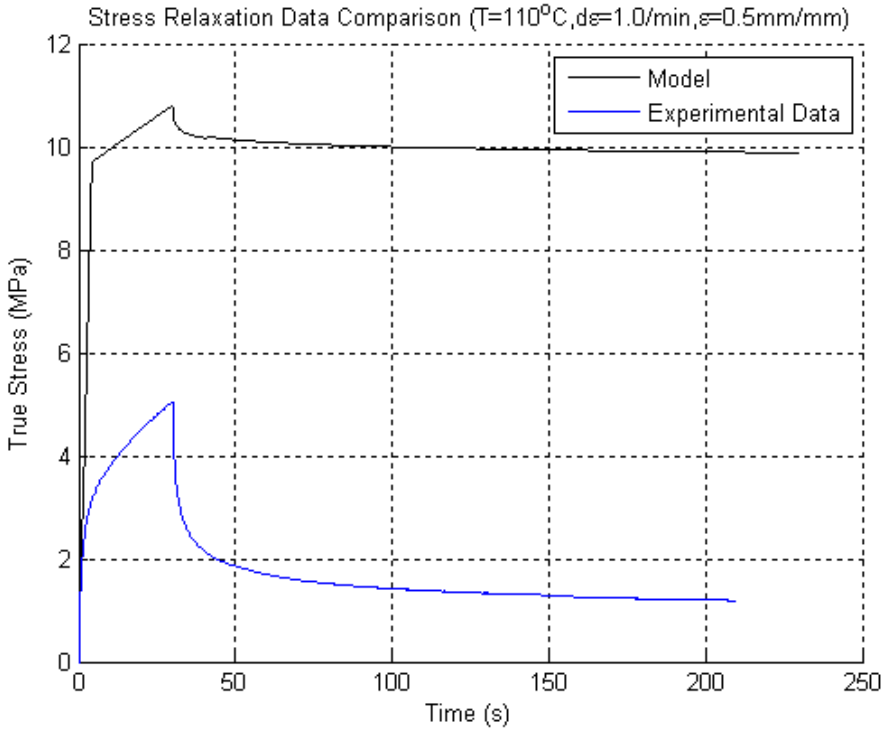
Stress Relaxation Data Comparison (T=110°C,dε=1.0/min,ε=0.5mm/mm)
Model
Experimental Data
True Stress (MPa)
Time (s)
0
2
4
6
8
10
12
0
50
100
150
200
250

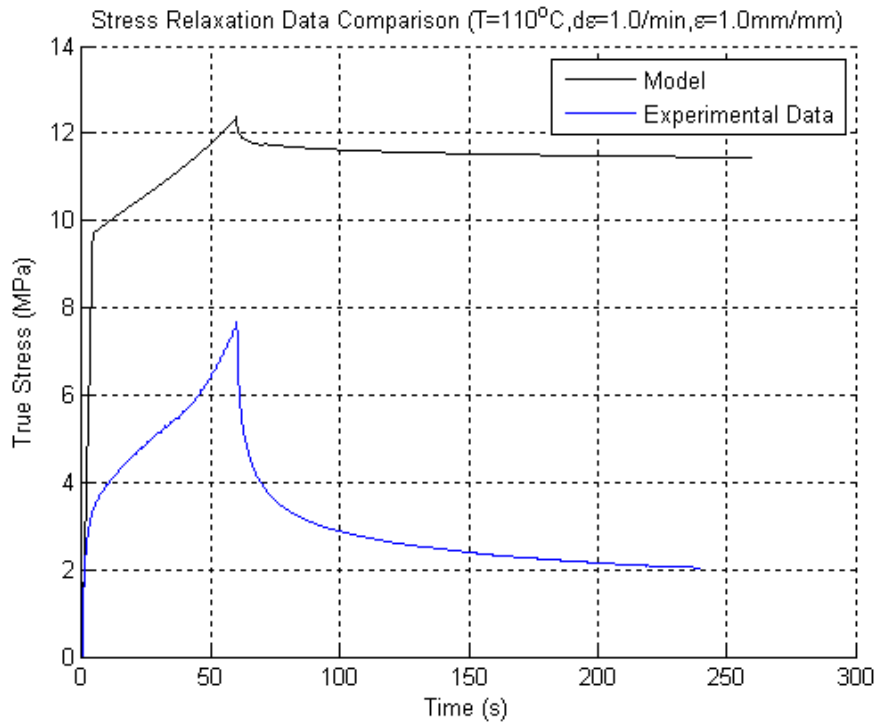
Stress Relaxation Data Comparison (T=110°C,dε=1.0/min,ε=1.0mm/mm)
Model
Experimental Data
True Stress (MPa)
Time (s)
0
2
4
6
8
10
12
14
0
50
100
150
200
250
300

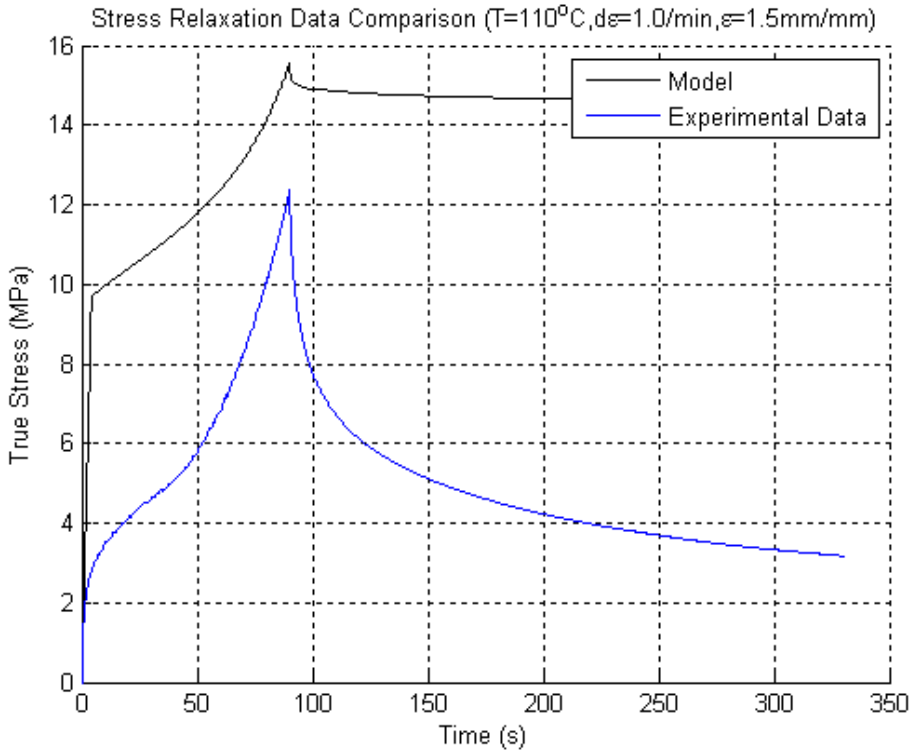
Stress Relaxation Data Comparison (T=110°C,dε=1.0/min,ε=1.5mm/mm)
Model
Experimental Data
True Stress (MPa)
Time (s)
0
2
4
6
8
10
12
14
16
0
50
100
150
200
250
300
350

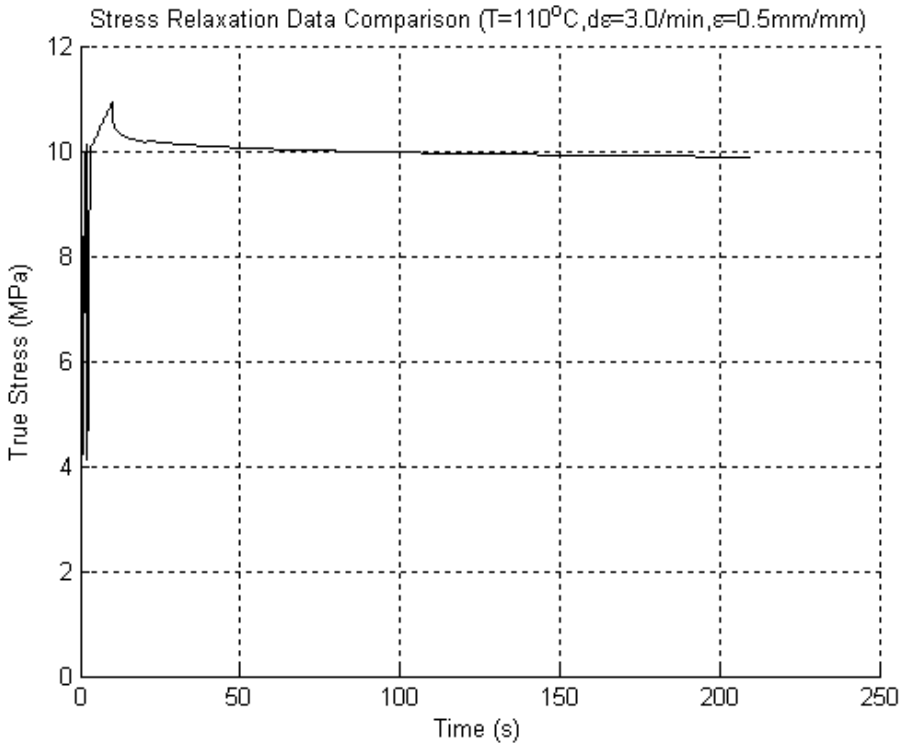
Stress Relaxation Data Comparison (T=110°C,dε=3.0/min,ε=0.5mm/mm)
True Stress (MPa)
Time (s)
0
2
4
6
8
10
12
0
50
100
150
200
250

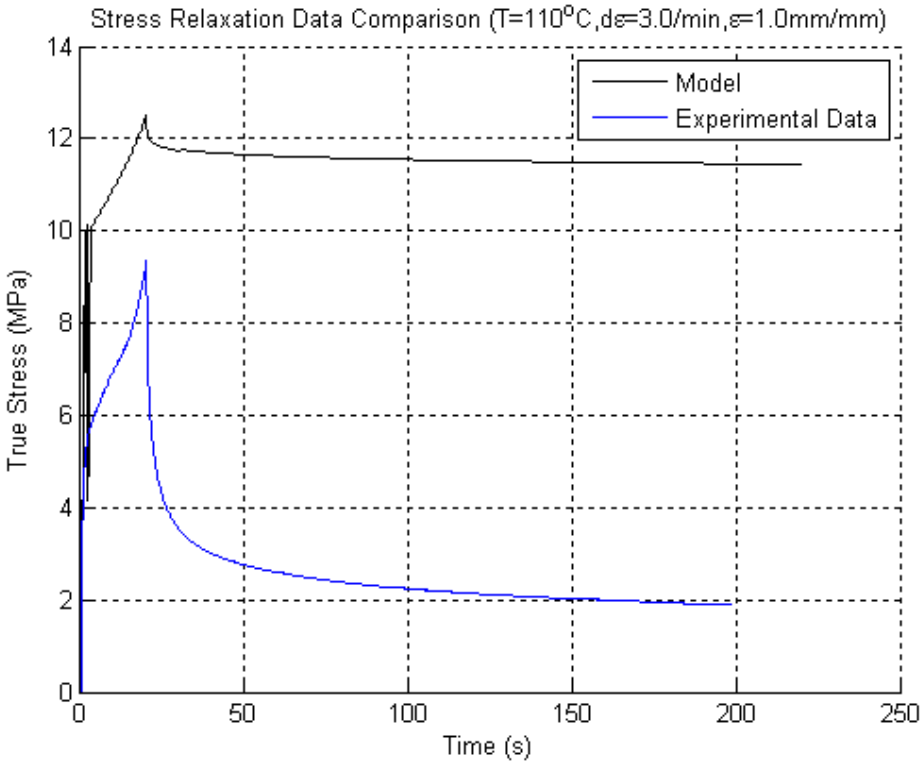
Stress Relaxation Data Comparison (T=110°C,dε=3.0/min,ε=1.0mm/mm)
Model
Experimental Data
True Stress (MPa)
Time (s)
0
2
4
6
8
10
12
14
0
50
100
150
200
250

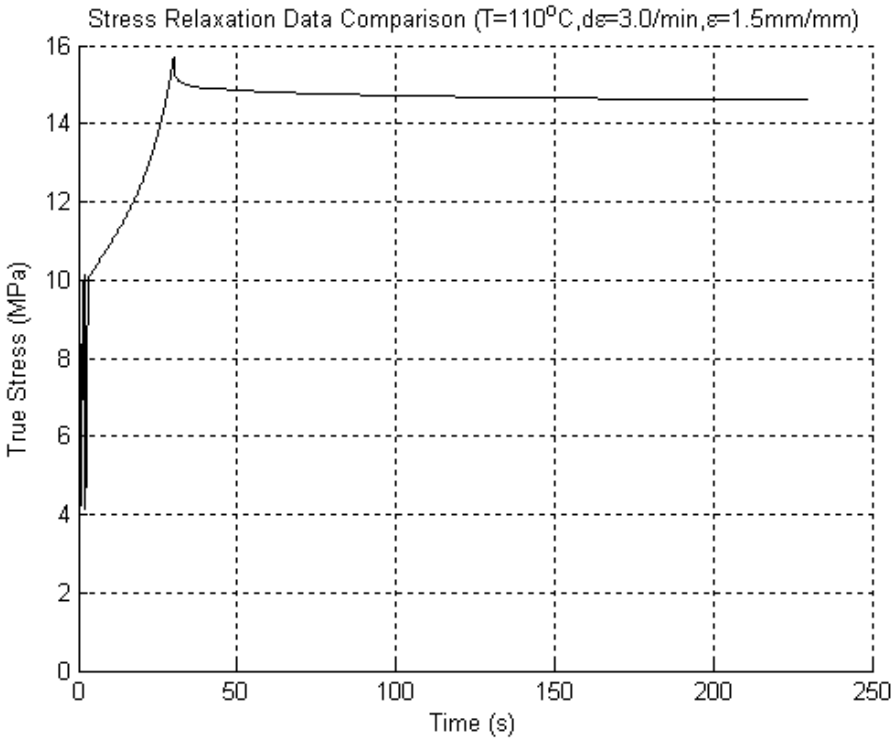
Stress Relaxation Data Comparison (T=110°C,dε=3.0/min,ε=1.5mm/mm)
True Stress (MPa)
Time (s)
0
2
4
6
8
10
12
14
16
0
50
100
150
200
250

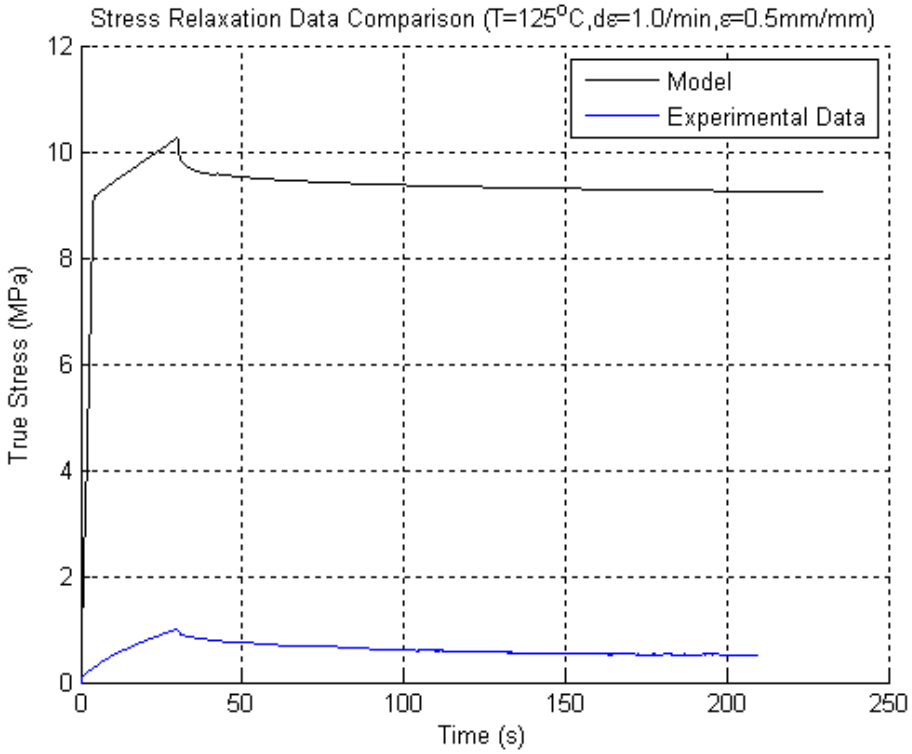
Stress Relaxation Data Comparison (T=125°C,dε=1.0/min,ε=0.5mm/mm)
Model
Experimental Data
True Stress (MPa)
Time (s)
0
2
4
6
8
10
12
0
50
100
150
200
250

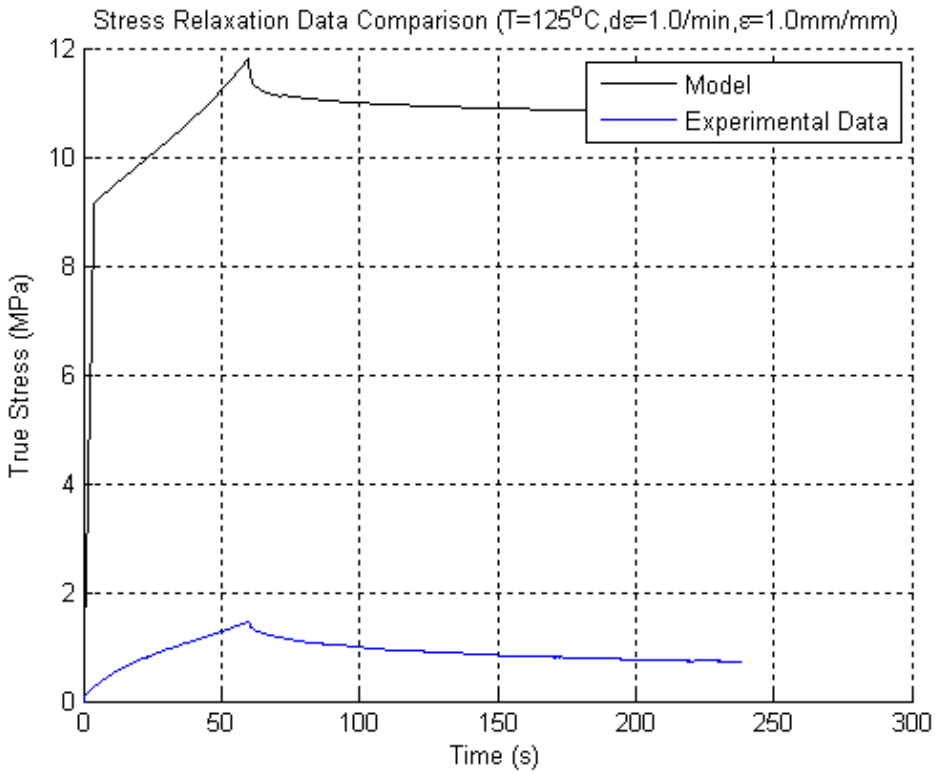
Stress Relaxation Data Comparison (T=125°C,dε=1.0/min,ε=1.0mm/mm)
Model
Experimental Data
True Stress (MPa)
Time (s)
0
2
4
6
8
10
12
0
50
100
150
200
250
300

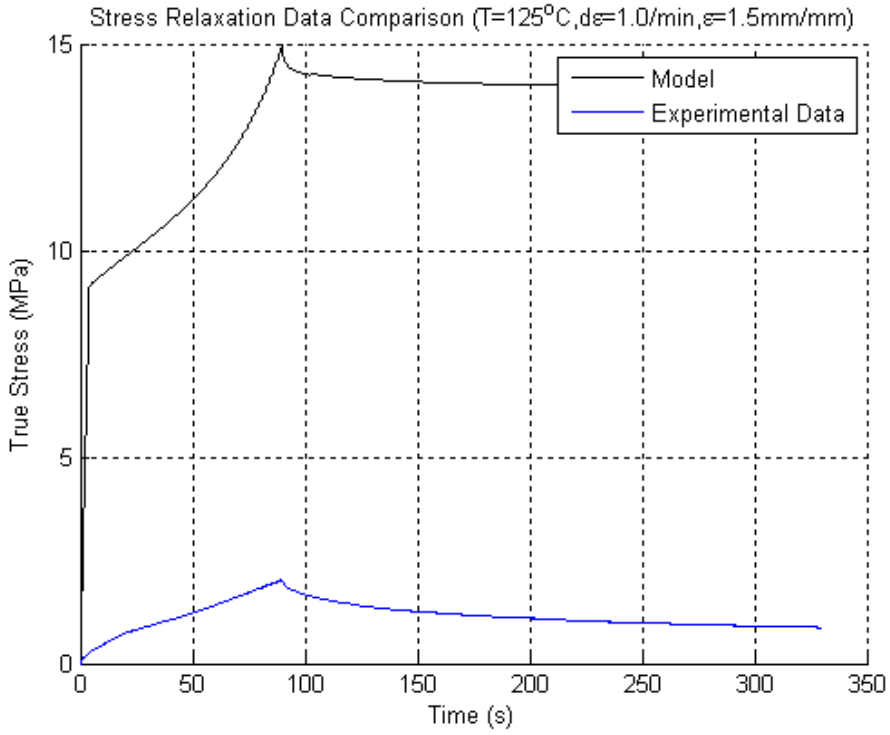
Stress Relaxation Data Comparison (T=125°C,dε=1.0/min,ε=1.5mm/mm)
Model
Experimental Data
True Stress (MPa)
Time (s)
0
5
10
15
0
50
100
150
200
250
300
350

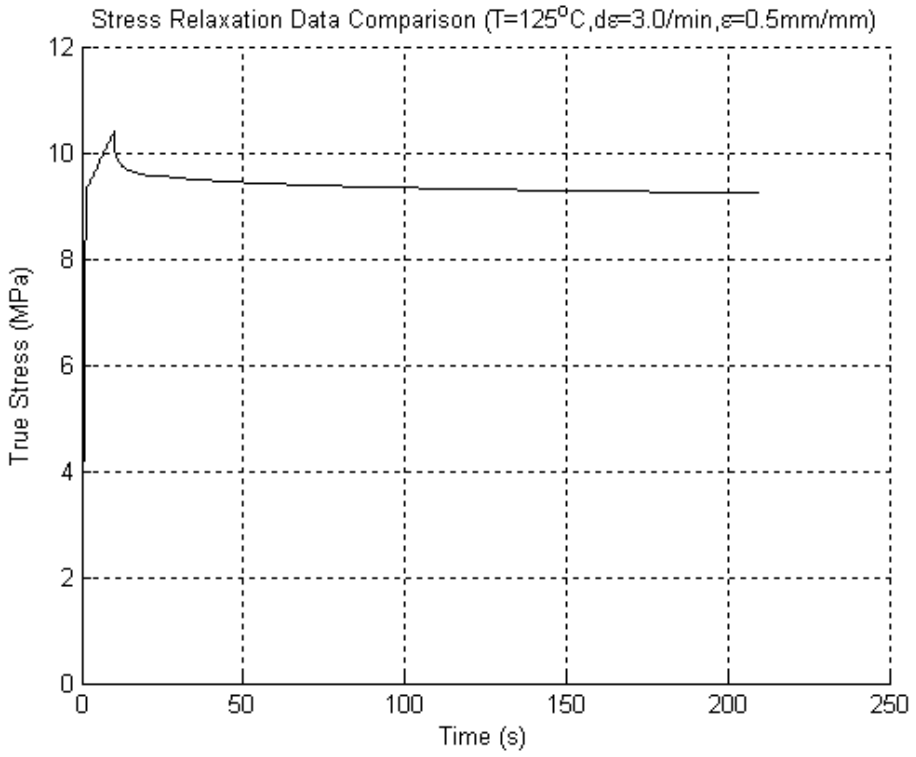
Stress Relaxation Data Comparison (T=125°C,dε=3.0/min,ε=0.5mm/mm)
True Stress (MPa)
Time (s)
0
2
4
6
8
10
12
0
50
100
150
200
250

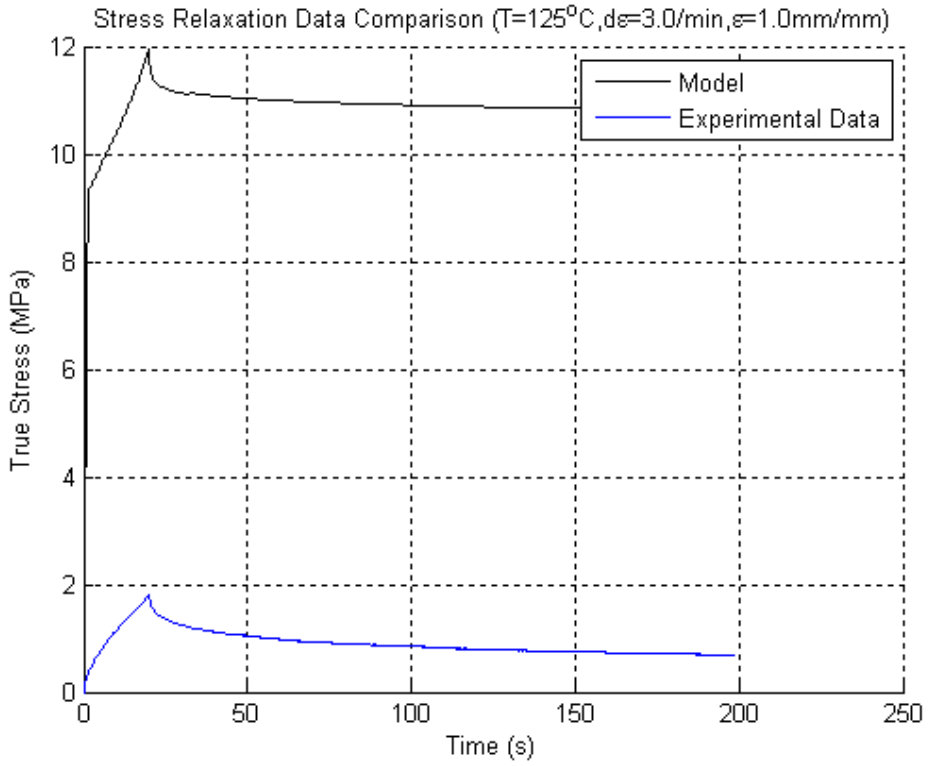
Stress Relaxation Data Comparison (T=125°C,dε=3.0/min,ε=1.0mm/mm)
Model
Experimental Data
True Stress (MPa)
Time (s)
0
2
4
6
8
10
12
0
50
100
150
200
250

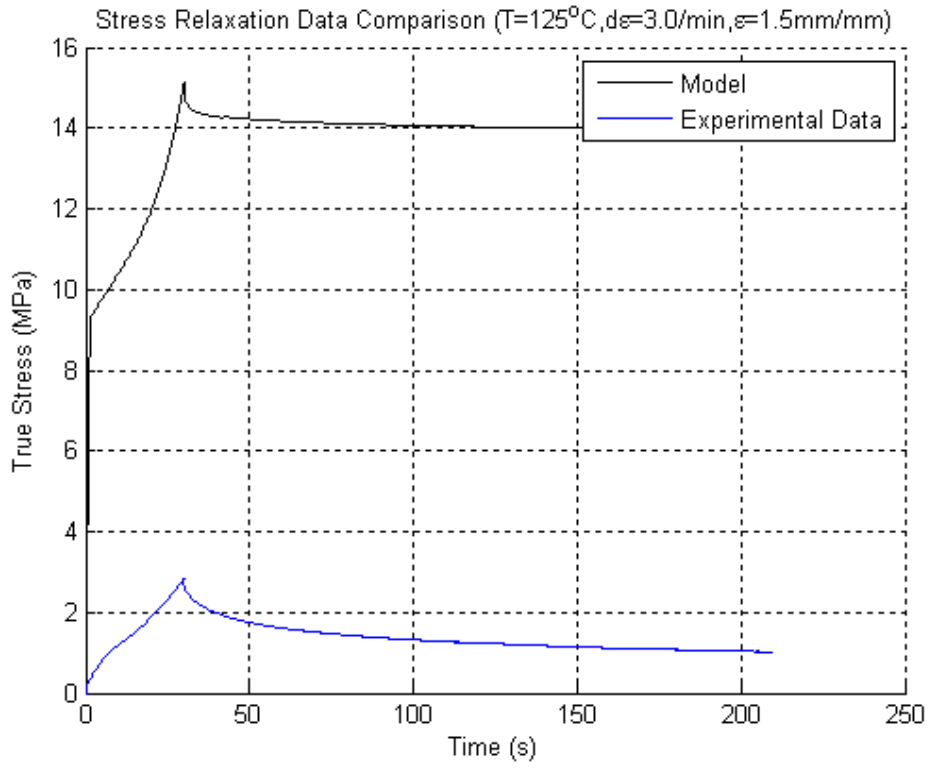
Stress Relaxation Data Comparison (T=125°C,dε=3.0/min,ε=1.5mm/mm)
Model
Experimental Data
True Stress (MPa)
Time (s)
0
2
4
6
8
10
12
14
16
0
50
100
150
200
250

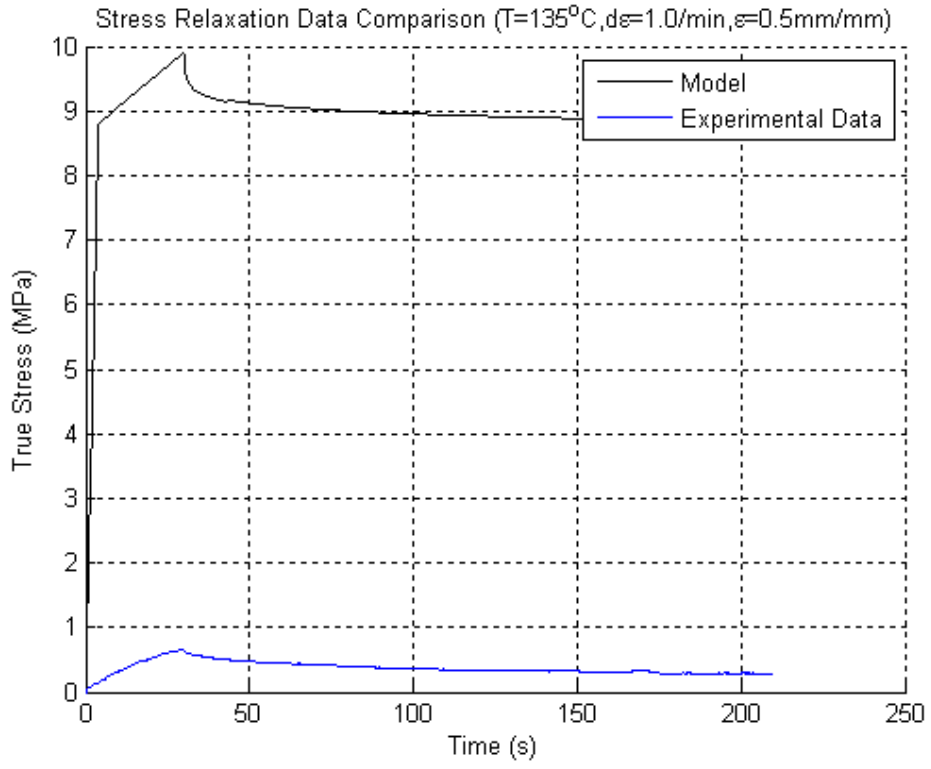
Stress Relaxation Data Comparison (T=135°C,dε=1.0/min,ε=0.5mm/mm)
Model
Experimental Data
True Stress (MPa)
Time (s)
0
1
2
3
4
5
6
7
8
9
10
0
50
100
150
200
250

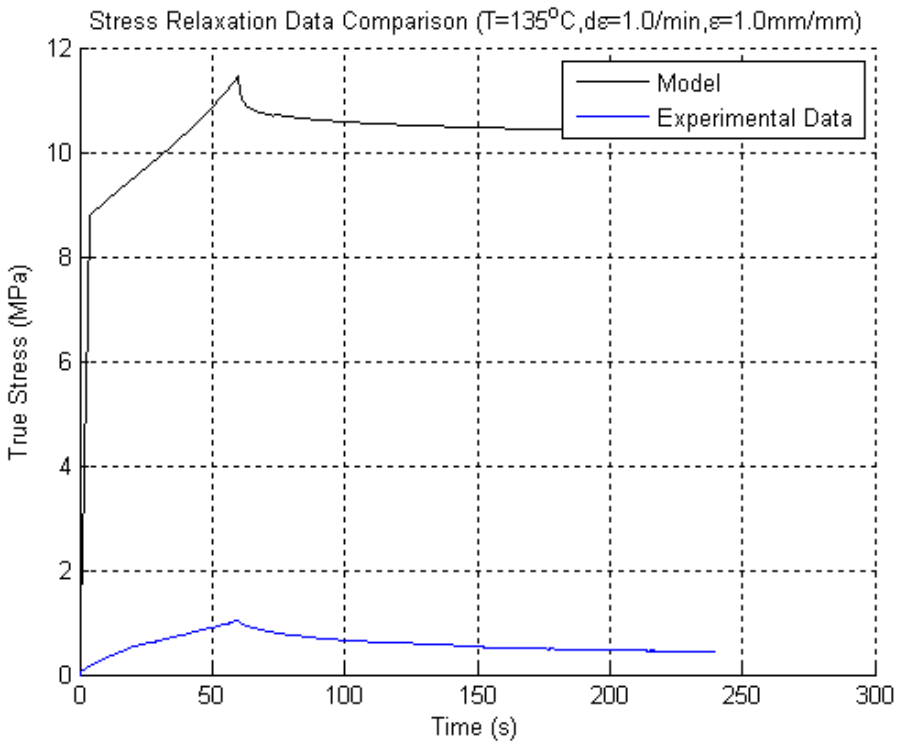
Stress Relaxation Data Comparison (T=135°C,dε=1.0/min,ε=1.0mm/mm)
Model
Experimental Data
True Stress (MPa)
Time (s)
0
2
4
6
8
10
12
0
50
100
150
200
250
300

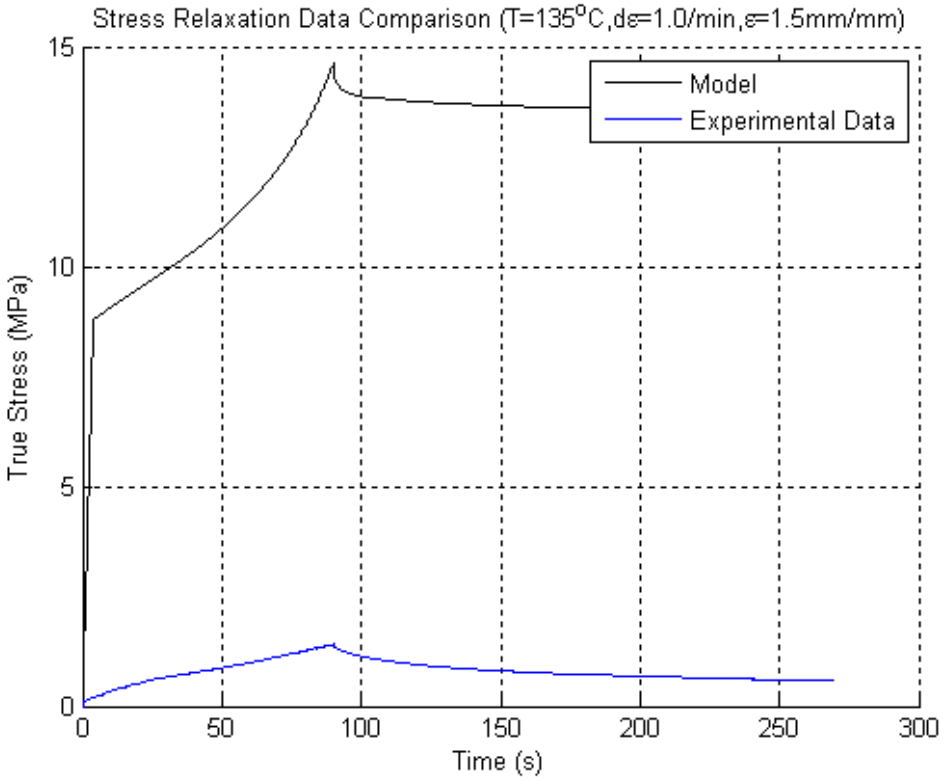
Stress Relaxation Data Comparison (T=135°C,dε=1.0/min,ε=1.5mm/mm)
Model
Experimental Data
True Stress (MPa)
Time (s)
0
5
10
15
0
50
100
150
200
250
300